# CHAPTER 7 LONGWALL MINING

## 7.1 INTRODUCTION

As the coal in a longwall panel is being extracted slice by slice, the surrounding strata are forced to move toward and fill the voids left by the extracted coal. This process induces a series of intensive activities which include (1) movements of the rock strata between the roofline and the surface, resulting in surface subsidence; (2) abutment pressures on both sides of the panel, in front of the faceline, and in the bleeder end of the panel; and (3) roof-to-floor convergence in the gateroads and face area. All of these activities and other related subjects are discussed separately in this chapter except surface subsidence, which is discussed in Chapter 13.

## 7.2 PANEL LAYOUT AND GATEROAD SYSTEMS

Figure 1.3.12 (p. 12) shows a typical U.S. longwall panel layout. The panels are normally rectangular in shape with a uniform width throughout the whole panel length, except in rare cases when panel width may be changed.

Panels are laid out side by side for 10 or more panels, provided the reserve allows. If there are strong, massive strata in the overburden, panels are grouped in districts of 4 or more panels and separated by a barrier pillar, which in general is sufficiently large to isolate, from a ground control point of view, the district of panels from the other adjacent districts (Peng and Su, 1983). The panels within a district are usually the same width and length provided the reserve allows. If the panel length is not the same, the bleeder ends are staggered. Gateroad stability problems at the staggered intersection between two adjacent panels could occur (A and F in Fig. 6.2.4 on p. 291) (Miller, 1998).

The gateroads on both sides of the panel are developed either by 2-entry, 3-entry or 4-entry systems. In a 2-entry system, there is one row of chain pillars; in a 3-entry system, there are two rows of chain pillars; and in a 4-entry system, there are three rows of chain pillars.

The great majority of U.S. longwall mines employ the 3-entry system. Normally the dimensions of two rows of chain pillars could be either the same or different (Fig. 7.2.1). They may be square, rectangular or diamond-shaped. For the same panel length, use of rectangular pillars cuts down the number of crosscuts. The longer the pillar, the less number of crosscuts required, thereby increasing the rate of development. The diamond-shaped pillars are for the convenience of machine movement, thereby speeding up development. Similarly, in the unequal sized pillar configuration, the smaller-sized pillars are located on the head side to reduce machine travel time. From a ground control point of view, numerical analysis (Peng and Chiang, 1984, p. 127) showed a slight advantage placing the larger pillar on the head side. However, in practice, the difference between the two types of pillar arrangements is insignificant, depending very much on their size differential and geological condition, for longwall mining, the overwhelming requirement for gateraod development is faster speed, not production.

For bump-prone, or deep, or highly gassy coal seams, the 4-entry system must be used in order to provide sufficient fresh air to the longwall face to meet the minimum required by law (Ray, 1987), or avoid safety hazards. Figure 7.2.2 shows the evolutionary change in gateroad arrangement for a bump-prone longwall mine in central Appalachia (Gauna et al., 1988). A and B had similar three-row equal-sized chain pillars, except that B had larger pillars than A. Thus from A to B, it represents the process of searching for a proper dimension of chain pillars

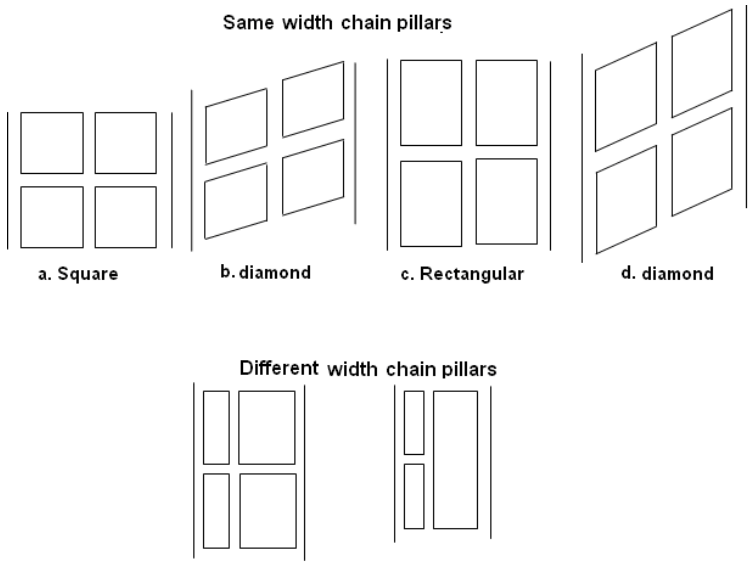


**Fig. 7.2.1 Types of pillar arrangement in 3-entry system**

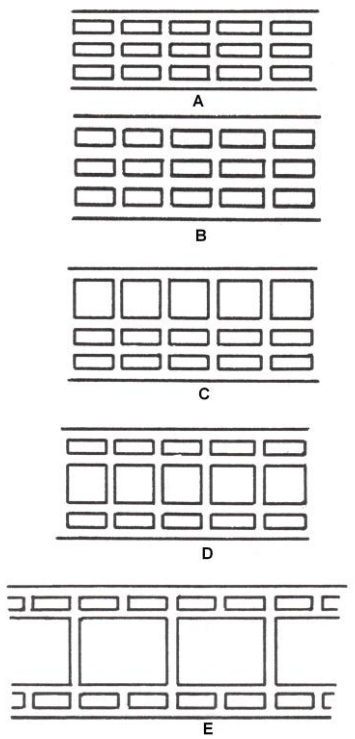


**Fig. 7.2.2 An example of evolution of 4-entry pillar system (Gauna et al., 1988)**

The evolution and adoption of the 2-entry yield pillar system for western bump prone longwall mines is discussed in Section 9.5.1 (p. 447) (Koehler, 1994).

## 7.3 OVERBURDEN MOVEMENT

### 7.3.1 Introduction

When a longwall panel of sufficient width and length is excavated, the overburden roof strata are disturbed in order of severity from the immediate roof toward the surface. Various methods, including physical modeling (Gaskell et al., 1988), time domain reflectometry (TDR) (Maleki et al, 1988; Su and Hasenfus, 1987; Wade and Conroy, 1980), multi-position borehole extensometer (Ingram et al., 1994; Khair et al., 1987a; Listak et al., 1986; Makusha, 2004), bullet perforation (Dahl and von Schonfeldt, 1976), and microseismic (X. Luo et al., 1998) had been used to measure overburden strata movement due to full extraction mining. In general, strata movement response to full extraction mining depends strongly on the location and thickness of the strong strata and mining geometry (mining height and panel width). For convenience of discussion, strata movement can be generalized as follows.

Figure 7.3.1 shows the four zones of disturbance in the overburden strata in response to the longwall mining below (Peng, 1992). The **caved zone,** which is the immediate roof before it caves, ranges in thickness from two to ten times the mining height. In this zone, the strata fall on the mine floor and, in the process, are broken into irregular but platy shapes of various sizes. They are crowded in a random manner. Thus, the rock volume in its broken state is considerably larger than that of the original intact strata. The volume ratio of broken strata to its original intact strata is called the **expansion ratio** or **bulking factor**. Expansion ratio is a very important factor because it determines the height of the caved zone. This is illustrated in Section 7.3.2 (p. 324). There are various estimates of expansion ratios for various rock types.

Above the caved zone is the **fractured zone**. In this zone, the strata are broken into blocks by vertical and/or subvertical fractures and horizontal cracks due to bed separation. The adjacent blocks in each broken stratum still maintain contact either fully or partially across the vertical or subvertical fractures. Thus, there is a horizontal force that is transmitted through and remains in these strata. With this horizontal force, the individual blocks in these broken strata cannot move freely without affecting the movements of the adjacent blocks. These broken strata are called the force-transmitting beams. The thickness of the fractured zone ranges from 28 to 52 times the mining height (or its upper limit is 30 to 60 times the mining height above the roofline). The combined thickness of the caved and fractured zones ranges from 30 to 60 times the mining height (Dahl and Von Schonfeldt, 1976; Jiang and Wells, 1998).

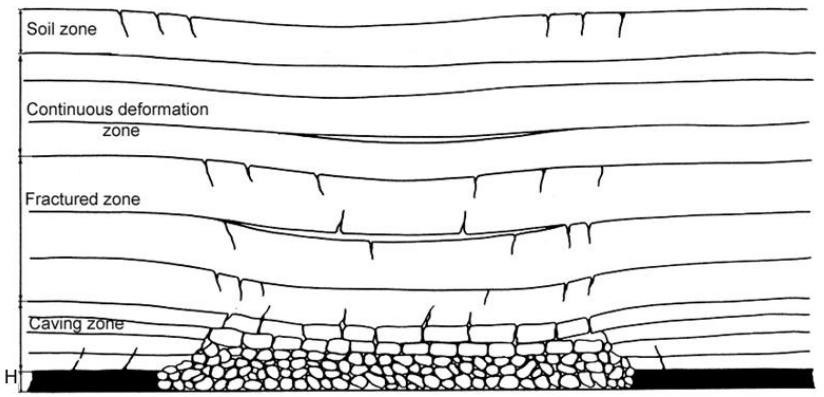


**Fig. 7. 3. 1 Overburden movement resulting from longwall mining (Peng, 1992)**

Between the fractured zone and the surface is the continuous deformation zone. In this zone, the strata deform gently without causing any major cracks that extend long enough to cut through the thickness of the strata, as in the fractured zone. Therefore, the strata behave essentially like a continuous or intact medium.

On the surface, there is a soil zone of varying depth depending on the location. In this zone, cracks open and close as the longwall face comes and goes. In general, cracks on and near the panel edges tend to remain open permanently, whereas those in and around the center of the panel will close back up when the longwall face has passed by. Cracks vary from less than one to 3-4 ft (0.3 to 0.91-1.22 m) wide and from less than 1 ft (0.3 m) deep to as deep as the soil zone.

In Figure 7.3.2, there are five zones of overburden strata movement based mainly on groundwater effect (Kendorski, 2006): the caved zone is in the zone of complete disruption; the fractured zone is vertically transmissive fractures; the dilated zone has increased storativity with little or no vertical transmissivity; the constrained zone has no significant effect on transmissivity or storativity; and the surface fracture zone potentially has vertically-transmissive surface cracks and disruptions (Kendorski, 1993). The dilated zone consists of two zones, a lower dilated zone and an upper aquiclude zone. The dilated zone has increased storage potential and can impact well observation, but it has no direct connection to the lower strata. The upper aquiclude zone is unaffected by mining and has no change in permeability.

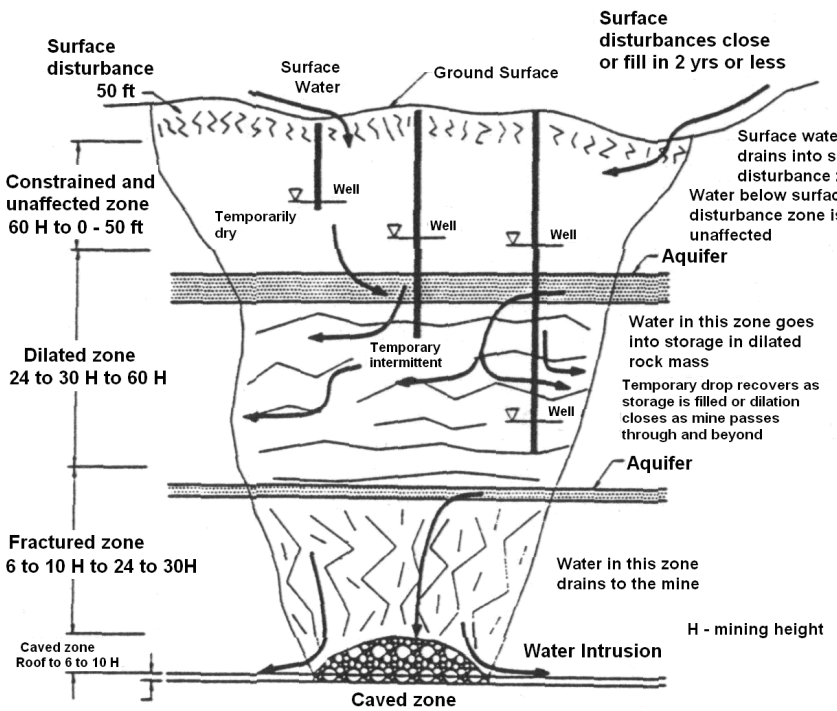


**Fig. 7.3.2 Overburden movement resulting from longwall mining (modified from Kendorski, 2006)**

Movement of the different zones has different degrees of effect on roof control at the longwall face. The effect decreases as the strata are located farther upward from the roof line. Those strata, the movement of which will affect roof control at the longwall faces, can be

classified into two types, immediate and main roofs. The ***immediate roof*** is that portion of the overburden strata lying immediately above the coal seam top, approximately two to ten times that of the mining height (Fig. 7.3.3). Above the immediate roof, the strata in the lower portion of the fractured zone are called the ***main roof***. The definition of immediate and main roofs, in this case, refers to their location with respect to the coal seam top or roof line, as generally perceived. Everything being equal, their severity of impact on roof control at the longwall face is proportional to their distance from the coal seam top or roof line.

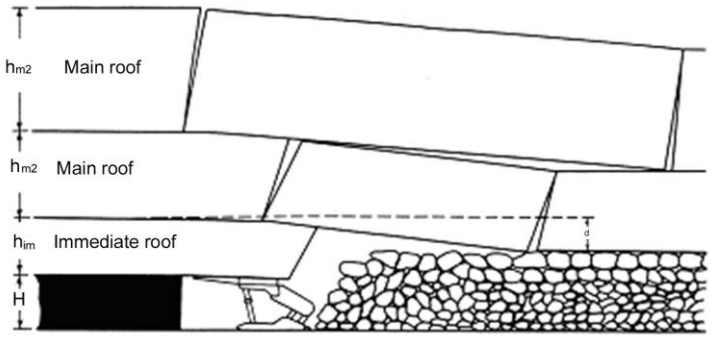


**Fig. 7.3.3 Immediate and main roofs (Peng, 2006)**

### 7.3.2 Immediate Roof

If the strata in the immediate roof will cave and fall in the gob following the advance of shield supports, and after having fallen, they are broken up and cannot transmit the horizontal force along the direction of mining, the shield support needs only to support that portion of the weight of the roof strata covered by the shield canopy area as soon as they are undermined. Conversely, if the strata in the immediate roof will not cave and fall in the gob following the advance of shield support, the rock weight that needs to be supported by the shield support covers not only the canopy area but also the overhung portion of the strata. Therefore, the immediate roof is the key to roof control at the longwall face. Its rock type and thickness or density of lamination and bonding strength in the immediate roof are the major factors governing the selection of shield capacity and various roof control techniques.

#### 1. Classification and Cavability of the Immediate Roof

There are many ways of classifying the roof for the purpose of powered support evaluation for longwall mining (Kidybinski, 1977). From the production point of view, the immediate roof can be divided into three groups, that is, unstable, medium stable, and stable (Peng and Chiang, 1982).

**A. Unstable immediate roof (Fig. 7.3.4). An unstable roof has the following features:**

(1) It consists of clay, clay shale, soft carbonaceous shale, slickensided shale, and well-jointed or fractured sandy shale.
(2) Right after the shearer's cutting, if the support is not advanced immediately, the unsupported roof between the faceline and the canopy tip will fall in a short period of time (less than 10 minutes). Head coal may be required to stabilize the roof.
(3) The roof in the gob caves immediately after support advance, i.e., there is no overhang. The caved fragments are small and the gob is well-compacted.

(4) Since the canopy length is generally three to five times the drum cutting width (or web), the roof, before its passage over the rear edge of the shield supports and onto the floor of the gob, is subjected to cyclic loading and unloading by the shield supports three to five times. This loading and unloading tends to break the roof, induce cavities, and move the caving line forward, resulting in the loading at the front half of the canopy being larger than at the latter half (Fig. 7.3.4).

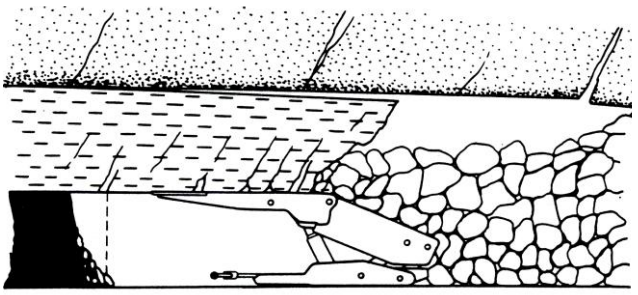

**Fig. 7.3.4 Unstable immediate roof (Peng, 2006)**

**B. Medium stable immediate roof (Fig.7.3.5). A medium stable roof has the following features:**

(1) It consists of hard or firm shale, sandy shale, and weak sandstone (e.g., fossilized or laminated sandstone). Joints and fractures are not well defined.

(2) Under normal conditions, the exposed roof area and time duration without roof fall allow coal cutting in a single direction, that is, shields are not advanced during the shearer's cutting trip. Instead they are advanced during the return trip.

(3) Generally, the roof caves in either immediately or shortly after the shields have been advanced. The caved fragments are larger in size. The caving line is located near the rear edge of the canopy or sometimes extends a little bit into the gob (Fig. 7.3.5).

(4) Canopy loading is distributed more uniformly between the front and rear parts of the shield support.

(5) Cyclic loading and unloading by the shield support will also affect the roof stability if the shield is not advanced rapidly and continuously. If the face sloughs severely and the type of shield selected is not suitable, an inherently medium stable roof may become an unstable one.

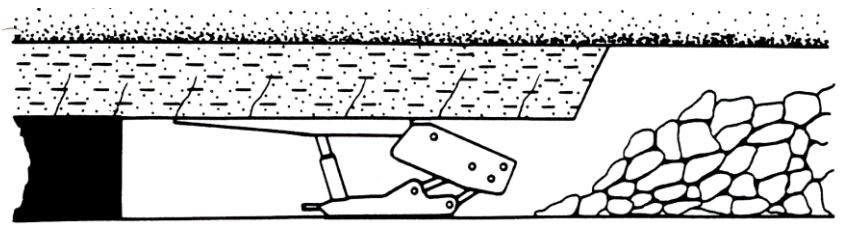

**Fig. 7. 3.5 Medium stable immediate roof (Peng, 2006)**

**C. Stable immediate roof. There are three cases of stable immediate roof:**

(1) The immediate roof is sandy shale or sandstone, which is thick and strong. It can be left unsupported for more than five to eight hours and still remain intact. Cyclic

loading and unloading by the shield support does not affect it. The resultant force acts toward the rear edge of the canopy. The roof cantilevers into the gob, and the roof in the gob falls periodically in large pieces. But if they fall near the rear end of the powered support, the impact force might affect the stability of the powered support, especially if the chock support type is used.

(2) The immediate roof is hard sandstone or conglomerate, which is very strong and massive. The roof will not only overhang in a large area, sometimes reaching 70,000-80,000 $ft^2$ (6,503-7,432 $m^2$) (Zhu et al., 1991; Jin and Sheng, 1992), but also will remain overhung for a long period of time (Fig. 7.3.6). During the non-weighting period, heavy roof pressure may not be obvious. But, once the periodic weighting period arrives, the roof over the gob acts vigorously en masse and produces an extremely large impact loading whenever caving occurs. Such impact loading occurs in a very short time and requires a very large capacity yield valve to relieve the pressure instantaneously. In addition, the sudden caving of a very large area generates a stormy wind (or wind blast) in the face area, damaging equipment and causing fatalities. The induced strong shock waves may be felt miles away. For this type of roof, it is necessary to perform properly induced caving, in terms of both time and operation.

(3) The immediate roof is hard limestone or sandstone or firm sandy shale and thicker than the mining height. Joints and fractures are well-developed and become the weak planes along which the rock breaks. As the face advances, it gradually sags and breaks in blocks. Further sagging causes the blocks to form a semi-arch with the gob end eventually rested on the gob floor. Thus, during the non-weighting period, the roof pressure may not be obvious. But as the width of the semi-arch grows, it will break at sufficient length, creating periodic weighting if certain conditions are satisfied. But in general, this type of roof strata does not cause roof stability problems.

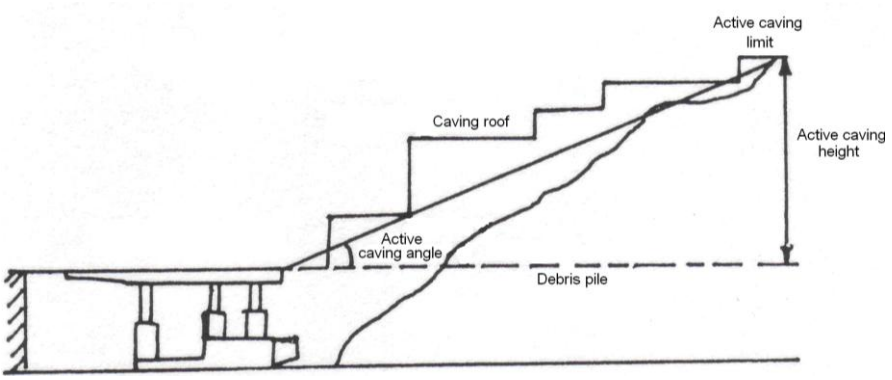


**A**

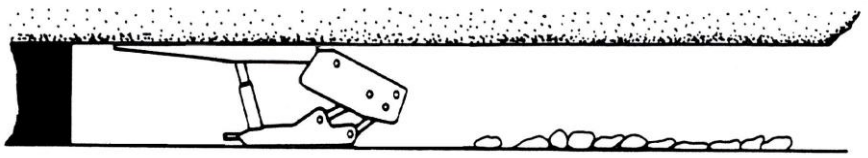

**B**

**Fig. 7.3.6 Stable immediate roof: A, from Sarkar (1998) and B, from Peng (2006)**

Both operational experience and research results have demonstrated that roof stability is relative. For an unstable roof, certain techniques are required to control and change the factors contributing to the unstable conditions and to upgrade its stability. For a medium stable roof, a powered support, properly selected and applied, is required to maintain roof stability. Very often a medium stable roof becomes an unstable one due to periodic weighting, poor roof conditions, or improperly selected powered supports. For the stable roof, with the exception of the gradually sagging one, its stability must be destroyed periodically and systematically by artificial means to avoid a sudden large area caving.

**2. Caving Height or Thickness of the Immediate Roof**

The thickness of the immediate roof is the basis for designing roof control techniques. The immediate roof is not necessarily the same throughout for a coal seam. Rather, it varies with stratigraphic sequence and method of mining.

Normally, caving initiates from the lowest strata in the immediate roof and propagates upward into the fractured zone. The process of caving in each stratum is that the stratum sags downward as soon as it is undermined. When the downward sagging of the stratum exceeds the maximum allowable limit, it breaks and falls. As it falls, its volume increases; therefore, the gap between the top of the rock piles and the sagged but un-caved stratum continues to decrease as the caving propagates upward. When the gap vanishes (i.e., the overlying strata have received the support of the caved rock piles), the caving stops. Thus the height of caving must satisfy the following condition (Fig. 7.3.3)

$$H - d = h_{im}(K - 1) \tag{7.3.1}$$

and $$d \le d_0 \tag{7.3.2}$$

where $H$ = mining height, $d$ = sagging of the lowest un-caved strata, $d_0$ = maximum allowable sagging (without breaking) of the lowest un-caved strata, $h_{im}$ = thickness of the immediate roof or caving height, and $K$ = bulking factor of the immediate roof.

From Eq. 7.3.1, the caving height can be determined by:

$$h_{im} = (H - d)/(K - 1) \tag{7.3.3}$$

It must be noted that $d$ and $K$ must be determined at the same location. The ideal place is within the area beginning from the point when the sagging but un-caved stratum first makes contact with the rock piles to the point when the rock piles have been compressed to the final stage.

From Eq. 7.3.3, it can be seen that there are several factors that affect the caving height:

A. *Mining height, H.* Based on Eq. 7.3.3, the caving height is proportional to the mining height. This relation can be used to control the caving height. But it must be noted that the caving height will not change immediately or continuously as soon as the mining height is changed. Rather, the caving height probably changes in leap steps in response to a sudden change in mining height.

B. *Maximum allowable sagging of the un-caved strata, $d_0$.* Based on Eq. 7.3.3, $d \le d_0$ has a profound effect on the height of caving. For instance, if $d = d_0 = H$, then $h_{im} = 0$, which means no caving; that is, the roof sags gradually until it touches the floor. On the other hand, if $d = d_0 = 0$, Eq. 7.3.3 becomes

$$h_{im} = H/(K-1) \tag{7.3.4}$$

Equation 7.3.4 assumes that the strata break and fall without any sagging. In this case, it predicts the largest caving height.

C. *Bulking factor, K.* **Bulking factor** is defined as the ratio of the volume of the broken rock strata to the original volume of the same strata before they are broken and cave. Since the volume of the broken strata is always larger than that of the original intact strata, bulking factor is usually larger than one.

The bulking factor varies with rock type, shape, and size of the caved rock fragments, the ways in which the caved rock fragments are piled up, and the pressure imposed on the rock fragments.

Peng (1980a) measured the volumes of underground roof fall cavities in the entries developed in the Pittsburgh seam and compared them with the volumes of the rock fragments piled up on the floor. He found that the bulking factor for the roof shale ranges from 1.25 to 1.30 with an average of 1.28. However, measurements using surface borehole multi-position extensometers, the bulking factor was determined to be 1.10-1.16 (Khair et al., 1987a) and 1.23-1.72 (Listak et al., 1986).

D. *Methods of roof control in the gob area.* Different techniques for controlling roof caving in the gob area can change the height of caving. For instance, if the gob is backfilled with waste rocks or tailing sands, the same effect is achieved as reducing the mining height. Thus Eq. 7.3.3 becomes

$$h_{im} = \frac{(H - h_f) - d}{K - 1} \tag{7.3.5}$$

where $h_f$ is the height of backfilling material and $K$ is the bulking factor of the immediate roof. Obviously, when the waste materials are backfilled to full mining height, i.e., when $H = h_f$, $h_{im} = 0$, there will be no caving.

However, it is interesting to note that through surface subsidence measurements, Das (1997) found that immediately behind the face, the bulk volume fills up around 45-60% of the total caving height and therefore, the bulking does not control caving.

### 7.3.3 Main Roof

Above the immediate roof, the strata in the lower portion of the fractured zone are called the ***main roof***. The main roof generally refers to the strata located in the lower portion of the fractured zone that are broken but un-caved and can still transmit horizontal forces, although the rear end of the strata is generally lower than the front end. Note the rear end of the strata is in the gob area, while the front end is located above the shield support and the immediate roof. The main roof may either be one or more layers depending on the stratigraphic characteristics and the gap of strata separation in that area. Its movements will greatly affect the stability of the immediate roof and, thus, the supports in the face area. Above the main roof, the strata movements are too far away to have a significant impact on the face area. The main roof generally breaks periodically along the direction of face advance and imposes periodic roof weightings on the face area.

The location and thickness of the main roof can be determined by examining the stratigraphic columns above the coal seam. The method involves the determination of number,

location, and thickness of the force-transmitting strata beams in the fractured zone. The guidelines are:

1 Strata separation will occur along the bedding planes, laminations, and weak layers because these are the weakest planes other than open fractures.
2 Strata separation and downward sagging occur first at the lowest stratum in the fractured zone and propagate upward.
3 The delay time for separation and downward sagging between adjacent strata depends primarily on the thickness and strength of the strata. If the upper strata are strong and thick, their movement is delayed far behind that of the lower strata. Conversely, if the upper strata are weak and thin, they will move simultaneously with the lower strata.

Therefore, by examining the stratigraphic column of the coal seam proposed for longwall mining, the caving characteristics of the overlying strata can be estimated. Fig. 7.3.7 shows an actual case study in the Lower Kittanning seam. The immediate roof is gray shale, 2 ft (0.61 m) thick. The main roof consists of two force-transmitting strata beams. The lower one is the 18-ft (5-m) thick sandstone plus the coal partings immediately above it, while the upper one is the 80-ft (24-m) thick gray shale plus the coal partings above it. The sandstone stratum above the 80-ft (24-m) thick gray shale is broken but retained to form a force-transmitting strata beam. However, it is so far from the immediate roof that its movement will not cause any significant effect on the movement of the immediate roof at the face area.

Sometimes the lower portion of the main roof is easily mistaken for the immediate roof, especially when the immediate roof is rather thick and strong. The best criterion to differentiate one from the other is whether or not it has the features of the periodic breakage and produces the periodic weighting pressure in the face area.

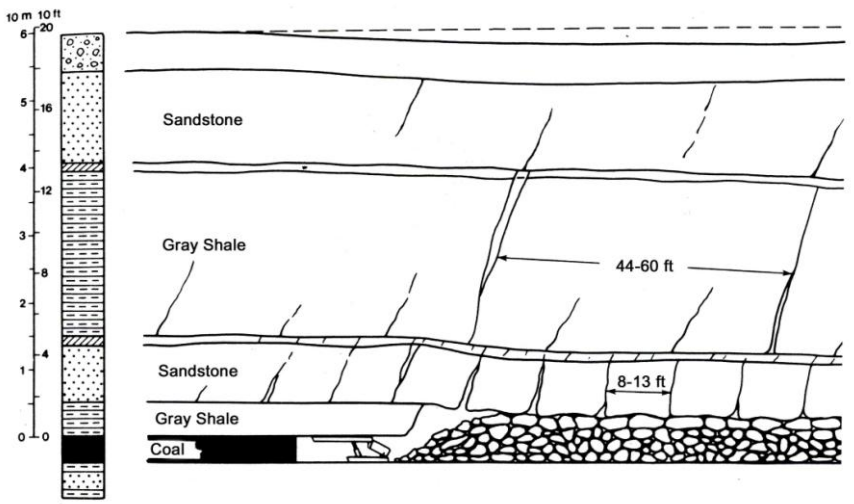


**Fig. 7.3.7 Immediate and main roof behavior in the Lower Kittanning seam (Peng, 2006)**

### 7.3.4 Sequences of Overburden Movements in a Longwall Panel

As longwall mining moves along the direction of mining in a longwall panel, there are two distinctive phases of overburden movements. The first phase of movement includes the distance from the setup entry to the point when the main roof first begins to break or, if the immediate roof does not cave right after support advance, the final stage of an interval that begins with a

large-area caving of the immediate roof and lasts until the complete breakage of the upper strata in the main roof. During such interval, the maximum roof pressure measured at the face area is called the ***first weighting*** (Fig. 7.3.8). However, if additional pressures due to the breakage of the main roof strata are not significant, the first weighting refers to the roof pressure immediately before and during the large-area caving of the immediate roof. The distance from the setup entry to the first weighting is defined as the ***first weighting interval, $L_0$***.

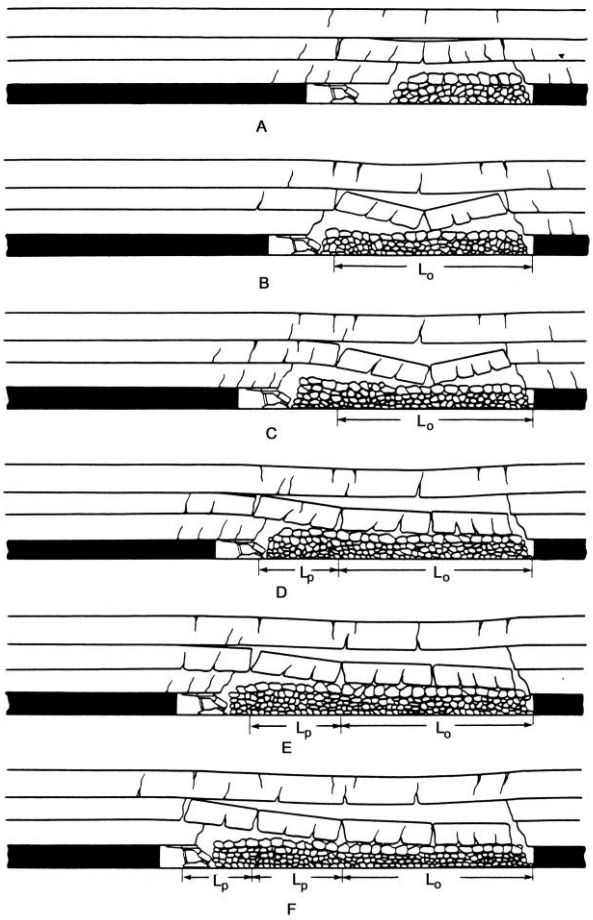


**Fig. 7.3.8 Idealized sequence of roof caving illustrating first caving and periodic caving (Peng, 2006)**

The second phase begins right after the first weighting and extends to the completion of the panel mining. During this period the roof pressure at the face area increases and decreases cyclically due to the cyclical breakage of the immediate roof or the main roof or both. This phenomenon is called the ***periodic roof weighting*** (Fig. 7.3.8). The maximum pressure occurring in each period is the ***periodic roof weighting pressure***, and the distance between two consecutive roof weightings is called the ***periodic roof weighting interval, $L_p$***. The severity of the first and periodic weighting depends very much on mining and geological conditions.

When the immediate roof is weak and thick, the first and second phases may not show significant difference. But, in general, the first weighting pressure and interval are larger than

the periodic roof weighting pressure and interval, unless the roof stratigraphic sequence changes to thicker and harder roof well inside the panel. For the stable roof, i.e., strong and hard-to-cave roof strata, if the powered supports are not properly selected, the first weighting is generally so severe that collapse of either a part of or the whole face may occur (Hsiung and Peng, 1985b).

**1. First Weighting**

Before longwall mining begins in a panel a set-up room of approximately 20-24 ft (6.1-7.3 m) wide is driven across the face at the starting end (or bleeder side) of the panel. The face equipment, including shield supports, shearer or plow, and chain conveyor, is installed in the setup room. In the initial period, as the mining proceeds, the roof remains intact and the gob is left open. As the width of the gob widens, the immediate roof begins to bend and sag. Eventually, it separates from the main roof along their bedding plane of contact when the gob span increases further. At this time, the immediate roof behaves like a fixed-end beam (or more exactly a thin plate anchored firmly at four edges); cracks begin to form on the upper surface at both ends of the beam. The cracks rapidly propagate through the thickness of the beam. As this happens, the beam becomes a simple-ended one. The location of the maximum axial tensile stress immediately switches to the lower surface at the mid span where the crack initiates and propagates through the thickness. After this, the immediate roof splits into two sections, both of which lose support and fall. In the falling process, they rotate and break into different sizes and shapes upon hitting the floor (Fig. 7.3.8A).

As the face moves farther toward the first weighting interval, $L_0$, the lower stratum in the main roof also separates from the upper one. Cracks form at both ends and the beam sags further until the mid span touches the top of the rock piles resulting from the caving of the immediate roof (Fig. 7.3.8B). The roof pressure reaches the maximum right before this happens. This is the ***first weighting***. As the face moves beyond $L_0$, the cracks in the front section of the main roof beam cut through the thickness causing the beam to break away. As this happens, the roof pressure drops suddenly and the overburden movements enter into the second phase.

The first weighting interval can be estimated by:

For the immediate roof

$$L_{oim} = \sqrt{\frac{2h_{im}T_{im}}{\gamma_{im}}} \tag{7.3.6}$$

For the main roof

$$L_{om} = \sqrt{\frac{2h_{m}T_{m}}{\gamma_{m}}} \tag{7.3.7}$$

where $L_{oim}$ and $L_{om}$ are first weighting interval for the immediate roof and main roof, respectively, $h_{im}$ and $h_m$ are thickness of the immediate roof and main roof, respectively, $T_{im}$ and $T_m$ are tensile strength of the immediate roof and main roof, respectively, and $\gamma_{im}$ and $\gamma_m$ are weight per unit volume of the immediate roof and main roof, respectively.

The larger of the two values from Eq. 7.3.6 and Eq. 7.3.7 should be used. But, in general, $L_{om} > L_{oim,}$ as stated earlier.

For jointed strata, the caving span is (Singh and Dubey, 1994)

$$L_{oim} = F\sqrt{\frac{2ih_{im}T_{im}}{\gamma_{im}}} \tag{7.3.8}$$

where $F$ is orientation factor, $i = KR$ is weakness coefficient factor, $K$ is jointing factor, and $R$ is stratification factor.

**2. Periodic Weighting**

After the first roof weighting (A and B in Fig. 7.3.8), the longwall face enters into the second phase of the overburden movement (Fig. 7.3.8, C-F). In this phase, the immediate roof, depending on rock types, caves immediately or with a little delay behind the powered support. The lower stratum of the main roof breaks periodically causing periodic high roof pressure at the face area. The breaking length or interval, such as $L_{P1}$, $L_{P2}$, and so on, varies with the strength, thickness, and joint conditions of the strata and the gap between the caved rock piles and the un-caved immediate roof, while the intensity of the periodic roof weighting depends on the breaking interval. On top of this, the upper stratum also breaks periodically.

Periodic weighting is a common feature for longwall mining in coal seams in which the overlying strata contain strong units in the immediate and main roof. The thicker and closer these units are to the roof line, the more severe and intense the periodic weighting (MacDonald, 1997; Matsui and Shimada, 1997; Park et al., 1992; Peng and Cheng, 1997; Sanford et al., 1999; Xiao et al., 1991). Underground operational experience indicates that periodic weighting seems to become less intense or disappear as the large-capacity powered supports are used, and the faces advance faster in high-production faces.

**3. Time-Weighted Average Resistance or Pressure (TWAR or TWAP)**

In a shield support cycle, the leg pressure varies. The final resistance (or pressure) of the support in each cycle usually appears at the moment when the adjacent support is released for advance. It generally lasts less than one minute or less than 3 percent of each supporting cycle. Although there are many contributing factors, TWAR or TWAP represents the maximum possible roof loading experienced by the support.

Since the roof pressure usually varies continuously with time, the time-weighted average resistance is more appropriate to illustrate the overall conditions of the support in a whole cycle. The time-weighted average resistance, $P_t$, is defined by the following equation

$$P_t = \frac{\sum P_i t_i}{t_t} \tag{7.3.9}$$

where $P_i$ is the average support resistance during the period of $t_i$. In other words, $P_t$ is the ratio of the area under the pressure variation curve to the total time in a mining (supporting) cycle.

**4. Methods of Identifying or Predicting Periodic Roof Weighting**

There are three events in the variational characteristics of the resistances of the shield supports that can be used to identify/predict the periodic roof weighting.

*A. Significant increase of time-weighted average resistance.* Both the maximum resistance and **time-weighted average resistance** (TWAR) of a support cycle rise greatly during periodic roof weighting. Since the maximum support resistance occurs almost instantaneously only when the neighboring support is being advanced, it is less desirable for identifying or predicting the onset of periodic roof weighting. On the other hand, the variation pattern for the

time-weighted average resistance, which reflects resistance changes in a mining cycle, is more representative. Figure 7.3.9 shows the variations of TWAR as measured for the Pittsburgh seam (Peng et al., 1982) for a distance of 78 ft (24 m) face advance. The periodic weighting interval $L_{PI}$ = 14.7 ft (4.5 m) consists of two parts, that is

$$L_{PI} = a_1 + b_1 \tag{7.3.10}$$

where $a_1$ = 4.2 ft (1.3 m) is the distance duration in which periodic roof weighting occurs; and $b_1$ = 10.5 ft (3.2 m) is the duration of relative equilibrium during which the roof pressures are relatively low.

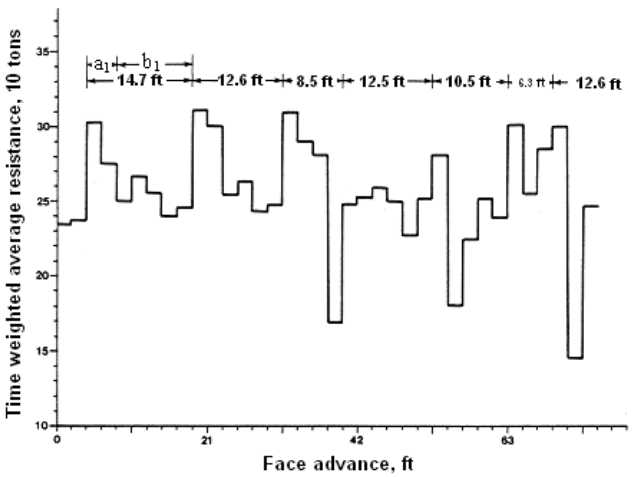


**Fig. 7.3.9 Variations of time-weighted-average-resistance (TWAR) measured in the Pittsburgh seam (Peng, 2006)**

The maximum TWAR occurring during periodic roof weighting is called maximum periodic weighting resistance, $P_{tm}$, which is related to the ***periodic weighting intensity factor, I,*** by

$$I = \frac{P_{tm}}{P_t} \tag{7.3.11}$$

where $P_t$ is the average TWAR during the non-periodic roof weighting period immediately preceding the periodic roof weighting where $P_{tm}$ is measured.

*B. High setting resistance or rapidly rising rate of resistance increase.* The rate of increase in support resistance after setting is one of the important markers in roof behavior. During the non-periodic weighting period, the rate of resistance increase generally increases gradually after setting but becomes much larger immediately preceding support advance. Conversely, during periodic roof weighting, the rate of resistance increase immediately before support advance is relatively low but increases significantly faster right after setting (Fig. 7.3.10). This feature indicates that the roof moves vigorously during periodic weighting and that immediately after setting, the supports rapidly receive the continuously increasing roof pressure. Therefore, the rate of resistance increase after support setting can be used to identify/predict the periodic roof weighting.

*C. Features of periodic roof weighting*. Two terms are most useful in describing the rules of changes in periodic roof weighting. One is the **periodic weighting interval, $L_p$,** which is the distance of face advance between two consecutive periodic weightings, and the other one is the time interval between them, **the periodic weighting period, $T_p$**.

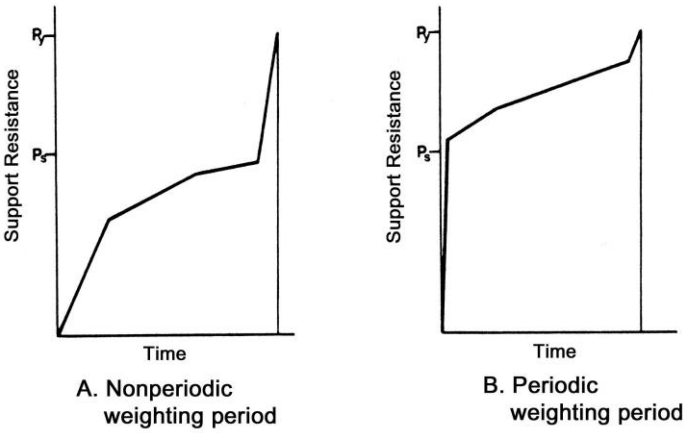


**Fig. 7.3.10 Example patterns of the rate of resistance increase during non-periodic and periodic roof weighting (Peng, 2006)**

The common feature concerning the main roof caving is that for every two to four smaller periodic roof weightings there is a larger periodic roof weighting. The smaller periodic roof weightings can be attributed to the deformation and caving of the lower portion of the main roof, and they last for one or two mining cycles. On the other hand, the severe movements from the upper portion of the main roof caused the larger periodic roof weightings, which last for three to seven mining cycles. Since there are differences in strata composition, and consequently strata behavior, the magnitude and characteristics of the roof weighting induced by the main roof are different from seam to seam or sometimes even from panel to panel in a coal seam.

The maximum periodic weighting resistance, $P_{tm}$ is affected by the periodic weighting interval, $L_p$.

$$P_{tm} = a + bL_p \tag{7.3.12}$$

where $a$ = 2.15-2.41 is a constant depending on the properties of the main roof strata and rock pile conditions in the gob, and $b$ = 4.5-17 is a constant related to the periodic weighting interval.

Equation 7.3.12 indicates that $P_{im}$ is linearly increased with an increase in $L_p$. This is only valid within a certain limit of $L_p$. The relation will change once $L_p$ exceeds this limit, due to the interaction between the fallen rock fragments and the broken main roof block, and the conditions in which gob piles exist.

On the other hand, the relation between the periodic weighting intensity factor, $I$, and $L_p$ is nonlinear,

$$I = \frac{L_p}{pL_p - q} \tag{7.3.13}$$

where $p$ = 0.80-0.87 and $q$ = 0.43-0.64 are constants related to overburden strata, rock piles in the gob, and the average TWAR during the non-weighting period. Equation 7.3.13 shows that within a certain limit $I$ decreases as $L_p$ increases, although the change is rather small.

Shield leg pressure data also show that in the 1980s, when powered support capacity was relatively low, periodic weighting was easily identifiable because it exhibited roof deterioration. But in the 1990s when shield capacity became larger and faces moved much faster, the intensity of periodic weighting was either reduced considerably or disappear.

### 7.3.5 Effects of Stratigraphic Sequences

It is well known that the stratigraphic sequence above a coal seam varies from seam to seam, mine to mine, panel to panel, and frequently even between different parts of the same panel. Differences in stratigraphic sequence will induce different degrees of overburden movement.

Numerous field studies in various coalfields in different parts of the world led to the conclusion that there are approximately five types of stratigraphic sequences (Fig. 7.3.11), each of which induces different types, and different degrees of severity, of strata movement, and thus, roof pressure at the longwall face area. Different intensities of roof pressure and roof activity require different methods of roof control. Therefore, analysis of the stratigraphic sequence and its changes within the reserves of interest is the prerequisite for shield support design.

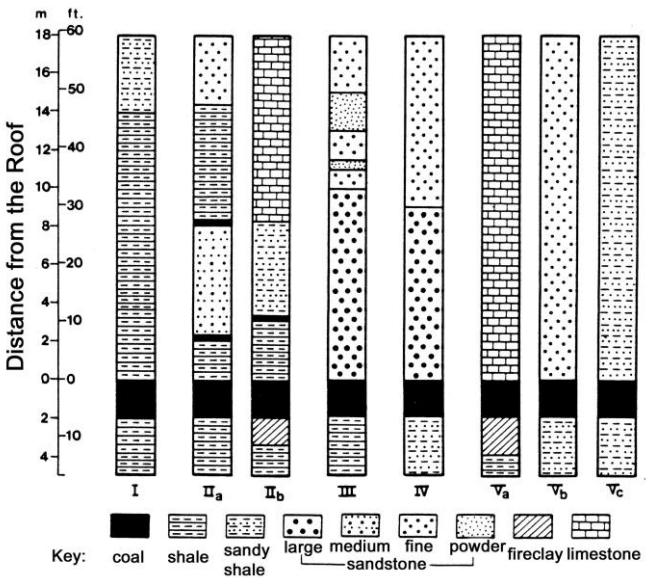


**Fig. 7.3.11 Five types of generalized stratigraphic sequence (Peng, 2006)**

#### 1. Type I Stratigraphic Sequence

In this type, the immediate roof is weak and very thick, usually more than four to five times the mining height (Fig. 7.3.4). Within this range, it may be a homogeneous shale or soft sandy shale with or without laminations, or it may be thin-layered shale interbedded with thin streaks of coals, clay band and sandstone, or it may be thinly laminated, coarse-grained sandstone due to preferred orientation of mica sheets or fossils.

This type of immediate roof caves immediately behind shield advance and fills up the whole gob space. Therefore, the main roof receives immediate support from the caved rock piles and maintains relative equilibrium all times. As a result, there will be no periodic roof weighting, or if any, a minor one that will not be identifiable without precise instrumentation.

Sometimes the immediate roof is not sufficiently thick, and the main roof, although hard and strong, is well jointed. Its sagging and resting on the gob piles will have little effect on the roof pressure at the face area.

**2. Type II Stratigraphic Sequence**

In this type, there is a weak immediate roof, but its thickness is less than four to five times the mining height (Fig. 7.3.5). Consequently, the caved rock piles from the immediate roof cannot fill up the gob space, leaving a large gap between the top of the caved rock piles and the lower un-caved strata in the main roof. Under such condition, the main roof, lacking support, will move actively, the severity of which depends on the stiffness of the strata, breaking periodically. This type of stratigraphic sequence will induce a clear periodic weighting. Fig. 7.3.12 shows an example of the roof strata caving sequence for Type II stratigraphic sequence (Peng and Park, 1977a and 1977b).

Alternatively, the shale/sandstone contact plane is considered the parting plane. The weak shale will separate from the overlying strong sandstone and cave.

**3. Type III Stratigraphic Sequence**

The immediate roof in this type is hard and strong, i.e., a strong roof stratum of medium thickness rests directly on the coal top (Fig. 7.3.6). It breaks only when it overhangs for a certain distance in the gob. Right before it breaks, the roof pressure at the face area is very high. Thus this type of stratigraphic sequence induces a clear and strong periodic weighting.

**4. Type IV Stratigraphic Sequence**

In this type, the immediate roof is not only very hard and strong, but also massive (i.e., homogenous and very thick) (Fig. 7.3.6). Conglomerates and thick, fine-grained sandstone are typical examples of this type (Mills et al., 2000; Xu, 1986). The roof tends to overhang in the gob for a very large area, sometimes up to more than 107,600 $ft^2$ (10,000 $m^2$) before it caves. When it caves, it is accompanied by strong and stormy winds that may further cause roof stability problems and safety hazards to the face crew. The shock waves may be felt as earthquake tremors miles away.

**5. Type V Stratigraphic Sequence**

In this type, the immediate roof is strong and thicker than the mining height. But, it is either well-jointed or not sufficiently stiff to overhang for a large distance. Thus, it can sag gradually until it touches on the floor in the gob and forms a semi-arch. The semi-arch will also break periodically. But it is usually not strong enough to be detected. This type of slow-sagging roof is more likely to occur in thinner coal seams.

In classifying the above-mentioned five types of stratigraphic sequences, only the roof strata are considered. However, it must be emphasized that floor rock property is also a critical factor for successful longwall mining. In high production faces, a strong, firm floor stratum is also required. In a soft floor, the shield base tends to sink into the floor. This causes difficulties for shield advance and slows down the speed of face advance. The degree of difficulty for

shield advance depends on the portion of the support base that sinks and its depth of sinking. The worst roof and floor strata combination is a soft floor in Type IV, III, and II roof stratigraphic sequences in descending order.

It must also be emphasized that the above-mentioned classification is based on strata strength and stiffness, not the commonly referred individual rock strength and stiffness. Shale as an individual rock is weaker than sandstone. But a very thick shale stratum is stiffer than a thin sandstone stratum, and thus, will overhang longer. Consequently, both strength and thickness (or spacing of laminations) of a rock stratum must be considered in the above-mentioned classification.

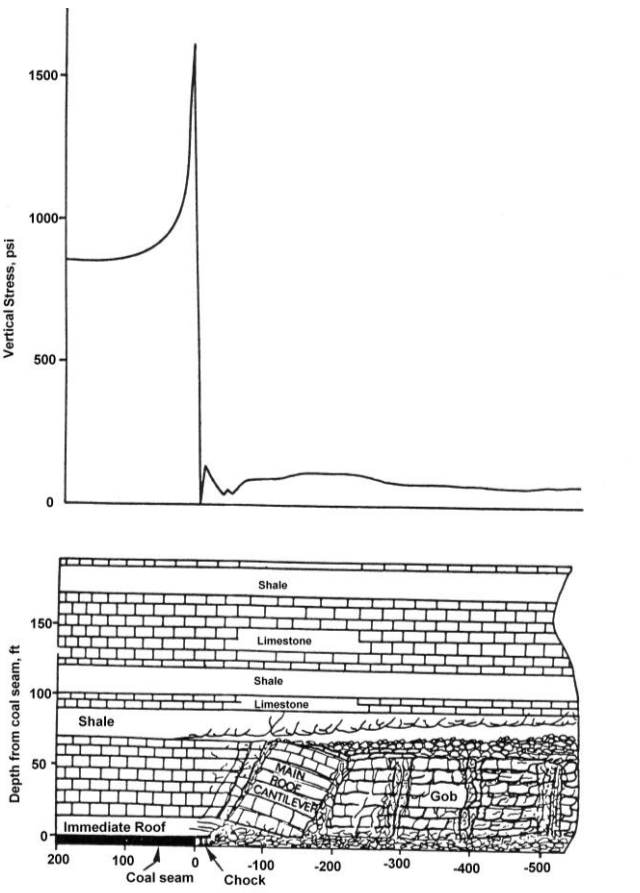


**Fig. 7.3.12 Example of type II strata caving sequence (Peng and Park, 1977a and 1977b)**

### 7.3.6 Effect of Time and Longwall Retreating Rate

It is well-known that laboratory experiments show that rocks exhibit time dependent behavior and that the stronger the rock is, the longer it lasts. This time-dependent behavior is more obvious in underground coal mines when in-situ strata are involved.

Extensive underground measurements of shield leg pressures in various longwall mines show that if a longwall stands idle over the weekend, the shield leg pressure will increases

quickly within the first 5-24 hours and become stabilized thereafter. Figure 7.3.13 shows an example of the shield load versus time curve during a weekend idle period that can be expressed by

$$\Delta p = 116.5(1 - e^{-0.72t}) + 1.39t \tag{7.3.14}$$

where $\Delta p$ is load increment of the shield support and $t$ is time. Equation 7.3.14 consists of two phases: In the first phase, $\Delta p$ increases rapidly with time. But the rate of pressure increase gradually decreases with time. In the second phase, the rate of pressure increase approaches a constant value and the leg pressure increases steadily, but slowly, with time.

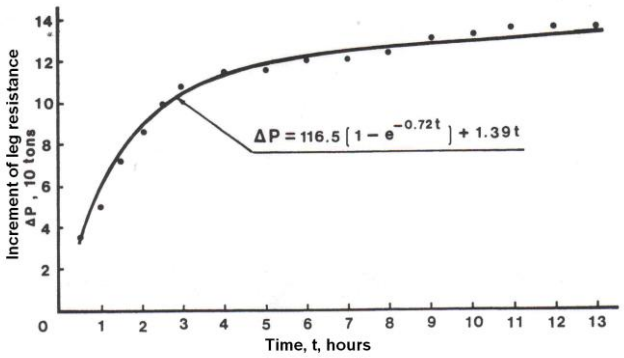


**Fig. 7.3.13 Leg pressure increment during idle period (YH Wang and Peng, 1986)**

## 7.4 ABUTMENT PRESSURES, GOB CAVING, AND GATEROAD CONVERGENCE

### 7.4.1 Computer Modeling

Conceptually, a softer coal seam is sandwiched between the relatively stronger roof and floor rocks and loaded by the weight of overburden. Stress is uniformly distributed in the coal seam under such conditions. When the panel gateroads are developed, the equilibrium conditions are destroyed due to the presence of openings. Stress distribution in the area has to be readjusted in order for a new state of equilibrium to be achieved. As a result, a de-stressed zone occurs in the roof of entries/crosscuts, and the load is transferred into the neighboring solid coal both in the panel and the pillars. As a result, zones of vertical pressure that exceed the average overburden pressure before mining are created in or near the edges of the panel and pillars. These zones are called the **abutments**, and the above-average pressures are the **abutment pressures**.

When longwall mining proceeds, abutment pressures will be formed around the edges of the gob and superimposed on those created during gateroad development. Figure 7.4.1A shows the vertical stress distribution in the coal seam from a three-dimensional, finite element modeling of multiple longwall panels using a three-entry gateroad system (Morsy and Peng, 2006).

The abutment pressure in front of the faceline is called the **front abutment pressure**; those along both sides of the panel in the gob area are the **side abutment pressures**. In the gob area, the maximum pressure realized is the overburden pressure, and thus, the existence of a rear abutment in the gob moving with the longwall face is unlikely except at the setup entry on the bleeder chain pillar side where a stationary abutment exists.

The front and side abutments intersect at the corners of the panel and superimpose on each other. In the coal seam, the location of the peak front abutment is located at the corners on both ends of the panel, whereas in the roof and floor it is located at the center of the panel (Fig. 7.4.1C). **Peak front abutment pressure** is the maximum value of the maximum front abutment pressures occurring in all cross-sections along the direction of mining. Both the front and side abutment pressures decrease exponentially away from the edges of the panel and return to the overburden pressure some distance away (C-C and R-R sections in Fig. 7.4.1B). Maximum side abutment pressure near the ribs of the headgate and tailgate begins to increase when the face is some distance inby. It increases continuously and reaches the maximum value when the face has passed. Thereafter it stabilizes, although in some cases yielding of pillars occurs (S-S section in Fig. 7.4.1B).

The vertical stress distributions in the roof and floor are quite similar (Fig. 7.4.1C), except the stress magnitude in the floor may be either smaller or larger, depending on the Young's modulus of the immediate roof.

When the roof rocks first cave in the gob, the weight of the caved fragments forms the gob pressure. As the caved fragments continue to pile up, so does the gob pressure. At some distance into the gob, the caved fragments start to take load from the upper strata. Fig. 7.4.1A shows a three-dimensional view of the gobs for two adjacent panels, one has been mined out and the other is being mined. Around the panel edges, the gob pressure is mainly due to the weight of the caved rock fragments. The gob pressure increases toward the center of the mined panel where the gob is more compacted. The maximum gob pressure is the overburden weight that occurs when the gob takes the full load of the overburden weight. Whether the gob pressure reaches the overburden weight or not, it depends highly on the panel width and the location and thickness of the self-supporting strata. If the panel is too narrow, the upper, unbroken strata will be bridged by the side abutments, resulting in gob pressure being more or less the weight of the rock fragments equivalent to the caving height.

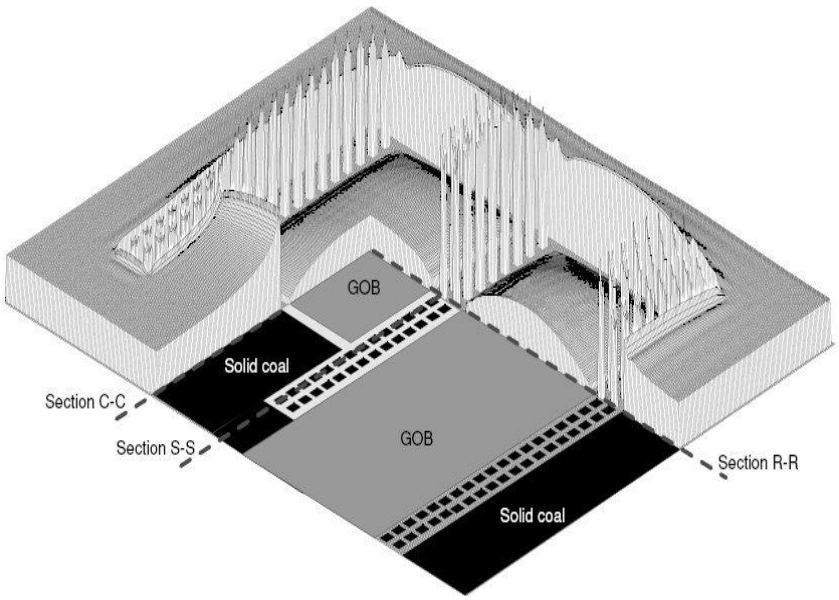


**Fig. 7.4.1A Three-dimensional view of vertical stress distribution in the coal seam (Morsy and Peng, 2006) (see enlarged color figure in Appendix 3)**

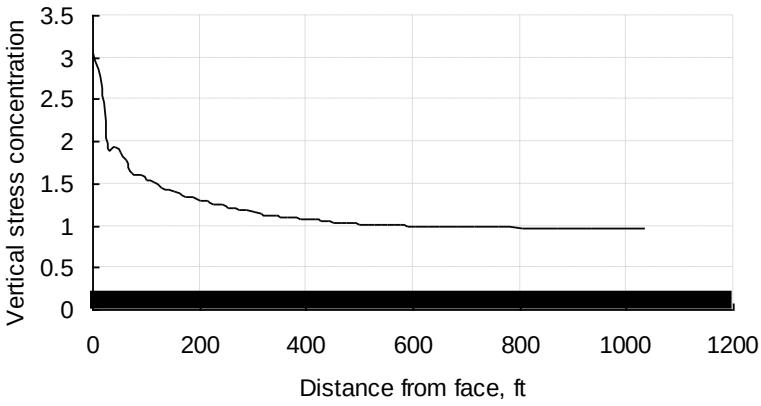


Section C-C

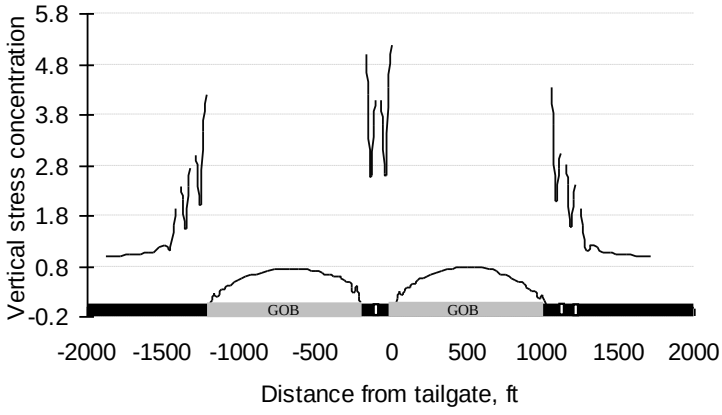


Section R-R

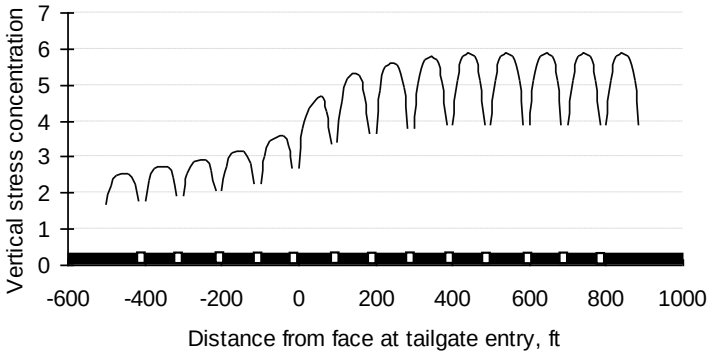


Section S-S

**Fig. 7.4.1B Vertical stress concentration at Sections C-C, R-R and S-S (Morsy and Peng, 2006)**

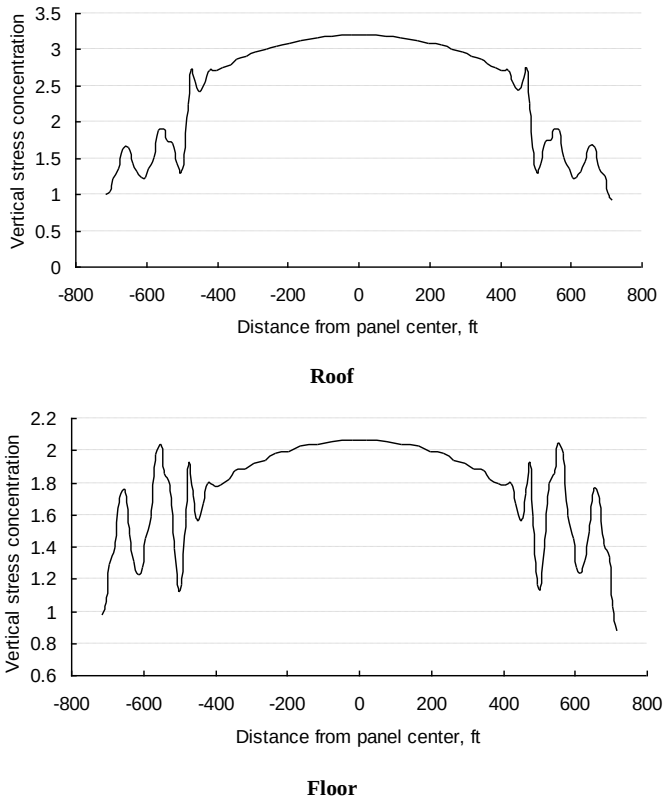


**Fig. 7.4.1C Vertical stress concentration in the immediate roof and floor (Morsy and Peng, 2006)**

### 7.4.2 Field Measurements

Since the mid-1970s, considerable underground instrumentation on pressure changes surrounding longwall panels have been performed. Peng and Chiang (1984, p. 54) summarized those studies performed prior to the mid-1980s. Those measurements covered the front and side abutment pressure distribution and gob pressure profiles. During this period, due to narrower panel and gateroad widths, abutment pressure measurements were able to cover the whole panel width. As panel width grew bigger in the late 1980s and 1990s, most stress measurements concentrated on side abutment pressures for gateroad chain pillar design purposes using mostly BPCs (Conover et al., 1989; Haramy and Kneisley, 1989; Koehler et al., 1989; Koehler et al., 1996; Larson et al., 1995; Payne and DeMarco, 1995; Rifenberg and Donato, 1993; Schuerger, 1985). Furthermore, many of those side abutment pressure measurements were designed to study the effect of horizontal stresses (Brasfield and Hendon, 1994; Matthews et al., 1992) using HI cells to measure the complete state of stress change. The results are summarized in the following sections.

#### 1. Abutment Pressure

#### A. Front abutment pressure

Depending on local conditions, the front abutment pressure in solid coal can first be detected at a distance of approximately 500 ft (152 m) outby the face. At this time, however, the pressure

is very small, but it begins to increase rapidly when the face approaches to within 100 ft (30 m). It reaches the maximum value (i.e., maximum front abutment pressure) when the face is 3-20 ft. (0.9-6.0 m) away. After that the pressure drops drastically and vanishes at the faceline (Fig.7.4.2).

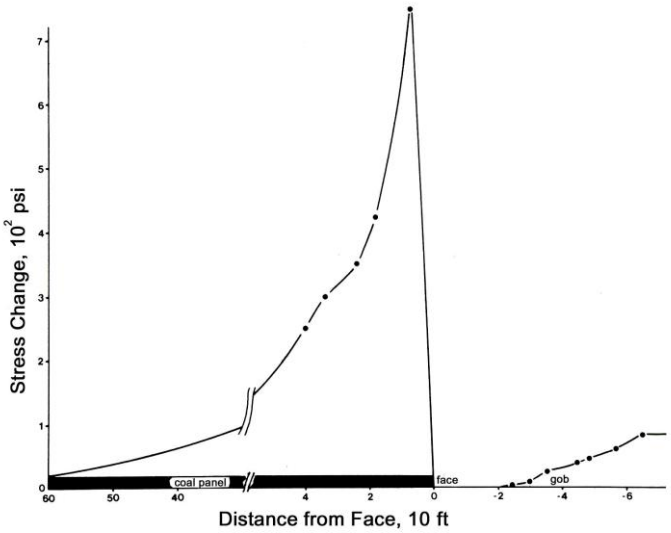


**Fig.7.4.2 An example of measured front abutment pressure in front of the longwall face (Peng and Park, 1977a)**

JS Chen et al., (2002) found that in western coal mines under a cover of 1,320 ft (402.4 m), the front and the side abutment pressures profiles can be divided into three zones in terms of pressure increment: initial influence zone, -650 to -350 ft (-198.1 to -106.7 m); obvious influence zone, -350 to -150 ft (-106.7 to -45.7 m); and significant influence zone, -150 to 0 ft (-106.7 to 0 ft) (Note that negative symbol means outby the face). However, Kneisley and Haramy, (1992) instrumented a virgin panel and found that there was no initial and obvious influence zone, the significant influence zone started at -100 ft (-30.5 m), that there was no yield zone at the face, and that the front abutment pressures between headgate and tailgate were similar. Cox (1994) found that for practical purposes, the front abutment extended ouby the face for a distance of about 230 ft (70 m).

The width of the front abutment depends not only on the overburden depth but also on the position along the face. It is not uniform across the panel width, being wider at both ends of the face and decreasing toward the center. The tailend is generally wider because of the effects of the adjacent mined-out panel.

The maximum front abutment pressure is not uniformly distributed, and the peak front abutment pressure occurs either at the corner or at the center, depending greatly on the physical properties of the roof rock (Peng and Chiang, 1984).

The **maximum front abutment pressure** is defined as the highest value in the front abutment profile and varies across the face width. The **peak front abutment pressure** is defined as the highest pressure in the maximum front abutment pressures found in all cross-sections. The peak front abutment pressure occurs usually at the corners (or T-junctions) of the panel when the immediate roof rock is weak. A weak immediate roof does not impose a strong weighting effect on the front abutment, because it caves immediately behind the shield

supports. The peak abutment pressure will remain at the corners as long as the weighting effects of the main roof do not come into play.

In general, the maximum front abutment pressure ranges from 0.2 to 6.4 $\sigma_0$ (where $\sigma_0$ is the average in-situ overburden pressure), depending on the geological conditions, face location with respect to periodic roof weighting and the setup entry, and adjacent mined-out areas. The front abutment pressure is smaller when the face is close to the bleeder pillars. If there is an adjacent mined-out panel, the maximum front abutment pressures are larger near that side. This is why in most cases the peak abutment pressure occurs at the tailgate T-junction.

The yield zone is the area between the faceline and the point where maximum front abutment pressure occurs. It is not uniform across the face width. The yield zone width ranges from 0.45 to 2.25 H (H is mining height) with the widest at the center of the panel. The yield zone is narrower when the face is near the bleeder pillars at the panel starting point. If the yield zone is wide, there will be more roof weight to be borne by the shield supports at the face.

**B. Side abutment pressure**

The side abutment pressure change is felt at the ribs of the headgate and tailgate at about the same time as the front abutment pressure. As the face advances farther, the side abutment gradually builds up as well as extends outward away from the ribs of the headgate and tailgate.

The side abutment pressure is largest at the ribs of the headgate and the tailgate and drops exponentially away from the active panel. The magnitudes of the side abutment pressure change for the first row of chain pillars range from 0.4 to 3.5 $\sigma_o$, depending on the location inside the pillar. For most cases, depending on the size of pillars with respect to seam depth, there is a pillar core where the pressure increase is smaller than all edges of the pillar.

Although it is possible that the side abutment pressure at the ribs reaches the maximum value before the face arrives, the side abutment pressure continues to extend outward from the active panel until the face has passed far beyond. It has been found that the side abutment (or the influenced zone) increases with the overburden depth such that (Peng and Chiang, 1984; JS Chen et al., 2002)

$$W_s = 9.3\sqrt{h} \tag{7.4.1}$$

where $W_s$ is the width of the side abutment (or influenced zone) in feet, and $h$ is the overburden depth in feet. No specific relations between the side abutment and panel width or seam thickness can be found. Because the zone of side abutment is limited, the chain pillar system can be properly designed such that the next panel is essentially undisturbed.

Depending on the total pillar width and the influenced zone of the side abutment, the stress change in the pillar, when the face of the second panel is passing by, may reach up to several times that of when the first panel is being mined. The magnitude due to second panel mining ranges from 1.6 to 10 $\sigma_0$ as compared to 0.4 to 3.5 $\sigma_0$ due to the first panel mining.

An example of using HI cell to measure the change of complete state of stress on side abutment pressure as the retreating face advances is shown in Fig.7.4.3 (Brasfield and Hendon, 1994). The influence of the retreating face was first seen in the No. 3 entry when the face was 328 ft (100 m) inby. Rapid stress changes began when the face was 164-196.8 ft (50-60 m) inby. At this time, the No. 3 entry saw overall stress reduction while No. 1 and 2 entries showed almost no change. When the face was 262.5-328 ft (80-100 m) outby, stress relief on the No. 3 entry side of the abutment pillar increased considerably, while the No. 1 and 2 entries

saw a very slight increase in vertical stress. At the final face position, the area around No. 3 entry and its adjacent yield pillar was completely de-stressed.

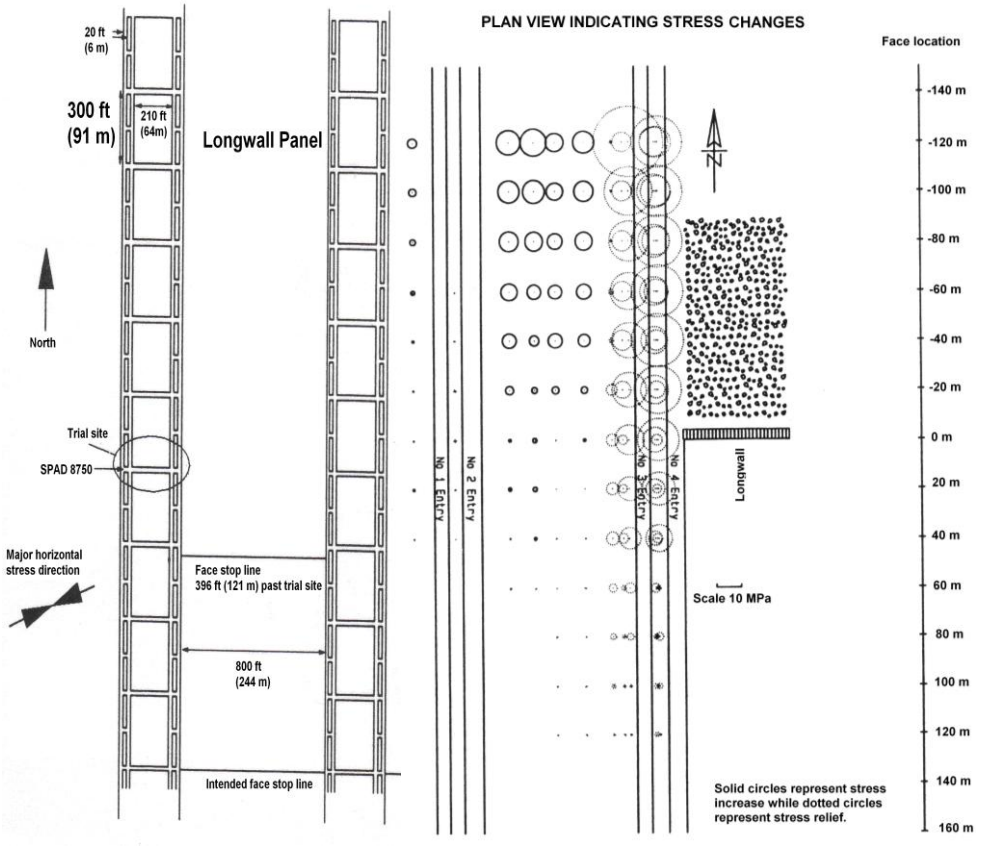


**Fig. 7.4.3 Stress changes in the gateroad chain pillars as the face advances (Brasfield and Hendon, 1994)**

## C. Gob caving and pressure

In full extraction mining with natural caving, such as longwall mining as practiced in U.S. coal mines, the nature of gob caving is a critical factor in mine design and production operations. The ideal condition is that the roof strata in the gob cave immediately or soon after shield advance so that the abutment pressures, especially the front abutment pressure, is greatly relieved. A small or insignificant front abutment pressure means stable roof conditions at the face for safe and efficient production. The reduction of front abutment pressure is proportional to not only the time after shield advance (or distance behind the shield), but also to the height of caving.

It is generally believed that when the gob is fully caved, the maximum pressure reached is the overburden pressure, i.e., restoration of the original pre-mining in-situ vertical pressure.

Several researchers conducted gob pressure measurements in the past three decades (Campoli et al., 1993; Haramy and Fejes, 1992; Maleki et al., 1984; Wade and Conroy, 1980; YH Wang and Peng, 1986). Gob caving may or may not be a continuing process and gob pressure build-up varies considerably from case to case; some show little increase (Haramy and Fejes, 1992), some show a stepwise increase until it approaches the overburden pressure

(YH Wang and Peng, 1986); and some show rapid increase; while others show slow increase (Wade and Conroy, 1980).

Figure 7.4.4 shows a case of gob pressure behavior at mid-panel for a panel 600 ft (182.9 m) wide and 430 ft (131 m) deep (YH Wang and Peng, 1986). The mining height was 5.5 ft (1.7 m). From A to B, the gob pressure increased from 0 to 112 psi (0-0.83 MPa), reflecting the immediate roof caving 10-12.5 ft (3-3.8 m) behind the shields. From B to C, pressure increased steadily at a small rate, indicating the immediate roof shale had fallen completely, but the main roof was cantilevering. From C to D, gob pressure increased from 138 to 400 psi (0.95-2.76 MPa), reflecting the breakage of the main roof cantilever beam. D was located 62.5 ft (16 m) behind the shield, which was the periodic caving interval of the main roof sandstone. The gob pressure reached the virgin stress around 115 ft (35.1 m) behind the shields.

Figure 7.4.5 shows the gob pressure history for a shortwall in the Pittsburgh seam where the panel was 150 ft (45.7 m) wide and 800 ft (243.8 m) deep with 5.25 ft (1.6 m) of mining height (Peng and Park, 1977a). The immediate roof was shale 12-15 ft (3.7-4.6 m) thick, overlaid by limestone 50-60 ft (15.2-18.3 m) thick. The pressure gage location was about 30 ft (9.1 m) from the panel edge. The vertical gob pressure became almost zero when the face passed the gage. The vertical gob pressure began to increase right behind the chock until it reached the peak stress of 820 psi at about 65 ft (19.8m).

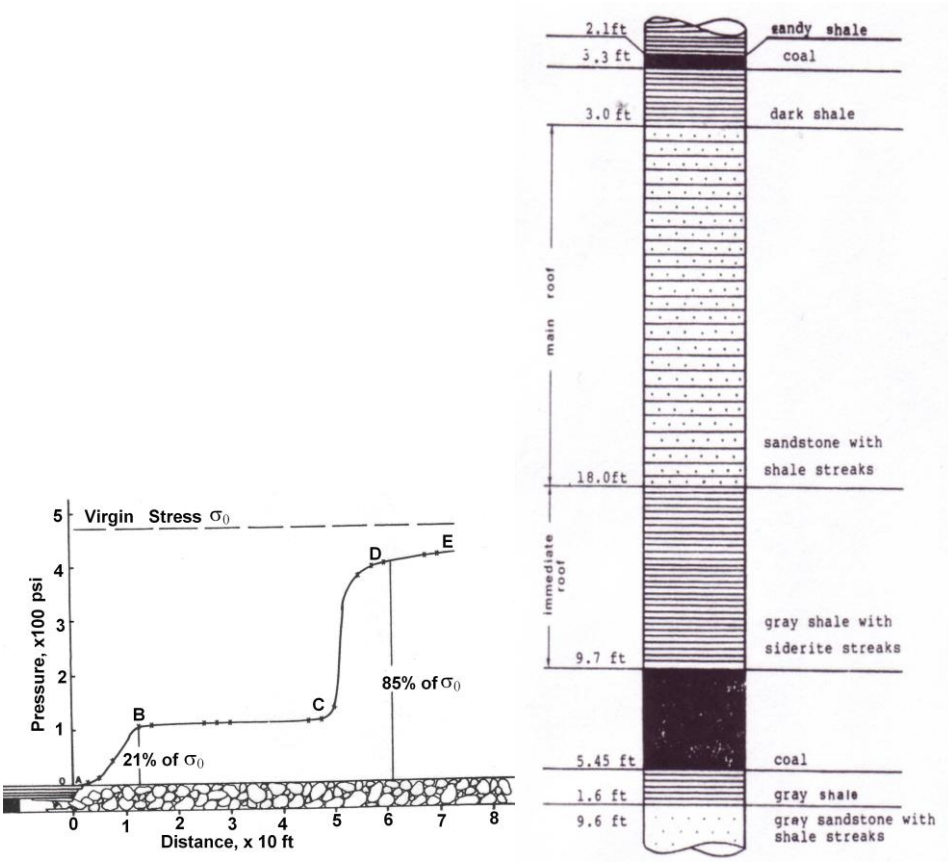


**Fig. 7.4.4 Profile of measured gob pressure at panel center (YH Wang and Peng, 1986)**

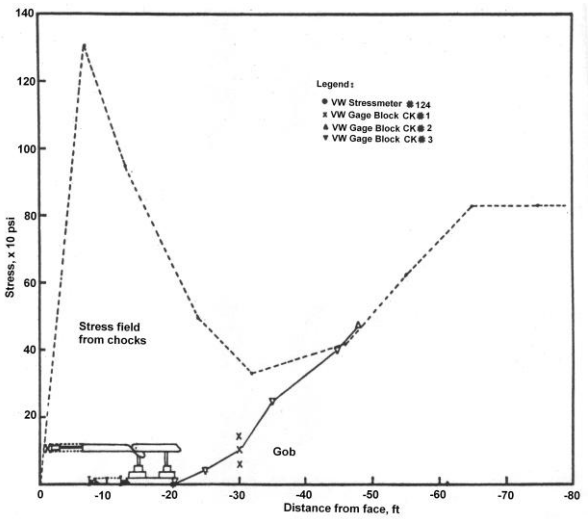


**Fig. 7.4.5 Profile of the measured gob pressure at panel edge (Peng and Park, 1977a)**

Figure 7.4.6 shows the gob pressure profiles for 9 gages located across a 600 ft (183 m) wide and 2,250 ft (685.8 m) deep longwall panel (Campoli et al., 1993). The floor pressure started about 500 ft (152.4 m) outby and reached peak stress around 20 ft (6.2 m) outby the face. The peak stress increased from panel edge to panel center. Floor stress vanished at the face area and began to increase right after the passage of shields. The rate of increase of the floor stress in the gob varied with location. In general, the rate of increase is small (or it even decreased) near the panel edge. The rate increased toward the panel center. The floor stress recovered to the virgin stress at about 400 ft (122 m) (0.2 times the overburden thickness) behind the face.

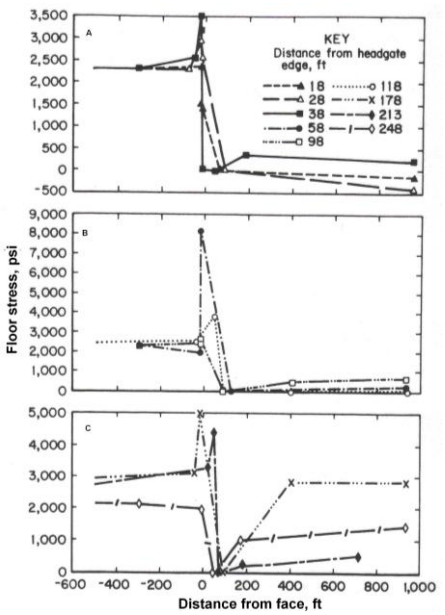


**Fig. 7.4.6 Floor pressure history across a longwall panel (Campoli et al., 1993)**

Figure 7.4.7 is the gob pressure profile at the mid-panel of a room-and-pillar panel with pillar extraction (Maleki et al., 1984). The panel was 1,804 ft (550 m) wide. The gob pressure did not begin to increase until the face was more than 0.2 times the mining depth outby and reached its peak pressure of 1.2 times the virgin stress when the face was 0.65 times the depth outby. This represents the behavior of a thick sandstone stratum in the western coal field.

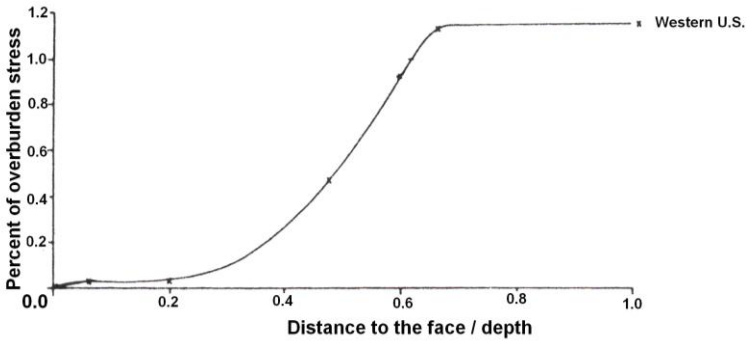


**Fig. 7.4.7 Gob pressure profile at mid-panel of a room-and-pillar panel with pillar extraction (modified from Maleki et al., 1984)**

Das (1997) found that the surface subsidence curves consisted of four periods (Fig. 7.4.8): steady, squeezing, stable and residual subsidence periods. In the steady period, OA, subsidence rises steadily, reaching up to 75-85% of the total subsidence but accounting for only 10-11% of the total subsidence time. The squeezing period, AB, that can be represented by a 4$^{th}$ degree parabolic curve, amounts to 10-15% of the total subsidence and 24-25% of the total subsidence time. In the stable period, BC, subsidence is negligible but takes up 43-45% of the total subsidence time. In the residual period, CD, 5-10% of the total subsidence occurs in 20-22% of the total subsidence time. Based on these data, it was estimated that the gob near the face area was filled only 45-60 % of the caved height, allowing the overlying strata to subside.

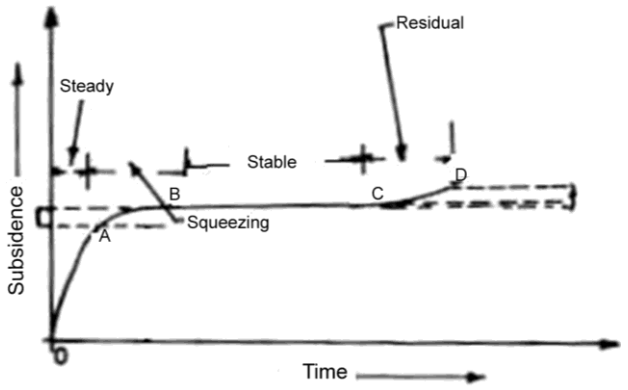


**Fig. 7.4.8 Measured surface subsidence versus time curve (Das, 1997)**

## 2. Height of Caving Zone

Because the uncaved roof rocks in the gob are supported mainly by the abutments, the caving height determines the magnitude of abutment pressures. A higher caving height represents a

smaller load to be supported by the abutments. The caving zone across the panel width is believed to assume more or less an arch shape with the highest points in or around the panel center, decreasing toward both sides (Mills and O'Grady, 1998). The caving height is highly dependent on geological conditions such as the location of the thick competent strata, the location of soft layer such as clay bands (Listak et al., 1986) and the bulking factor of the caved strata (Maleki et al., 1988; Makusha, 2004). Caving stops when a self-supporting stratum is encountered, or the overlying strata are fully supported by the caved fragments. Strong roof strata tend to delay the caving process and extend further into the gob. This condition will increase the front and side abutment pressures.

An example of the caving process is shown in Fig. 7.4.9. After initial face advance of about 15 ft (4.92m), the immediate roof did not cave. As the face continued to advance, the overlying shale layer about 60 ft (18 m) thick tended to overhang for at least 50 ft (15.3 m) before it caved in. It was at least because the location of the borehole where the measurements were made was not necessarily in the starting position of a weighting cycle for that shale layer. The weighting effect of the shale layer is believed to have limited impact on the front abutment because it was 60 ft (18.3 m) above the coal seam. The caving zone reached its maximum height when the face was at least 240-280 ft (73.2-85.3 m) outby. This indicates that the 50 ft (15 m) thick sandstone layer was strong enough to self-support for at least 220-260 ft (67.1-79.2 m) into the gob.

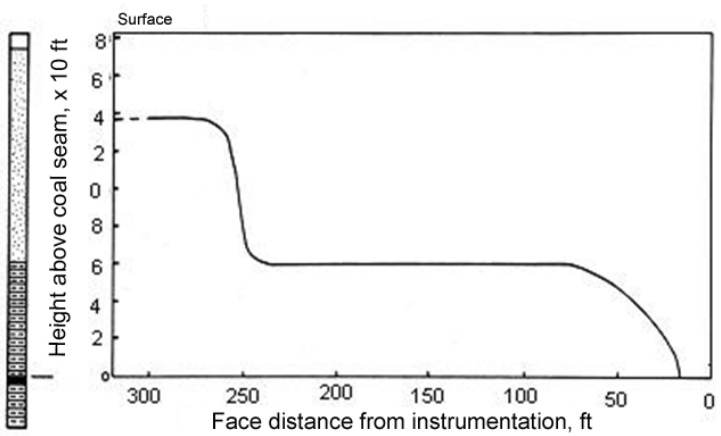


**Fig. 7.4.9 Development of caving height as face advance (Wright et al., 1979)**

In addition to the sequences of weak and strong strata above the coal seam and the bulking factor of caved fragments, caving height is also affected by the seam thickness, panel width, and overburden depth. More caved fragments are needed to fill up the void created by mining in a thick seam than in a thin one. Also, the caved fragments in the thick seams are more compressible than those in thin ones because their piles will be higher. The wider the panel, the larger the roof deflection, especially at the panel center, thereby causing the strata to break sooner. A larger depth of overburden causes more caving due to higher overburden pressure.

An approximate relation between the caving height, seam thickness, and the overburden depth is expressed as

$$h_{im} = h^{0.439} H^{1.5444} \tag{7.4.2}$$

where $h_{im}$ is caving height, $h$ is overburden depth, and $H$ is seam thickness or mining height. Thus, the influence of seam thickness on caving height is greater than that of overburden depth.

### 3. Gateroad Convergence

Convergence is the reduction in the entry height due to the stress redistribution resulting from various mining activities. Entry convergence is mostly assumed to be solely due to roof sag, while floor heave is negligible. Entry convergence can be first felt at the same time as the side abutment or front abutment pressure is first detected. Convergence at this time, however, is very small. It increases at an accelerating rate as the face approaches. After the face has passed, entry convergence continues to increase until it collapses

Entry convergence varies with the distance from the active panel. Convergence in the headgate is obviously larger than that in the second entry or the third entry. Convergence in the headgate is largest near the panel rib and decreases toward the first chain pillar. The amount of decrease depends on local geology, entry width, and pillar width. There are no obvious trends in the track entry (or second entry).

Convergence in the tailgate is much more severe than that in the headgate. The maximum convergence in the tailgate can be as high as three times that in the headgate. Maximum convergence in the headgate is toward the active panel but that in the tailgate is toward the previously mined-out panel. Cox (1994) found that tailgate convergence outby the face can be expressed by

$$y = 0.48\, e^{-0.01x} \text{ (Imperial unit)}$$
$$= 13.85 e^{-0.034x} \text{ (SI units)} \quad (7.4.3)$$

where $y$ is convergence and $x$ is distance outby the face.

A strong roof tends to resist deformation due to mining activities. Therefore, convergence with a strong immediate roof is less than that with a weak one.

## 7.5 SHIELD DESIGN

### 7.5.1 Introduction

Shields installed in the U.S since the early 1990s have been of the two-leg design. Prior to that period, several types of powered supports were in use, and there were research efforts devoted to determining which types of powered support is most compatible with various geological conditions. All of the current 53 longwalls operating in the U.S. employ two-leg shields Therefore, based on current industry practice, there is no need to choose the type of powered supports, greatly simplifying the whole design process. This chapter will concentrate on the design and selection of two-leg shields.

The average capacity of powered supports for all U.S. longwalls has been increasing year after year during the past three decades, although there seems to be a stabilizing trend in recent years (Peng, 2006). The reasons the support capacity seems to have stabilized are: the restriction in shield width to accommodate the two large legs (maximum diameter > 420 mm); shield control unit, etc., for ergonomically safe operation; and shield weight for floor stability and safe handling. To state this differently, many supports built prior to the late 1980s were under capacity. Conversely, most supports currently being used are overrated. Against this background, the design of a powered support is less related to capacity and more related to

enhanced reliability, service life, and diagnostic monitoring capabilities. With the trend toward two-meter width in recent years, the one remaining structural design is shield width. Shields wider than two meters may need to be further strengthened for torsional and asymmetric loading (Barczak, 2001b).

There are many positive advantages for employing an over-rated shield support. For one thing, all theories developed for support capacity determination relate to static loading and do not account for the fact that shields are moving with the longwall face. As such, they are loaded and unloaded cyclically, which causes wear and tear cycle after cycle. This normal wear accumulates over years, and with an expected service life of seven to ten years, it has considerable impact on the integrity of the shield, and thus, performance. In this respect, in addition to improved structural design over the past two decades, a larger capacity shield can withstand cyclic loading and unloading much better than a smaller one. Consequently **fatigue life**, not **static life**, should be used in shield support design.

### 7.5.2 Elements of Shield Design

Traditionally, support design meant the determination of support capacity. This concept ignores certain elements of the supporting system, including support itself and the foundation floor on which the support rests. The traditional method is adequate when the support itself is simple in structure, such as a coal pillar but completely inadequate for standing supports that must transmit the roof load to the floor through itself. For the case of shield supports in longwall mining, a shield has a complicated structure, the design of which must be compatible with the requirements of controlling roof and floor, and it must also have a long service life. Consequently a complete shield support design consists of four elements: the amount of roof and lateral loads to be supported, structural design and testing of the shield itself, determination of floor load distribution, and fatigue life span.

#### 1. Roof Load or Support Capacity

As the roof is undermined, some roof collapses immediately, some gradually deflects until it touches the floor or gob piles, and other roof overhangs for various lengths of time. All of these will induce various degrees of roof loadings and movements in the face area. Therefore, the behavioral characteristics of the immediate and main roofs are paramount in determining the loading conditions on the supports.

#### 2. Structural Integrity and Stability of the Powered Support

The dimension of each component of the support and its interconnection must be adequate for proper functioning at the face area. The size and strength of each component and welds as well as connections between stressed parts must also be adequate to withstand the expected loadings, static, and fatigue.

#### 3. Interactions among Support, Roof, and Floor

Certain types of powered supports are best suited for certain types of roof and/or floor behaviors and vice versa. For two-leg shields, the selection of the dimensions of shield elements should take into account the expected interactions among roof, support, and floor.

#### 4. Service Life

Nearly all supports used in underground coal mines are stationary, i.e., once installed they stay in place long after the supported areas have been abandoned. Conversely, shield supports are

moving, cut by cut or supporting cycle by supporting cycle, with the retreating longwall face. Therefore, it is loaded and un-loaded cyclically. This is **fatigue** as opposed to static loading throughout the service life of the support. Fatigue life is shorter than static life.

In order to cover these four factors, a procedure consisting of six sequential steps as shown in Table 7.5.1 is necessary (Peng, 2006). The recommended shield design procedures represent the elements that need to be considered for a complete shield design. In practice, however, due to lack of qualified personnel and the required length of time involved in the analysis, mine personnel, when ordering new shields, exercise only steps one and six, leaving step two through five for the shield manufacturers.

**Table 7.5.1 Procedures for designing a shield support**

| |
|---|
| 1. Preliminary determination of component sizes by considering: |
| (a) Mining height |
| (b) Prop-free front and space for crew travel |
| (c) Ventilation requirements |
| (d) Other considerations |
| 2. Determination of the roof and lateral loadings by considering: |
| (a) Characteristics of the immediate roof thickness and caving conditions |
| (b) Gob loading on the caving shield |
| (c) Characteristics of main roof movements |
| 3. Determination of the bearing capacity of floor rocks and water conditions. |
| 4. Determination of geometrical configuration based on preliminary analyses of: |
| (a) Stability based on external loadings and geometrical configurations |
| (b) Supporting efficiency |
| If necessary, revise the geometrical configuration and repeat the analyses until the desired stability and supporting efficiency are obtained. |
| 5. Structural design: determine the actual size and stiffness of each element by performing static stress analyses of the support, including simulation of critical loading conditions for each element. Revise the design and repeat the whole procedure, if necessary. |
| 6. Testing of the full-sized prototype shield model and electronic and hydraulic units. |

### 7.5.3 Determination of External Loadings

External loadings on shield supports consist of those applied on the canopy and on the caving shield. The former includes the vertical load due to the weight or movement of overburden strata and lateral forces, both parallel and perpendicular to the face, due to the horizontal movements of roof strata. The latter is the weight of caved rock fragments that are piled up on the caving shield.

Most researchers (Barry et al., 1969; Jacobi, 1976; Wade 1977; Wilson 1975) in past years have concentrated on the derivations of the vertical load due to the weight of the roof strata. Although there are differences in roof load models, they can be summarized by a model as shown in Fig. 7.5.1. The immediate roof breaks along or some distance outby the faceline

and at the gob edge of the support either vertically or sloping upward at an angle $\theta$ toward the gob. Depending on the roof rock property and geological conditions, sometimes the roof overhangs and sometimes it breaks along or in front of the gob edge of support.

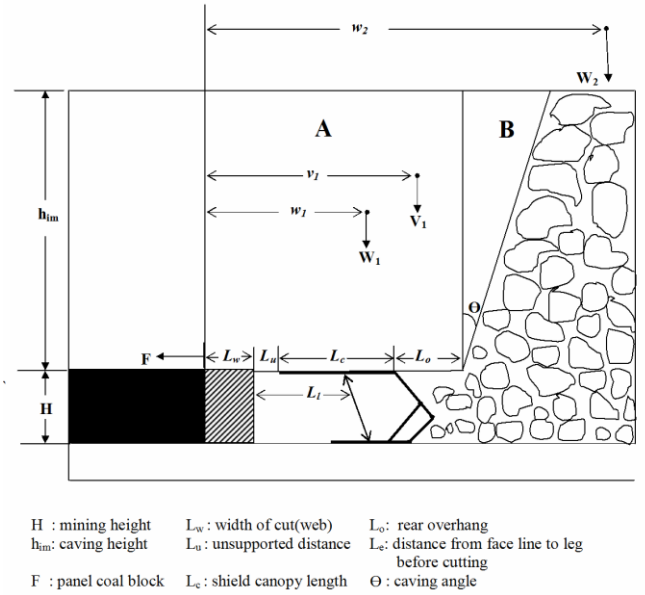


**Fig. 7.5.1 A generalized roof loading model (Peng, 2006)**

Just like pillar design, there have been many methods developed for the determination of shield roof loading by researchers in various countries where modern longwall mining is practiced (JS Chen et al., 1999; JS Chen and Peng, 1999; Barczak, 1990; Barczak and Conover, 2002; Barczak and Oyler, 1991; Chadbourne, 1994; Jiang et al., 1993; Park et al., 1992; Peng ,1998a; Peng et al., 1987b; Sarkar, 1998; Smart and Aziz, 1986; Su et al., 2004; Trueman et al., 2005; Wilson,1975). In this section, a few of the more commonly used or more effective ones are covered.

### 1. Detached Roof Block Method

The detached roof block method is simple (Fig. 7.5.1) and has been commonly used by support manufacturers and coal operators. Two factors are used to estimate the height of a detached roof block: stratigraphic sequence and bulking factor. Initially, the stratigraphic sequence of boreholes is used to determine the contact plane (or parting plane) between the immediate roof that will cave following shield advance and the main roof that will overhang. (Note that the immediate roof is not necessarily a single layer, but that it may consist of several different rock types and thicknesses). The location of the contact plane above the coal seam top is the thickness of the immediate roof, which, in turn, is used to determine whether it will fill up the void created by the complete mining of the coal seam (or mining height, H). The required caving height of the immediate roof that needs to fill up the void created by a certain mining height is governed by the bulking factor, e.g., Equation 7.3.3 (p. 324). If after mining, the height of the bulked material equals or exceeds the caving height determined by Equation 7.3.3, it means the caved rock fragments can fill up the voids and provide support to the overlying strata. Consequently, the height of the rock block determined by Equation 7.3.3 will

be that which is to be supported by the shield support. The weight of the detached rock block, $W_f$, is then:

$$W_f = \frac{HC\gamma_{im}L}{K_o - 1} \tag{7.5.1}$$

where $C$ is shield support spacing,

$L = L_w + L_u + L_c + L_o$ after shearer's cutting

$L = L_u + L_c + L_o$ before shearer's cutting

and $K_o$ is the original bulking factor of the immediate roof. If $K_o$ = 1.5 -1.1, then

$$W_f = (2-10)HC\gamma_{im}L \tag{7.5.2}$$

Therefore, the amount of rock weight on the canopy is equivalent to the rock weight of 2 to 10 times the mining height, depending on the selection of $K_o$. The support capacity employed by the coal industry increased continuously from the 1970s through the late 1990s, and in order to match the increasing load capacity, this design method required that the bulking factor must be decreased correspondingly from 1.5 to 1.1 or less which is a considerable range. As stated previously, support capacity determined by using the largest bulking factor of 1.5 in the 1960s to 1970s resulted in an underrated static powered support capacity, whereas the use of a bulking factor equal to or less than 1.1 produced over-rated static shield capacity in recent years. If the bulking factor method is adopted for determining the support capacity, the actual bulking factor of the roof strata must be used, and the support capacity so determined may be less than what is in practice today. Peng (1980a) recommended a bulking factor of 1.25. However, the measured values by Khair et al., (1987a) was 1.10-1.16 and by Listak et al., (1986) was 1.23-1.72.

The increasing roof loading can be attributed to the existence of overhung strata within the caving height determined by the chosen bulking factor, because the overhung strata produce an additional weight on the shield, the magnitude of which depends on the length and thickness of the overhung strata.

If within the required caving height calculated by using a more reasonable bulking factor such as 1.10-1.25, there is a stratum or strata that will overhang, the effect of those overhung strata must be considered in order not to under-rate shield capacity (Richardson et al., 1996; Singh and Dubey, 1994). JS Chen and Peng (1999) calculated the overhanging length of each stratum separately and then summed their total weight on the shield (Fig. 7.5.2) using the following equations:

$$L_b = t\sqrt{\frac{T_o}{3q}} \tag{7.5.3}$$

$$L_c = A + B + C + \ell_c \tag{7.5.4}$$

$$F_{rd} = (DF)\frac{\sum_{i=1}^{k} W_i x_i}{\ell_r} \tag{7.5.5}$$

$$W_i = L_{bi} S t_i \gamma_i \tag{7.5.6}$$

$$x_i = \frac{L_{bi}}{2} \tag{7.5.7}$$

where $DF$ = 1.10-1.25 is a design factor, considering the adjacent support's advance after the shearer's cutting, $k$ is number of rock layers within the required caved zone, $L_b$ is the length of a fix-ended cantilevered beam, $L_{bi}$ is the length of cantilevered beam of the $i^{th}$ rock layer, $q$ is the uniform load on the beam per unit length, $S$ is support spacing, 5.75 ft (1.75 m) or 6.56 ft (2 m), $t_i$ is thickness of the $i^{th}$ rock layer, $T_o$ is in-situ tensile strength of the rock beam, which can be estimated by multiplying its lab-determined strength by a reduction factor such as

| | |
|---|---|
| Coal, claystone, or fireclay | 0.20 |
| Shale or mudstone | 0.25 - 0.30 |
| Sandstone, siltstone, limestone, or laminated sandstone | 0.30 - 0.50 |
| Massive sandstone | 0.50 - 0.80 |

$x_i$ is the distance from the center of gravity of the $i^{th}$ rock layer to the first supporting point of the coal face, $W_i$ is weight of the $i^{th}$ rock layer, $\gamma_i$ is density of the $i^{th}$ rock layer. $l_c$ is shield canopy length, $l_r$ is distance from face line to leg, and $F_{rd}$ is resultant force.

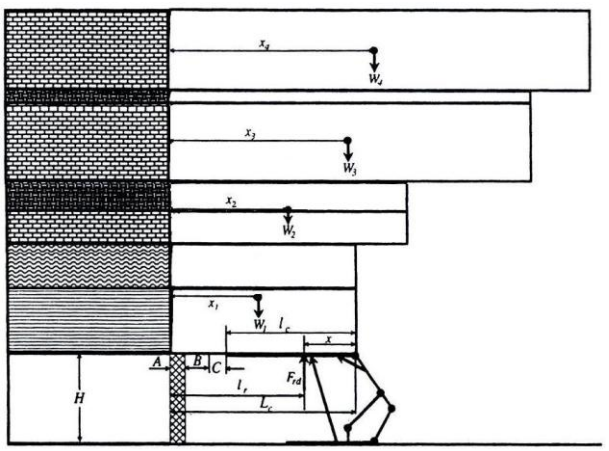


**Fig. 7.5.2 Beam roof loading model (JS Chen et al., 1999; JS Chen and Peng, 1999)**

## 2. Shield Leg Pressure Measurement Method

This method is only applicable for existing longwalls for evaluation of the adequacy of existing shields and improvements needed for the next generation of shields. However, it can also be used for new mines in the same seams or seams with similar geological conditions.

Peng (1998a) reported that pressure changes within a supporting (or mining) cycle vary from cycle to cycle and shield to shield. But, in general, pressure change can be divided into three major types: increasing, steady, and decreasing types, depending on whether the leg pressure, increases substantially after setting, stays more or less the same, or decreases substantially, respectively. Shields of the increasing pressure type receive the largest pressure (or load) increment in a mining cycle (Fig. 7.5.3A). The increasing type of pressure curve can be divided into three segments according to its rate of pressure change. The first segment is the initial rapidly increasing segment and usually lasts less than 10 minutes after setting. The second segment covers the portion of relatively steady increase after the initial rapid increase and accounts for most of the cycle time. The third segment is the final rapid increase portion

and occurs usually within five minutes before the shield is released for advance. This type of pressure curve denotes a relatively intense roof loading. If the roof movement is very intense, the leg pressure may reach the yield load before and cease to increase further until the end of the mining cycle. Shields with the steady type of pressure curves (Fig.7.5.3B) receive less load than those with the increasing type. This type of pressure change also can be divided into three segments. But the first two segments are quite different from those of the increasing type. The pressure in the first segment may remain constant, decrease, or increase, while the second segment is normally flat. This type of pressure curve denotes a relatively weak roof loading. The decreasing type of pressure curve (Fig.7.5.3C) denotes that either the roof is extremely weak, it has too much rock/coal debris between the canopy and roof strata and/or under the base plates, or a leg leakage. The leg pressure decreases rapidly after setting and continues to decrease at a decreasing rate. In some cases it increases suddenly at the end of the cycle, while in others cases it finishes at the same decreasing rate.

The final pressure in a shield supporting cycle of an increasing loading type is the maximum load attained in that cycle. Since all shields are equipped with transducers for pressure monitoring, analysis of the leg pressure history for all shields over one or more panels will provide sufficient data for statistical analysis. The average final pressure may be adopted as the desired shield capacity. One may argue that this is a very conservative approach because the final pressure in a supporting cycle usually occurs in a very short period of time when the adjacent shields are released for advance, and that it should better be handled through a yield valve. If this is the case, the time-weighted average resistance or pressure (TWAR or TWAP) may be used.

The above-mentioned methods are most applicable for cases when the measured shield leg pressures in a supporting cycle do not or rarely exceed the pre-set yield pressures. Trueman et al., (2005) noted in thick seam mining or shields used with low setting pressures that leg pressures often involved one or more yield cycles. The time interval from one opening of a yield valve to the next is defined as a yield cycle. Based on the yield cycle characteristics, they proposed the following:

A. Adequate capacity and appropriate setting pressure – when leg pressure cycles are compatible to those shown by Figs. 7.5.3A and 7.5.3B, the setting pressure is appropriate and the yield capacity is adequate.

B. Adequate capacity but too high a setting pressure – after one or more yield cycles, the roof convergence and pressure increment reaches equilibrium (Fig. 7.5.4).

C. Inadequate shield capacity – when the yield cycle continues without signs of reaching equilibrium between shield leg pressure and roof convergence (Fig. 7.5.5).

In any event, the shield leg pressure data can provide a wealth of information, and they should be used to statistically compare and determine the most likely scenarios of shield loading to be encountered.

As noted previously, the recorded shield leg pressures vary from cycle to cycle and from shield to shield. Furthermore, the amount of data from the whole face is overwhelming. So in order not to be biased in analyzing the data, statistical methods must be used. Bessinger (1996) stated that the characterization of pressure variations can allow a rational, statistical assessment of the required yield capacity of a new shield design, and he developed a method of estimating the cumulative probability of peak load. He suggested that as a minimum, the 87 percent cumulative probability roof load value may be chosen. Below this value, an increased

frequency of undesirable outcomes may be experienced. In the range of 87 to 93 percent the results may appear marginal with occasional large-scale roof control problems.

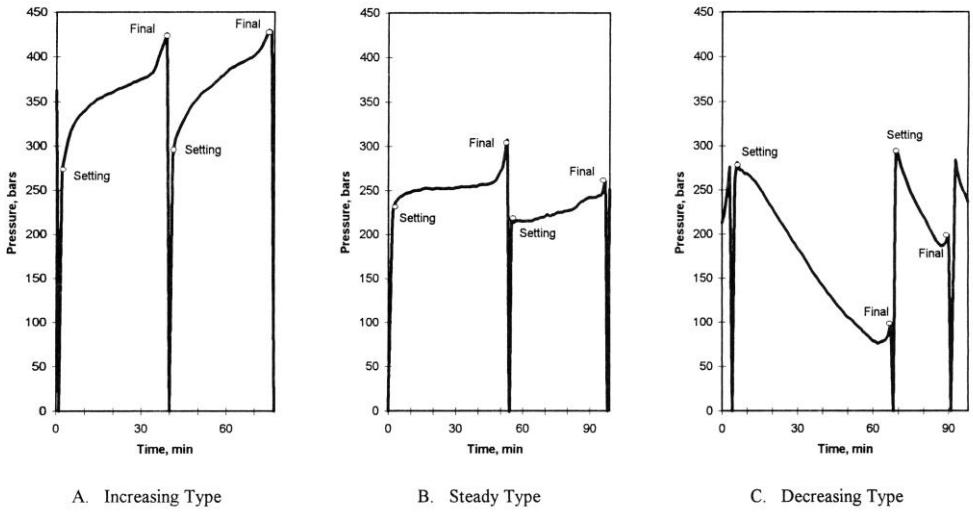


**Fig. 7.5.3 Three types of pressure changes in a shield supporting cycle (Peng, 1998)**

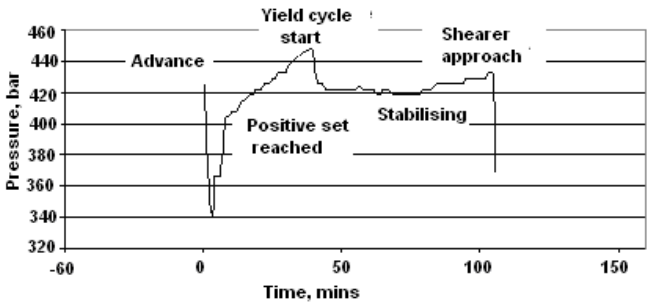


**Fig. 7.5.4 Support loading showing stabilization after yielding (Trueman et al., 2005)**

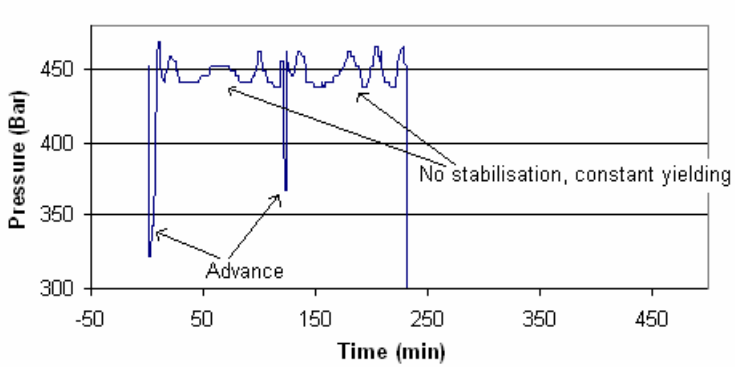


**Fig. 7.5.5 Support loading showing continuous yielding (Trueman et al., 2005)**

### 3. DEPOWS (Design of Powered Support Selection Model)

DEPOWS is a user friendly, menu-driven PC computer model developed by Jiang et al., (1989). It consists of four elements, i.e., required vertical load capacity, most suitable support type, minimum horizontal force, and maximum allowable floor pressure. Peng et al., (1987b) developed a roof-support-floor interaction, displacement-controlled model for determining the required roof load capacity based on the hydraulic leg pressure history monitored over 23 longwall panels in the Appalachian coalfields. Since all of those studies were performed prior to the introduction of electrohydraulic control, manual support settings were employed. They found that face (roof-to-floor) convergence is different due to varying geological conditions and that change in support resistance varies with face convergence. In other words, under the same geological condition, the final load or the increment of support resistance (i.e., load increment) in a mining cycle is proportional to the setting load. Similarly, under the same setting load, the final load or load increment will be different due to varying roof conditions. Figure 7.5.6 shows the characteristics curve of the model based on this concept, in which

$$\Delta q = a q_s^2 e^{-c q_s} \tag{7.5.8}$$

where $\Delta q$ is the increment of load density, $q_s$ is the setting load density, and $a$ and $c$ are constants relating to the characteristics of main and immediate roofs, respectively. Factors $a$ and $c$ are determined empirically, and for convenience of determination, a separate nomograph has been constructed for each of them (Figs. 7.5.7 and 7.5.8).

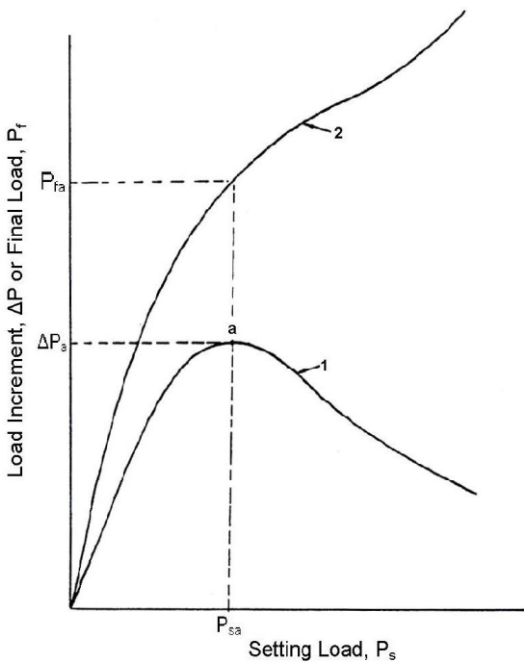


**Fig. 7.5.6 Characteristics curves of the DEPOWS model (Peng et al., 1987b)**

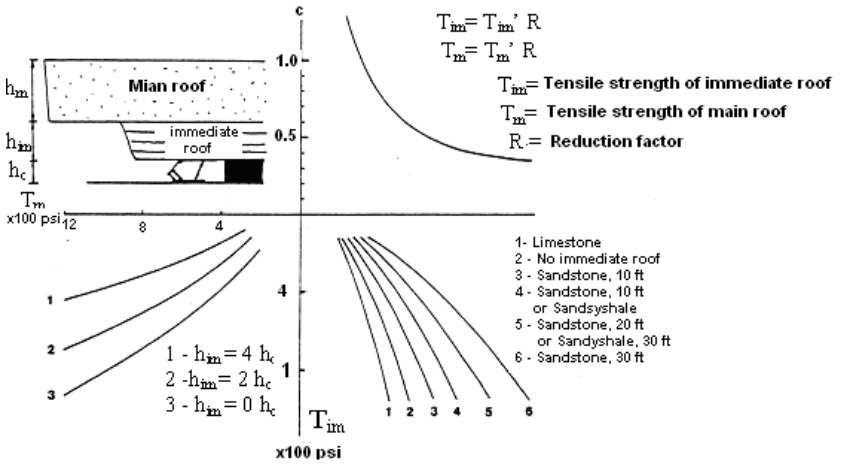


**Fig. 7.5.7 Nomograph for determination of constant *c* (Peng et al., 1987b)**

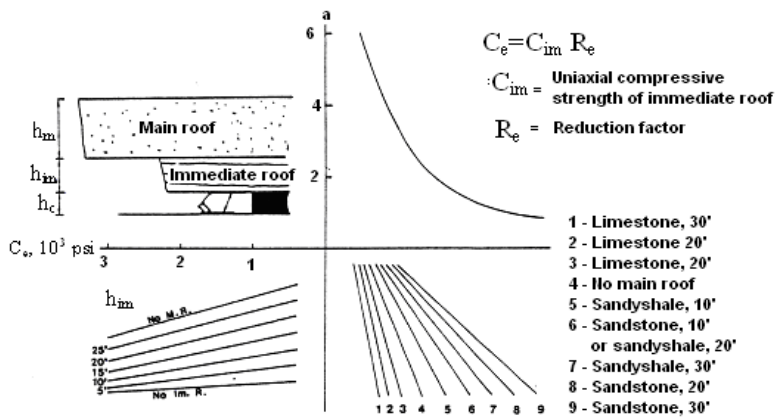


**Fig. 7.5.8 Nomograph for determination of constant *a* (Peng et al., 1987b)**

The equations for determining the required load capacity are:

$$\Delta P = 0.4174 aA / c^2 \eta \tag{7.5.9}$$

$$P_s = 3.2A / c\eta \tag{7.5.10}$$

$$P_y = P_s + \Delta P \tag{7.5.11}$$

where $\eta$ is the supporting efficiency and is defined as the ratio of the vertical component of load to the total leg load, $A$ is the canopy area, $P_s$ is setting load, and $P_y$ is the final load in a mining cycle. Note that yielding is not implicit in this analysis.

It must be emphasized that leg pressure data on which this model was developed were obtained prior to the mid-1980s when support capacity ranged from 280 to 800 tons with an average of less than 500 tons. The recommended support capacities using these empirical equations are considered to be of rational values for static capacity and the prevailing support capacities at that time.

## 4. Yielding Foundation Model

In this model the powered support is considered to be one of three yielding foundations (Fig. 7.5.9A) that support the immediate roof and the bridging beds (Smart and Redfern, 1986). The other two foundations are the coal ahead of the face and the waste in the gob. The powered support is assumed to control the subsidence of the roof strata around the coalface sufficiently to prevent fractures that are generated ahead of the face. The force required to achieve this purpose depends on the contribution of the other two foundations. In the bulking factor control caving (Fig. 7.5.9B), the waste piles offer immediate support to the subsiding bridging beds, assisting the powered supports to control subsidence, thereby leading to moderately-rated powered supports. In parting plane control caving (Fig. 7.5.9C), the immediate roof is stronger, and the first major parting plane is farther into the roof. In this type of caving, the caving height is controlled by the location of a dominant parting plane. The thickness and bulking factor of the rock below this parting plane may not be sufficient to fill the waste void, creating a foundation that offers no immediate support to the subsiding bridging beds, thereby requiring more heavily rated supports.

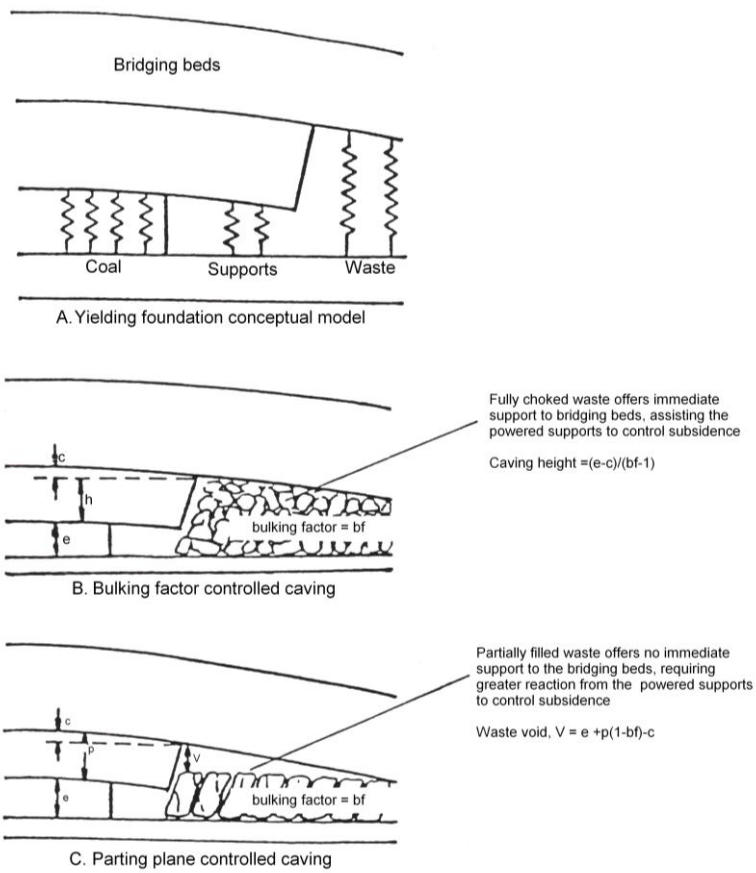


**Fig. 7.5.9 Yielding foundation model (Smart and Redfern, 1986)**

The specification of powered support capacity can be done either by geotechnical appraisal or finite element numerical modeling. In the geotechnical appraisal method, the

required data are the geological and rock mechanics properties of strata in a geological column 32.8 ft (10 m) above and 16.4 ft (5 m) below the coal seam of interest, including grain size, location of parting plane, fracture log, core recovery, UCS, Young's Modulus, tensile strength, and slake durability. Comparison is made between the unknown operating conditions for which a support system is to be specified and two known operating conditions for which the support capacity is known. Based on the results of comparison, the required support capacity is estimated.

### 7.5.4 Floor Pressure under the Base Plate

**1. Rigid Base Plate**

Traditionally the determination of floor pressure is always based on the assumption that the base plate is rigid. Depending on the location of the vertical resultant force under the base plate, pressure distribution in the floor can be simplified to a triangular shape, a trapezoidal shape, or a rectangular shape (Jackson 1979).

If $0< s <L / 3$ (Fig. 7.5.10A), the pressure distribution is triangular. But the length of the pressure envelope, $l$, is less than the contact length, $L$, between the base plate and floor. The magnitude of the pressure can be determined by

$$p_{avg} = \frac{R_v}{lw} \times 2000 \tag{7.5.12}$$

$$p_{\max} = 2 p_{avg} = \frac{2R_v}{lw} \times 2000 \tag{7.5.13}$$

where $P_{avg}$ = average floor pressure in psi, $l$ = length of the floor pressure envelope in inches, $R_v$ = resultant load, $P_{max}$ = the maximum floor pressure at the front end of the base plate in psi, and $w$ = width of the base plate in inches.

If $s = L / 3$ (Fig. 7.5.10B), the pressure distribution is still triangular, but $l = L$. Equations 7.5.12 and 7.5.13 can be rewritten as

$$p_{avg} = \frac{R_v}{Lw} \times 2000 \tag{7.5.14}$$

$$p_{\max} = 2 p_{avg} = \frac{2R_v}{Lw} \times 2000 \tag{7.5.15}$$

If $L/3 < s < L / 2$ (Fig. 7.5.10C), the pressure distribution is trapezoidal, and the magnitudes of the pressure are

$$p_{\min} = \frac{2R_v}{Lw}\left(\frac{3s - L}{L}\right) \times 2000 \tag{7.5.16}$$

$$p_{\max} = \frac{R_v}{Lw}\left[2 - \frac{6}{L}\left(s - \frac{L}{3}\right)\right] \times 2000 \tag{7.5.17}$$

If $s = L / 2$ (Fig. 7.5.10D), the pressure distribution is rectangular and uniform

$$p_{\max} = p_{avg} = p_{\min} = \frac{R_v}{Lw} \times 2000 \tag{7.5.18}$$

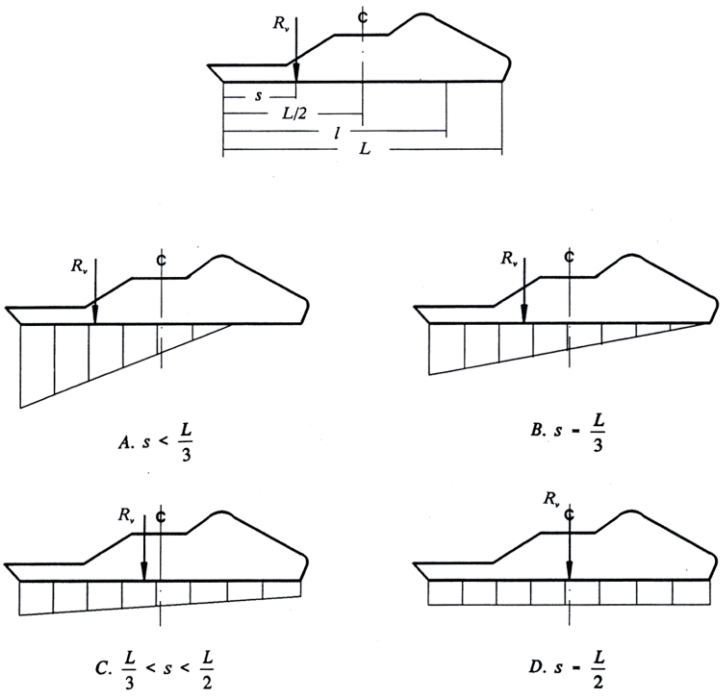


**Fig. 7.5.10 Floor pressure distribution – rigid base (Peng and Chen, 1993)**

### 2. Elastic Base Plate

Finite element analysis was performed to analyze the effect of four factors (i.e., Young's modulus of the floor rock, vertical resultant force, the contact width between the base plate and the floor, and location of the resultant force) on the magnitude of the maximum floor pressure under the base plate of powered supports using orthogonal factorial experimental design (Peng and Chen, 1993). The distribution of floor pressure is illustrated in Fig. 7.5.11 and is completely different from those of the rigid base plate. The maximum floor pressure is always located directly under the vertical resultant force, and the magnitudes of floor pressure are nearly the same for the same resultant force, floor property, and contact width between base plate and floor.

Based on the finite element computer analysis, a regression equation was developed to determine the maximum floor pressure as follows

$$p_{\max} = 1233 + 213x_1 + 2.72x_2 - 38x_3, psi \tag{7.5.19}$$

where $x_1$ is the Young's Modulus of the floor material in $10^6$ psi, $x_2$ is the vertical resultant load in tons, and $x_3$ is the contact width between the plate and the floor along the faceline direction in inches.

## 7.5.5 Testing of Full-sized Prototype Shields

The final step in support design is the manufacturing of a full-sized prototype model for testing. Testing of a full-sized prototype model will provide information about the design deficiencies from which corrections can be made before full production is scheduled. A

properly designed testing program can uncover weak points for full design changes. Most important of all, there is no design method currently available to consider the fatigue life which, in practice, is what a shield is subjected to throughout its service life. A full-scale prototype model testing for 50,000 – 75,000 supporting cycles of various loading conditions is the best and most assuring way to account for fatigue life.

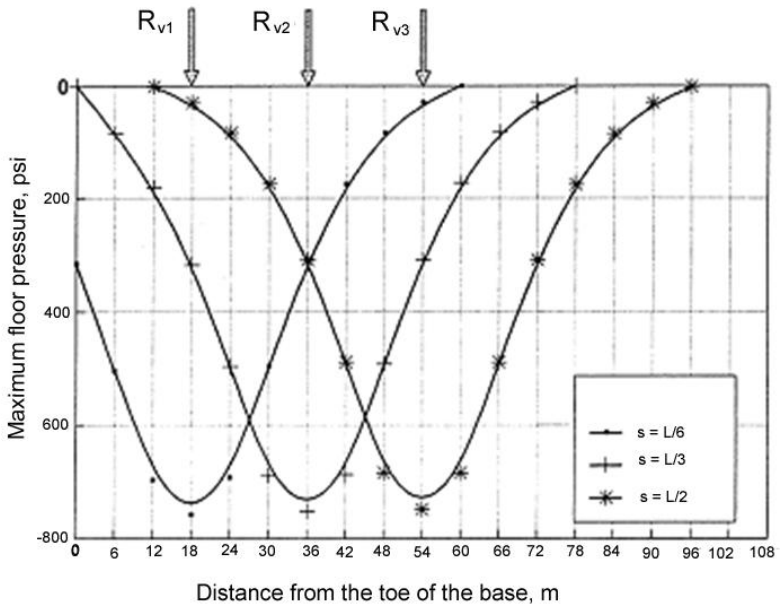


**Fig. 7.5.11 Floor pressure distribution – elastic base (Peng and Chen, 1993)**

There are two types of testing machines. One is a static frame in which the external loadings are generated mainly by applying the hydraulic leg pressures of the support being tested against the test frame. The other is the active testing machine in which all external forces are applied. A typical example is the NIOSH Mine Roof Simulator (Fig.7.5.12) (Garson et al., 1982) which is a computer-controlled electromechanical hydraulic press. The lower platen is capable of applying 1,500 tons vertically and 800 tons horizontally. Full load can be applied anywhere over an octagon pattern on the lower platen. Horizontal and vertical travels are programmable and can be applied simultaneously.

The testing programs vary with the OEMs (original equipment manufacturers). They should include the most severe loading conditions expected during the service life of the support. In this respect, any testing program will be less meaningful if the actual loading conditions expected during the service life of the supports are not properly simulated in the testing program (Matthews, 1986).

## 7.6 ROOF /RIB FALLS AND FLOOR HEAVE AT LONGWALL FACES

Ground control problems at longwall faces are, just like in entries/crosscuts, roof falls, coal face spalls, and floor heaves. At the longwall face, the cross-section configuration is such that one rib is the coal face, while the opposite rib is the shield's caving shield: the roof is covered with a shield canopy, except the unsupported distance between the canopy tip and coal face,

while the floor is also protected by the base plates of the shield except for the distance between the base toe and coal face.

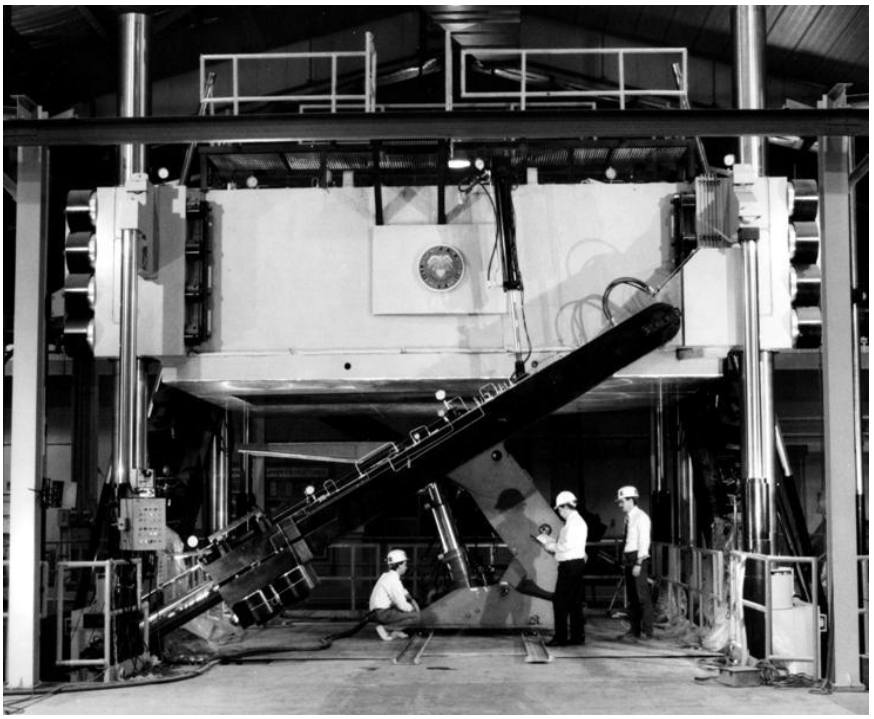

**Fig. 7.5.12 NIOSH mine roof simulator (Garson et al., 1982)**

### 7.6.1 Roof Falls

#### 1. Mechanisms

Based on in-situ monitoring and observation, it is believed that a passive horizontal force acting toward the gob exists in the immediate roof generated by the overburden strata movement toward the gob. Since rock is much weaker in tension, the tensile force moving toward the gob may cause the immediate roof to fail and fall down. On the other hand, when the immediate roofs are thinly-laminated or contain vertical joints, roof falls will occur if an active counter horizontal force is not available (Peng and Chen, 1991).

The immediate roof between the canopy tip and the coal face is the most sensitive area with respect to the convergence of the roof. Frith (2005) divided the roof falls at the face into two categories; cutter type failure of the immediate roof skin and above it, the weighting-induced, sub-vertical, large intact blocks dipping toward the face. They are caused by the roof strata acting as cantilever beams with the coal face as the fulcrum point. Beam bending generates compressive and tensile horizontal stresses, causing cutters at the coalface. If the vertical displacement of the beam is large, it may adversely affect the shield support's ability to set correctly, thereby causing unstable roof to propagate higher (Frith et al., 1992).

Underground observation in German coal mines indicated that roof falls are related to the following two sets of factors: (1) a critical distance between the canopy tip and the coal face.

$TF_{cri}$ which is predictable and related to the thickness and UCS of the first roof layer, and (2) roof falls are related to: (A) measured support resistance (MSR) of the shield support, (B) the calculated vertical stress ($P_v$), (C) the fracture direction index (DI), and (D) the distance by which $TF_{cri}$ is exceeded ($\Delta$TF). These factors are related to the measured roof fall frequency (FF) by (Langosch et al., 2003) (Fig. 7.6.1),

$$FF = c_1 \cdot \frac{p_v^{c_2} \cdot DI^{c_3}}{MSR^{c_4}} \cdot \Delta TF \cdot (\%) \tag{7.6.1}$$

where *FF* is the measured fall frequency (%), which is defined as the ratio of the number of observed shields with roof falls to the total number of observed shields per face, and *DI* is the direction of roof fractures with respect to mining direction: *DI* = 2 when the fractures are so oriented that the roof blocks can fall through the unsupported distance; *DI* = 1 when the fractures are so oriented that the roof blocks are supported by the coal face, $c_1$, $c_2$, $c_3$, and $c_4$ are constants. The model assumes that the tendency of the roof to fail is dependent on the stability of the first series of strata between coal face and canopy tip.

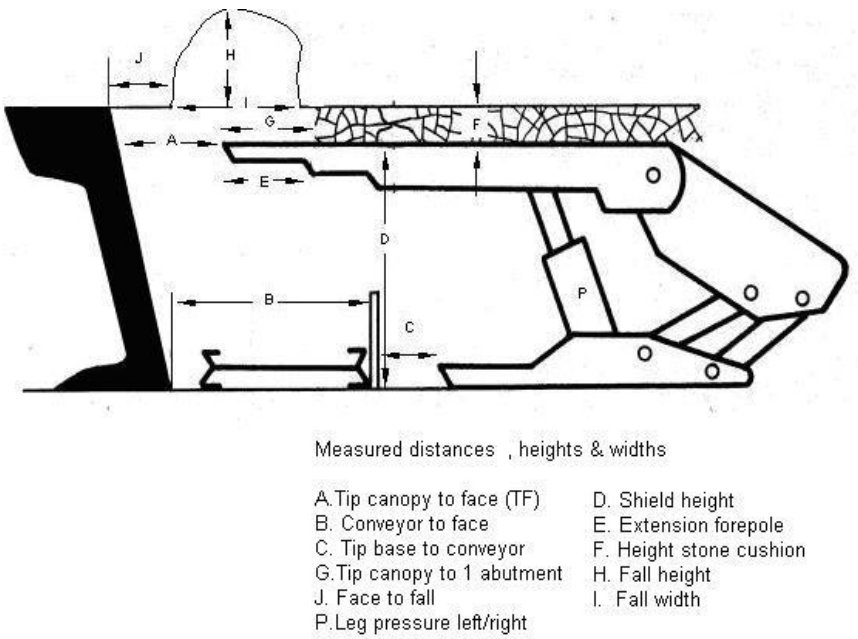


**Fig. 7.6.1 Underground roof fall investigation method (Langosch et al., 2003)**

Roof fall statistics in China (Kang and Yang, 2005) showed that the great majority of roof falls occurred in areas when the immediate roof contains at least one coal streak within the lower portion of the immediate roof, the thickness of which ranged from 1.2 to 22.5 in. (0.03-0.57 m). The stability of the first immediate roof layer depends on its own structure, formation, and rock mechanic characteristics.

## 2. Methods of Preventing Roof Falls at the Face

The unsupported distance between canopy tip and coal face is by design 18-24 in. (457.2-609.6 mm) to avoid accidentally cutting into the shield canopy by the drum during coal cutting. However, in practice the unsupported distance is much larger and often up to 3-4 ft (0.9-1.2 m)

wide. For medium stable and stable roofs, such large unsupported distances can be self-supporting, but for unstable roof, roof falls will occur.

Shield supports are able to handle smaller roof cavities (e.g., less than 3 ft long by 3 ft high or 0.9 m long by 0.9 m high). Shield supports may not be able to handle larger roof cavities, thereby causing production delays.

The easiest and most effective way to prevent roof falls in the unsupported distance is to keep the canopy close to the coal face, provided the shield capacity, especially tip capacity, is sufficient. Many roof falls are due to insufficient shield capacity. In such cases, increasing the shield capacity or replacing it with a larger capacity shield is required.

Adoption of the two-leg shield can reduce/prevent roof falls in the unsupported area, because two-leg shields can provide an active horizontal force during setting to counter the passive face-to-gob horizontal force resulting from the tendency of roof strata moving toward the gob. This way, the immediate roof in the unsupported area is always subjected to compressive force and consequently is more stable (Hafera et al., 1989; Nemcik et al., 1998). The ability of two-leg shield to generate an active horizontal force is related to the following 7 factors; Young's modulus of the coal and immediate and main roof, ratio of the immediate roof thickness to mining height, distance between canopy tip and coal face, inclination angle of the shield hydraulic leg, and shield capacity (Peng and Chen, 1991). Everything being equal, the larger the setting load and the smaller the hydraulic leg angle from the horizontal, the larger the active horizontal force and consequently, the more stable roof in the unsupported area.

If the roof fall cavities are large, the most common remedy is to pump foam materials via surface boreholes and fill up the cavities (Frith, 2006; Peng, 2007). The foam material should cure quickly with suitable strength so that the shield supports can make use of it for initiating the advance.

Experiments with the four-entry, yield-abutment-yield system in the Pittsburgh seam (Peng 1991b) showed that the yield pillar on the headgate side can protect the headgate T-junction against roof falls and cutter roof based on the measured pillar stress and entry convergence. The pillars were 50-150-50 ft (15.2-45.7-15.2 m) centers with entries 16 ft (4.9 m) wide. The previous design, a 100-100-50 ft (30.5-30.5-15.2 m) system with a large pillar on the headgate side, frequently encountered cutter roofs.

### 7.6.2 Face Spall

Most longwall coal faces exhibit some degree of face spall. Face spall occurs more frequently in high coal seams or during face weighting periods. Face spall may be confined to the top portion of the coal face, or it may occur in full seam height. In the former case, the unsupported distance between canopy tip and coal face may become too large, resulting in roof falls.

Face spall is related to the rate of convergence of the roof. During roof weighting, roof convergence accelerates, and face spalling also intensifies. Therefore, it is very important that shields should have sufficient capacity and be in good working order because with proper working conditions, shields can slow or prevent accelerated roof convergence, thereby reducing load transfer to the coal face. A solid straight face signals little or no front abutment pressure, while a broken face indicates heavy abutment pressure or inadequate shield capacity/working conditions.

A well-cleated coal will spall in small pieces, posing no threat to crew safety and AFC transportation. On the other hand, coal with poorly-developed cleat systems tend to spall in large lumps causing safety and production problems (Frith et al., 1992).

### 7.6.3 Floor Heaves

Floor problems at the face occur when the floor strata are soft and thick, where shields are liable to dig into the floor, preventing safe and speedy advance of shields. This subject is discussed in more detail in Section 10.6 (p. 498).

Floor failure can also occur in competent floor (Nemcik et al., 1995). When a weak slip plane is present at a shallow depth into the floor, the shear force in the floor may fail the bedding, generating large lateral stresses in the upper floor resisting the lateral displacement of coal toward the gob. If the immediate floor is relatively thin, its strength may be exceeded, and subsequently the floor will buckle or fail in compression, resulting in a floor heave in front of the shield support.

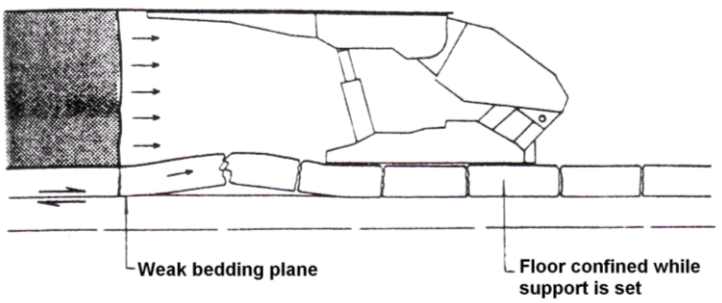


**Fig. 7.6.2 Floor buckling induced by lateral stress (Nemcik et al., 1995)**

## 7.7 EFFECT OF PANEL WIDTH

Ever since the adoption of modern longwall mining by the U.S. coal industry in the mid-1970s, the average panel width (or face length) has increased steadily year by year from slightly over 400 ft (121.9 m) in 1976 to more than 900 ft (274.3 m) in 2007. There are plenty of signs indicating that this trend will continue. Increasing panel width reduces the number of longwall moves and gateroad developments per year, increases the production time, and thus, lowers the operation cost.

From a ground control point of view, two general questions must be answered satisfactorily when planning to increase the panel width: (1) will the increase of panel width change the characteristics of the strata movement in the longwall face and (2) how much will the shield support loading increase and if so, will the current shield support capacity be sufficient?

Three-dimensional finite element analyses (Tsang and Peng, 1994; Peng and Tsang, 1994) showed that (1) the shield support load distribution in a longwall face is affected by roof condition and the degree of gob compaction. In multi-panel longwall mining, maximum shield load occurs near the tailgate side (Fig. 7.7.1). But under strong roof condition, shield support load is rather uniform across the whole panel when the panel width is less than 500 ft (152.4 m); (2) the increase of panel width will cause the shield load to increase. The amount of load increase is a function of panel width, roof condition, and degree of gob compaction. Overall,

the percentage of load increment on the shield support ranges from 3.5 to 8 percent per 100 ft (30.5 m) increment of panel width, with an average of 6 percent. When the panel width is larger than 700 ft (213.4 m), the load increment becomes smaller under both weak and strong roof conditions (Fig. 7.7.2); (3) the effects of panel width on the gateroad system are generally small compared with mining depth effect.

When the panel width is larger than 700 ft (213.4 m), such effect becomes insignificant under both weak and strong roof conditions. In numerical modeling, strong roof condition consists of 10 ft (3 m) of shale overlying by 30 ft (9.1 m) of sandstone, whereas weak roof condition consists of 14 ft (4.3 m) of interbedded shale, coal siltstone and sandstone overlying by 20 ft (6.1 m) of massive shale. For hard-to-cave roofs, however, increasing panel width from 492 to 656 ft (150 to 200 m) was reported to have adverse effects in roof weighting and roof control at the face (Frith et al., 2000).

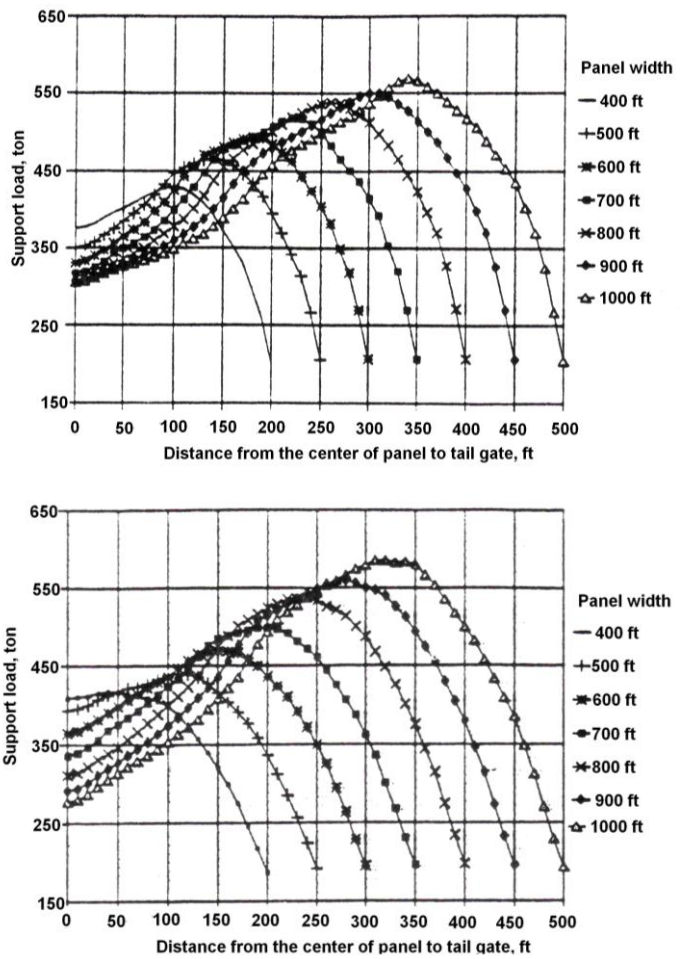


**Fig. 7.7.1 Shield support load distribution on the tailgate side under weak (upper) and strong (lower) roof conditions (Peng and Tsang, 1994)**

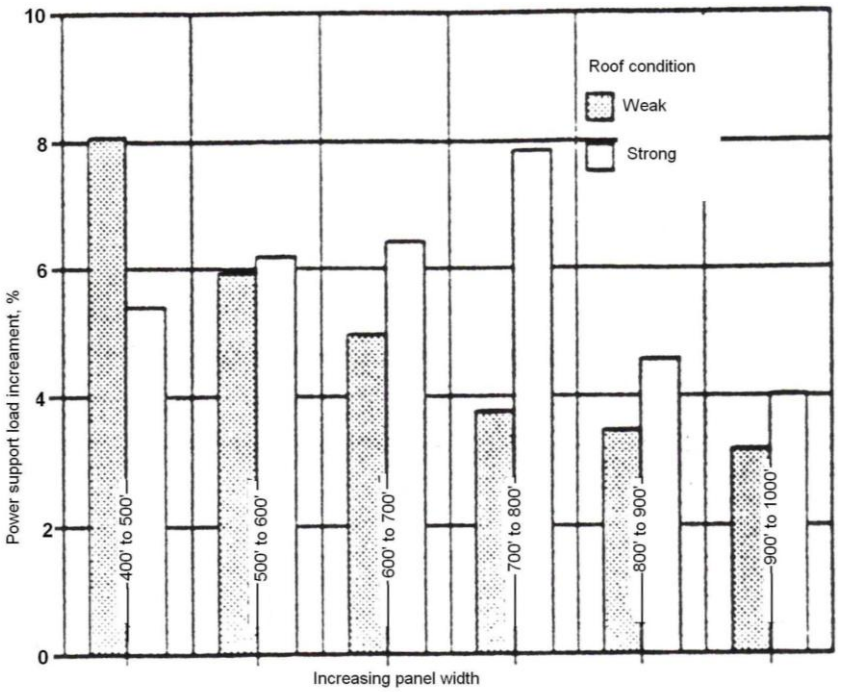


**Fig. 7.7.2 The maximum percentage load increment on the shield support as the panel width increases (Peng and Tsang, 1994)**

The effect of panel width on overburden movement depends very much on the stratigraphic sequence, especially the location and thickness of massive strong strata. Fig. 7.7.3 shows the difference in overburden movement between two adjacent panels. Panel A was 656 ft (200 m) wide and panel B was 524.8 ft (160 m) wide (Mills and O'Grady, 1998). The zone of overburden movement extended upward to a height of approximately 1.0-1.1 times the panel width (or 43-59 times mining height). Movement height was maximum at panel center and decreased toward the gateroad chain pillars on each side, i.e., it was domed-shaped. Movements of the overburden strata were downward in discrete blocks. Separation was concentrated at horizons 65.6 ft, 164 ft, 328 ft and 426.4 ft (20 m, 50 m, 100 m, and 130 m) above the coal seam with major strata units between 164 and 328 ft (50 and 100 m) above the coal seam. This major unit may be a factor in the observed periodic loading of longwall shield supports and appeared to be a more significant factor in the wider panel.

The effect of panel width was investigated by Strawson and Moodie (2007) for three panel width, 574 ft, 869.4 ft, and 984.2 ft (175 m, 265 m, and 300 m) (Fig. 7.7.4). Microseismic data showed that microseismic events in the narrower 574 ft (175 m) panel were predominantly well behind the face, but generally ahead of the face for the wider, 869.4 ft (265 m) panel. Tensile fractures dominated in the narrower face, while shear fractures were prevalent in the wide panel. Reduction of shield loading at the center of the narrower panel was significant, indicating bridging of the main roof. But cutters occurred in the headgate.

In the narrow panel (inby portion of LW 106 in Fig. 7.7.4), a reduction in face weighting issues (roof falls and face spalls) and face stoppages were observed, whereas a number of face weighting issues occurred in the wide panel portion (869.4 ft or 265 m wide) of LW 106,

where it was deeper. In the 984 ft (300 m) wide panel, there were only a few minor geotechnical issues, mainly due to the larger seam split area. In summary, the experiments proved that the overburden strata in this mine will bridge for a panel width of 574 ft (175 m), resulting in reduction in shield loading and face weighting issues.

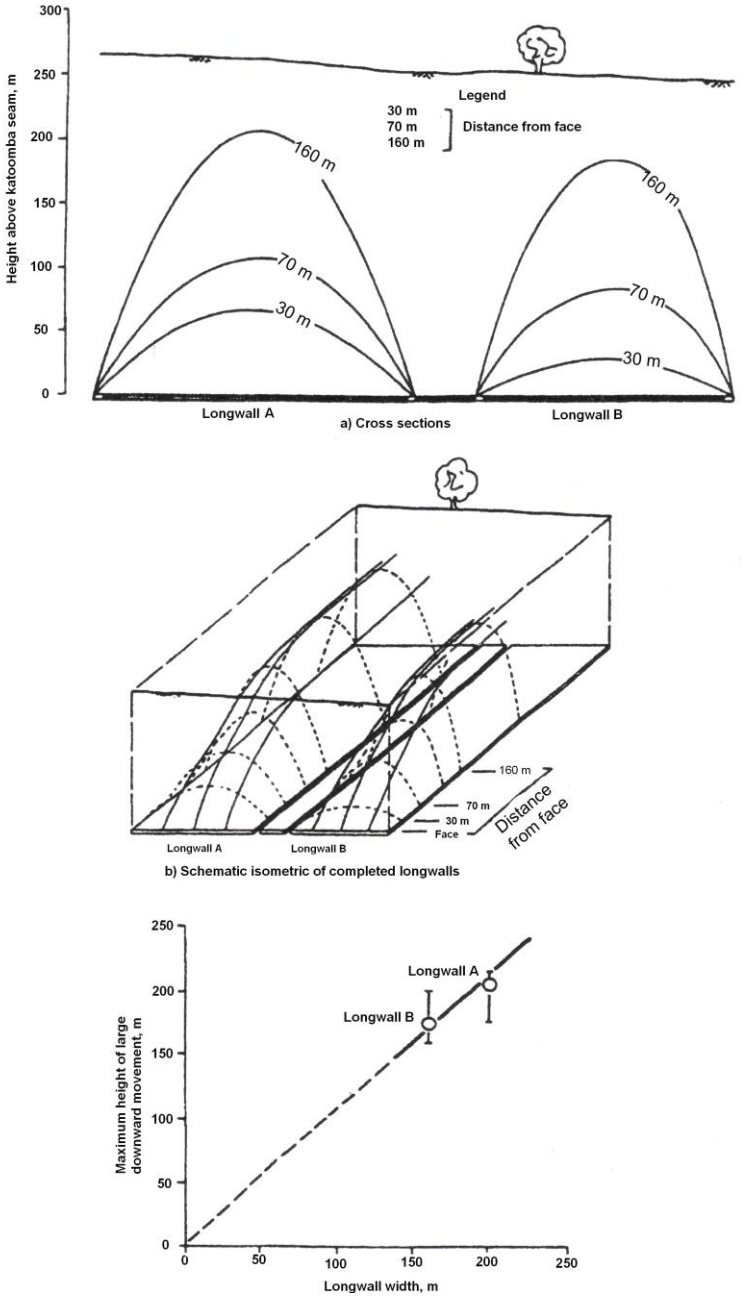


**Fig. 7.7.3 Relationship between panel width and height zone of large downward movement in the overburden (Mills and O'Grady, 1998)**

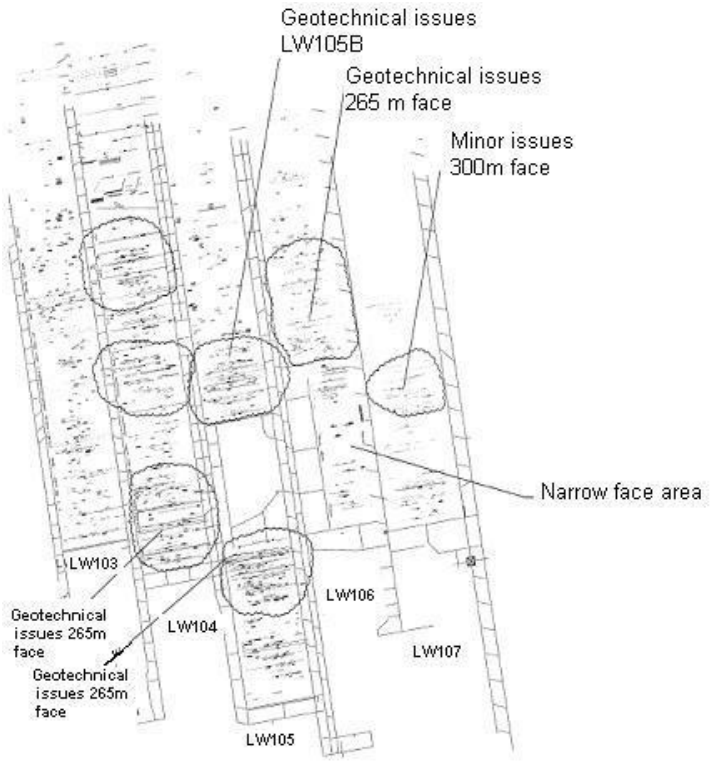


**Fig. 7.7.4 Face weighting events (Strawson and Moodie, 2007)**

## 7.8 FAULTS AND GEOLOGICAL ANOMALIES

### 7.8.1 Introduction

Geological faults of various types have been encountered in many coal seams. Depending on the offset displacement between the two opposite sides of the fault and the extent of fractures around it, it may or may not present problems for mining through it. In general, mining through a fault presents ground control problems. Therefore most coal mines try to avoid trouble by leaving the faults out of the mining plan.

If the reserves contain many faults or the faults occur in such a way that a mining plan will encounter one or more of them, many potential hazards exist in mining through faults, including sudden changes in horizon and grade, thinning of the coal seam, weak and disturbed strata, less stable gateroads, increased gas and water, and potential for equipment damage. Longwall preparation and planning for mining through faults should include (Rowland, 2002):

1. Gateroad preparation upon development - additional supports, such as cable bolts and cable trusses, may be needed in an area on either side of the fault.
2. Equipment must be prepared and configured correctly for cutting through the fault zone.
3. Gateroad reinforcement, such as polyurethane injection to strengthen the roof and ribs, should be implemented when the face is within 150-300 ft (45.7-91.5 m) of the fault zone,

4. Longwall navigation plan – all geological structures of the panel as exposed through gateroad development should be mapped.
5. If necessary, the longwall face crew should receive training on the navigation and gateroad preparation plans.

If the offset of the fault is less than the difference between the seam thickness and the closed height of the shields, the coal face can pass through the fault area without roof ripping and floor brushing. If the offset of the fault is greater than that difference, it is necessary to make an artificial slope on the floor by roof ripping and/or floor brushing so that the shearer and shields can pass through successfully. If both the roof and floor are soft, the shearer can cut through them easily. On the other hand, if the roof and floor are very hard, it may be necessary to blast them off.

### 7.8.2 Fault Mapping and Pre-Consolidation

If the coal reserves are suspected or known to contain many faults of different types, detailed mapping of fault occurrence in the property must be performed using geophysical methods (Koontz, 1994; also Section 3.6 on p. 122). In recent years, the seismic method is preferred for fault mapping. The smallest faults that can be mapped by 2-D seismic reflection surveying have offsets of 16.4-32.8 ft (5-10 m), depending on the quality of the data. For high quality 3-D surveys, faults with offsets as small as 6.56-9.8 ft. (2-3 m) may be detectable (Hatherly, 2006). In some cases, drilling of boreholes at strategic location is the most effective way to map the fault (Kendorski, 2003).

If the faults to be mined through have a large offset and a wide zone of broken, weak rock and coal, mining through them will result in difficult mining conditions such as roof falls, high longwall cross grades, and redistribution of in-situ stresses (Gou and Hu, 2006). In order to minimize the risk to personnel and maintain consistent production, a proactive strengthening of the fault zone is required (Pastars and Medthurst, 2007).

The fault strengthening program involves drilling, in-seam or from surface-to-seam, of an array of boreholes in and around the faults. Rock and coal cores are used to determine the zone of weakness and the quality of materials in and around faults. Pressurized grout consolidation of fine cement is then performed through these boreholes. Grout will permeate under pressure to fill voids and close joints, thereby strengthening the fault materials, while reducing water flow and providing for adhesive strengthening (NGCM, 1999).

Fig. 7.8.1 shows a flow chart for determining the feasibility of pre-consolidation. Note if pre-consolidation is not selected, then roadway and face stability program must be implemented. If pre-consolidation grouting is chosen, fault characterization and drilling and grouting programs follow. Once the orientation, offset, and dip of faults are determined, drilling and grouting programs follow. A drilling program involves the number, location, and direction of boreholes, and grouting programs include type, pressure, and volume of grout.

Active mining seldom triggers fault movement. In fact, a survey by Kendorski (2003b) showed that almost all mines carefully avoided faults in mining layouts and that fault reactivation has not been known to occur in coal mines in North America. He also presented a case study where a fault lay within a panel at the mine level, inclining away from the panel but within the angle of draw on the surface. The fault had about 1.5 ft of tight clay gouge and shuttered rock on the hanging wall, totaling about 4 ft (1.2 m) thickness perpendicular to the fault. The fault did not reactivate during or after mining.

Fault reactivation may occur in multiple-seam mining conditions where the strata are softer due to repeated mining. In such cases, Lee (1966) found that faults may be reactivated when: (1) the fault dips over and toward the panel center with the panel in the footwall, (2) the fault trace on the surface is about 0.3 times the depth toward the gob from the panel edge, and (3) if the fault extends beyond the edge of the panel. It is less likely to be reactivated when undermined by the panel.

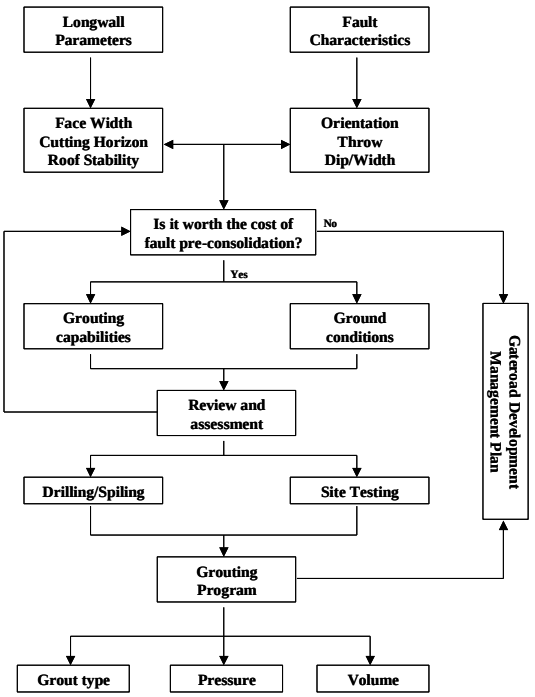


**Fig. 7.8.1 Flow chart for determining the feasibility of pre-consolidation (AMC Consultants, 2006)**

### 7.8.3 Geological Anomalies

As compared to room-and-pillar mining, longwall panel layout is very rigid, and since longwall is highly productive, any delay due to unexpected appearance of geological anomalies will cause dramatic reduction in panel and subsequently mine production.

There are many case studies demonstrating the adverse impacts of geological anomalies on the stability of longwall faces and gateroads (Miller, 1998; Su et al., 1999; Su et al., 2002b) leading to safety and production issues. Taking a proactive approach to map out the panel geology and develop a strategy to deal with the geological anomalies are pre-requisites for safe and consistent longwall production.

Jiang and Wells (1998) described a case study in which the geological anomalies in the longwall panels included severe seam undulation accompanied by drastic changes in coal thickness, changes in parting thickness, and massive sandstone channels. Roof falls and face failures due to parting failure occurred when a difficult mining condition existed, i.e., severe undulation of the mine floor and thick partings or a massive sandstone channel in the main roof. Analysis of shield leg pressure data indicated that mine roofs behave differently under different geological anomalies, including sandstone channels, floor undulation, and roof joints.

Severe roof or face stability problems occurred during several idle periods when a severe roof weighting event occurred. The effect of severe roof weighting can be minimized by advance knowledge of increased roof weighting and mining through the area without stopping. Early preparation is the key to continuous operation.

## 7.9 GATEROAD PILLAR EXTRACTION

For safety reason, the gateroad chain pillars described in Section 7.2 (p. 317) were not recovered during panel retreat mining. Therefore, the maximum coal recovery in a panel ranges from 70 to 85 percent. Recovery of chain pillars in the gateroad system involves supporting the entries and crosscuts, which, as described in Section 7.10 (p. 371), is expensive and time consuming.

In the past decade, however, gateroad pillar extraction has become a routine practice in one southern Appalachian coal mine (Hendon, 1998). This deep and gassy coal mine employs the 4-entry yield-abutment-yield system. Entries and crosscuts are 20 ft (6.1 m) wide. The yield pillars on both sides are also 20 ft (6.1 m) wide. The center abutment pillar is 200 ft (61 m) wide. In the past, the belt conveyor was located in the #2 or # 3 entry during section advance. After completing the development, the section belt was taken out and a longwall belt was installed in one of the outside (#1 or #4) entries. This required two belt installations. If the section belt could be used as the longwall belt, significant savings could be realized. So the decision was made to re-use the section belt in the #3 entry as the longwall belt, which required the extraction of the yield pillar between the #3 and #4 entries during retreat. This setup made the #4 entry an open entry during longwall retreat. Fig. 7.9.1 shows the conditions in the #4 entry and the yield pillar between #3 and #4 entries (Peng, 2007). On the face (looking outby), the 4$^{th}$ entry was supported by two rows of wood posts, 6 x 6 in. (152.4 x 152.4 mm) at the center. The roof stayed intact. But the floor heaved severely at the entry center, and some posts punched deeply into the floor, while others buckled. The yield pillar was stable with heavy spalling at the top. The 3$^{rd}$ entry was stable at all times. The roof was sandy shale.

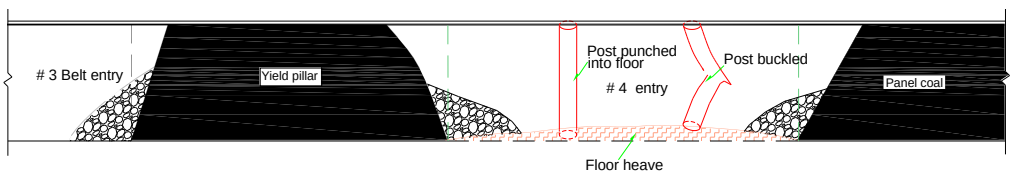


**Fig. 7.9.1 Headgate side of the face looking outby, showing the conditions of #4 entry and the adjacent yield pillar (Peng, 2007)**

Longwall panels in underground trona mine are also developed by the 4-entry system using borer type continuous miners producing curved ribs. Entries and crosscuts are 16 ft (4.9 m) wide. The three rows of chain pillars are equal in size, 125 ft (38.1 m) wide by 200 ft (61 m) long center-to-center. Trona has a UCS of 7,000 psi (48.3 MPa), which is stronger than the roof and floor, i.e., oil shale with a UCS = 3,500 psi (24.2 MPa). Arrangement of section and longwall belts is similar to that described previously (Steenberg and Davis, 1998).

Figure 7.9.2 shows the headgate side of the face covering only the open entry during longwall retreating. There were several moon-shaped rib cracks at the mid-height following the curved-rib shape of the entry, parallel to each other extending 3-4 ft (0.9-1.2 m) deep. Face spalling occurred as usual in this area. In fact, these curved cracks that were perpendicular to

the face intersected those that were parallel to the face and formed smaller slabs than in other areas of the face. This open entry did not cause any instability problems during shearer cutting. When the shearer was approaching this open entry, it lowered its cutting height and avoided cutting the roof bolts and straps. There was no supplementary support installed at the open entry before or during longwall retreat.

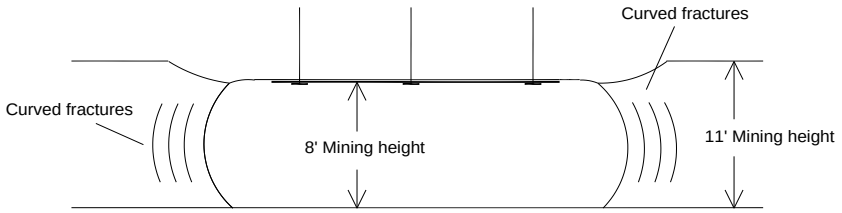


**Fig. 7.9.2 #4 entry cutting condition of Trona mine**

## 7.10 PRE-DRIVEN RECOVERY ROOM AND MINING THROUGH OPEN ENTRIES

### 7.10.1 Introduction

The continuing effort to increase productivity always calls for the design of wider and longer panels to reduce the number of longwall moves in a budget year, and in a longwall move, to reduce the move time. In addition, due to ventilation requirements, safety concerns, and other mine-specific conditions, cut-through entries from the headgate side to the tailgate side may be required somewhere near the middle of a very long panel. For instance, if the development work for the next panel to be mined runs late, creating cut-through entries at convenient locations to block out the next panel is a frequently used option. The main problem with those open entries is that the longwall needs to cut through those entries during retreat mining, which generates the front abutment and raises concern regarding the stability of those open entries.

The longwall recovery plan at the end of panel retreat mining calls for wire-meshing the roof for 10-13 cuts before the stop line. This is a tedious operation and slows down the rate of face advance considerably. In order to reduce this low-production period, the pre-driven open recovery room concept was developed in the late 1980s (Bauer et al., 1988; Listak and Bauer, 1989). Another reason for adopting an open recovery room is that if the roof condition in the designated location is bad, an open recovery room provides an excellent opportunity to pre-support the roof and insure its stability during the recovery operation.

There are other occasions when an open entry is beneficial. For instance, if a geological fault causes a poor roof condition and is encountered on the panel side during gateroad development, this weak zone may be taken out during development by driving an open entry along the fault line and installing necessary supporting systems for the entry to prevent premature instability during retreat mining. In other instances, mine management may, for whatever reasons, decide to extend the length of the previously driven shorter panels so the bleeder entries in those shorter panels or other previously driven transportation entries can become open entries in the new panels.

### 7.10.2 Methods of Supporting Open Entries or Pre-driven Recovery Rooms

The primary supports for open (or cut-through) entries and recovery rooms are normally similar to other development entries in the same mines. The secondary or supplementary

supports installed to handle the abutment pressures during retreat longwall mining can be divided into the following three types (Fig. 7.10.1) (Peng, 2000a):

1. Complete backfill of open entries
2. Supplemental roof and/or rib bolt reinforcement only - no standing support
3. Rows of standing supports with or without supplemental roof and/or rib bolt reinforcement

**1. Complete Backfill of Open Entries**

The most commonly used material for backfill is flyash mixed in various proportions with artificial cements, e.g., a grout mix consists of flyash, 10-23% cement, and a foaming agent. By entraining air in the mixture, the foaming agent reduces the amount of material required to fill the entries, improves the pumping characteristics of the mix, and reduces problems associated with excess bleed-off water underground (Seymour et al., 1998). Depending on the coal and roof rock properties, backfilled materials with a designed uniaxial compressive strength of 300-1,000 psi (2.07-6.90 MPa) and modulus of deformation around 1 x $10^5$ psi (0.7 GPa) have been used (JS Chen et al., 1997). In this method, the backfill material is pumped into the entries via surface boreholes until it completely fills up the open entries. Pressurized pumping may be required in order to make sure the gap between the roof and the top surface of the grouting material is as small as possible. Instrumentation of backfilled cross-panel entries during longwall retreat indicated that most of the mining-induced load was supported by the cross-panel entry pillars. The backfill provided stability for the roof and floor of the cross-panel entries/crosscuts and also confined the pillars, significantly improving their load-carrying capacity (Seymour et al., 1998; JS Chen et al., 1997).

This method is the safest of the three and must be used when the roof is very weak and cannot maintain any entry roof span when the front abutment pressure arrives. However, since it requires a vast quantity of material to backfill entire entries/crosscuts, it is normally the most expensive. Figure 7.10.1A shows an example of this backfill system.

**2. Supplemental Roof Supports with or without Rib Reinforcement**

If the main and/or the immediate roofs are strong and free of major fractures or geological defects, supplementary roof supports alone (without any standing supports) may be used (Smyth et al., 1998; Oyler et al., 2001). The supplemental support system must be well designed to cope with the incoming front abutment pressure, the shields must be in good working condition, and they must have sufficient capacity to support the roof structure as the face cuts into the open entry. The most critical period occurs when the face is approaching an open entry with less than 10 to 15 ft (3.1 to 4.6 m) of coal block left, or according to Thomas (2008), when the ratio of fender pillar width-top-height is between 0.7 and 1.2. Because this is approximately the influence zone of the peak front abutment pressure, and if the coal is soft, sloughing off on both sides of the remaining coal block will cause the unsupported region between the remaining coal block and the most inby row of support in the open entry to increase greatly and suddenly, thereby increasing the roof load. The supplementary support system usually consists of heavy-duty high strength cable bolts and cable trusses. The cable bolts must be sufficiently long and installed vertically to reach the main roof. For the cable trusses, the inby side of the inclined bolts must be sufficiently long (minimum 12 ft or 3.66 m) and installed at lower angles so that they can prevent premature roof falls in front of the shields as the face approaches the open entry. The inby side of the open entry ribs should be supported with rib bolts and wiremesh. Figure 7.10.1B shows an example of the roof support system. It is

also important that shields should have sufficient capacity to maintain the roof level as they approach the open entry, because at this point the strong roof beam built by the supplemental supports over the open entry is bridged between two abutments: one is the coal pillar on the outby side and the other is the shields (plus whatever is left off the solid coal panel) on the inby side.

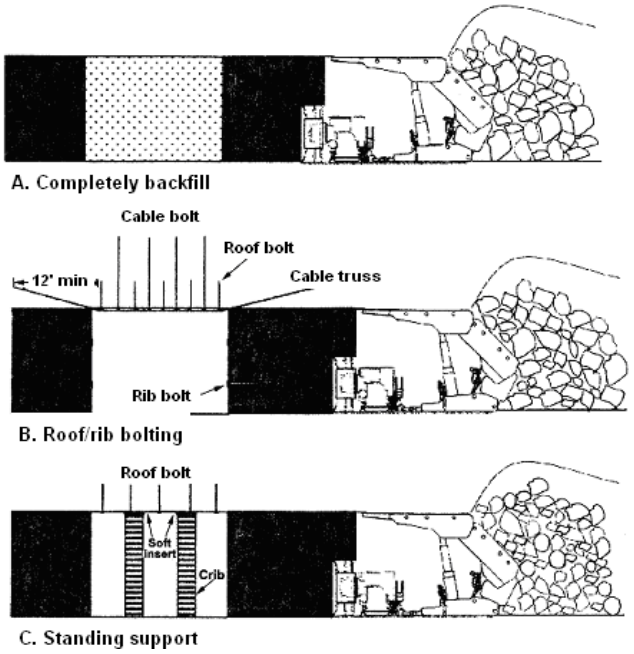


**Fig. 7.10.1 Three general types of roof and rib supports for open entries (Peng, 2000)**

### 3. Supplemental Standing Supports with or without Supplemental Roof Supports

In-between the two extreme methods described above, there are several others that have been used (Fig. 7.10.1C) (Barczak, 2007; Bauer et al., 1989; Bookshar et al., 1998; Heasley et al., 2003: Tadolini et al., 2002; Zhang et al., 2006). Support density varied considerably from a low of 68 psi (0.47 MPa) to a high of 756 psi (5.21 MPa). Depending on roof strength and entry width, open entries can be supported by one or more rows of standing supports with or without supplemental roof reinforcement. For stronger roofs devoid of any geological anomalies, one row of high strength cribs at specified intervals may be sufficient. Conversely, for weaker roofs or wider recovery rooms, three rows (one row each against the inby- and outby-side ribs and the third row at entry center) of cribs at the specified interval are preferred (Wynne et al., 1993). The most common one is two rows of cribs for 16-20 ft (4.9-6.1 m) wide entries. Again, the inby side cribs are critical and must be designed to act as an abutment to support the constructed roof beam as the face approaches. Various types of cribs have been used successfully, including wood, concrete, and flyash cribs. In recent years, cribs made of concrete-like synthetic materials have been used. There are two kinds of concrete-like crib materials available: one is prefabricated and the other is pumped in. The former requires underground vehicular transportation, while the latter requires one or more surface boreholes and surface pumping facilities, therefore it is exclusively used. The crib material should have a uniaxial compressive strength varying from 2,000 to 3,000 psi (13.7 to 20.7 MPa) and be

spaced so that it provides a support density varying from 300 to 1,000 psi (2.07 to 6.9 MPa). In addition, it is important that a softer material like wood blocks or a pumpable cement bag be inserted between the top of the standing support and the roof to allow initial elastic convergence of the roof as the abutment pressure sets in so that the cribs are not subjected to undue localized pressures making them crack up prematurely.

An example of successful ground control design for a pre-driven recovery room in the Pittsburgh seam was demonstrated in a case study. 3-D finite element computer modeling was used to design the roof support system for the pre-driven recovery room (Fig. 7.10.2) (Zhang et al., 2006). The standing support consisted of three rows of pumpable cribs, 30 in. (762 mm) in diameter with 6 ft. (1.8 m) spacing. The primary supports were combination bolts with steel straps and wiremesh on 4 ft (1.2 m) centers. One row of cable bolts, 12 ft (3.7 m) long, was installed on each side. The panel was 1,250 ft (381.1 m) wide and 500-700 ft (152.4-213.4 m) deep. Mining height was 8 ft (2.4 m), and entries and crosscuts were 16 ft (4.8 m) wide. The roof consisted of, in ascending order, gray clay shale, 5-15 ft (1.5-4.6 m), shale, 0-30 ft (0-9.1 m), and limestone 0-35 ft (0-10.7 m).

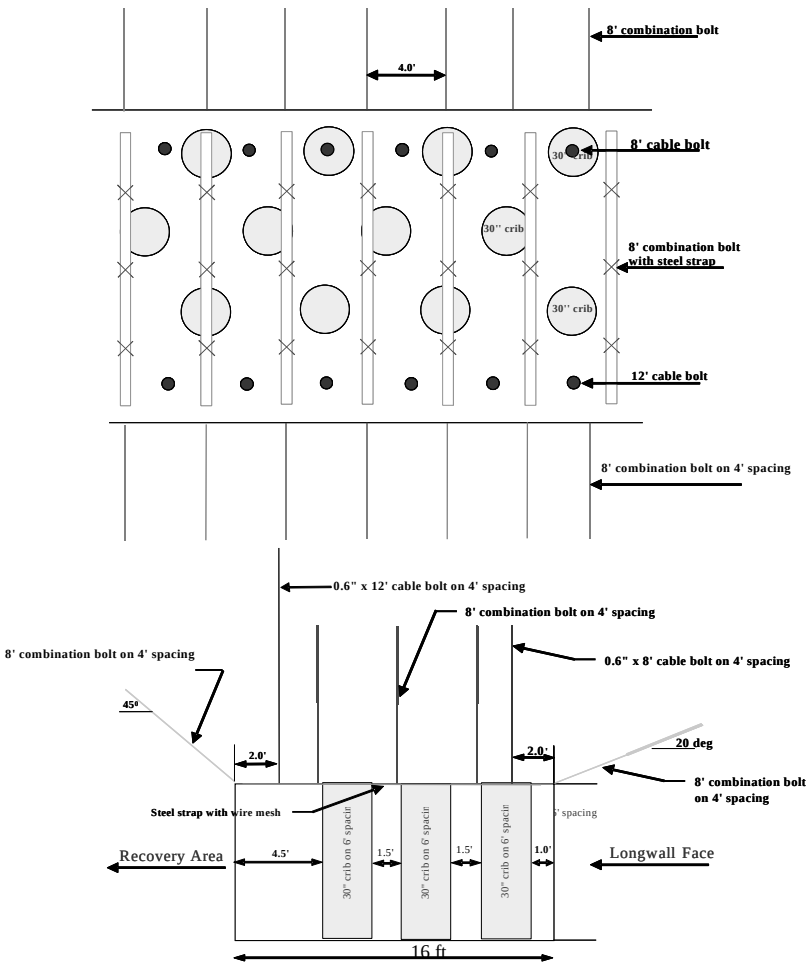


**Fig. 7.10.2 Support design for the longwall recovery (Barczak et al., 2007)**

The front abutment began to show up when the face was 100 ft (30.5 m) inby (Barczak et al., 2007). The increase was very gradual until the face was 25 ft (7.62 m) inby. The pumpable cribs, panel fender pillar, and longwall shields all yielded during this period (Fig. 7.10.3). When the face was about 21 ft (6.4 m) from the recovery room, the inby side of the fender pillar yielded, forming an isolated pillar. Pillar stress continued to increase and reached the peak stress of 7,500 psi (51.7 MPa) at 21 ft (6.4 m). Pillar stress began to drop when the face was 15 ft (4.6 m) inby. Pillar stress dropped rapidly and failed at 11 ft (3.4 m) (Tadolini and Zhang 2007).

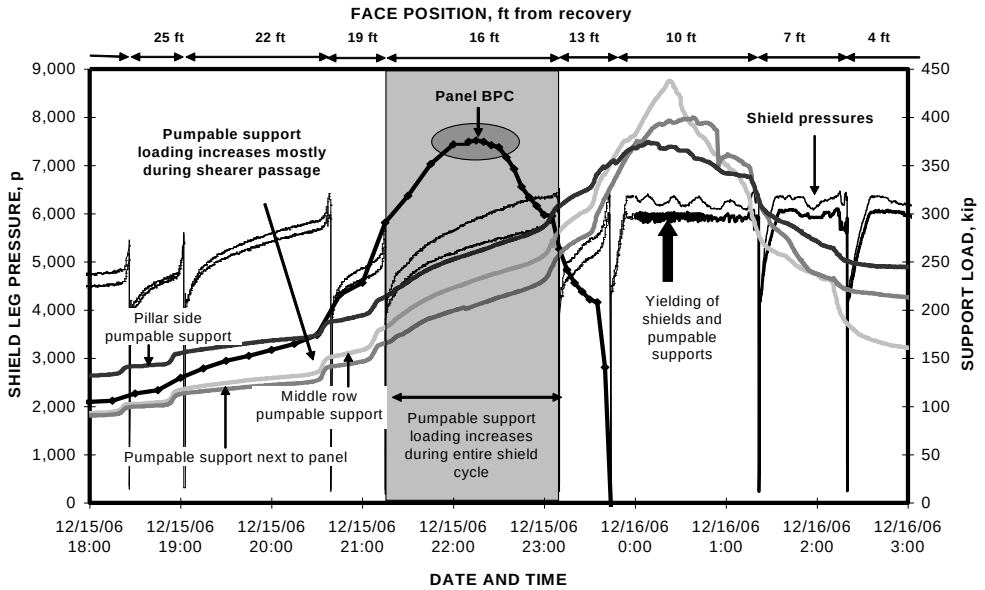


**Fig.7.10.3 When the longwall face was approximately 16 ft (4.9 m) inby the recovery room, the pumpable supports loading increased during the full shield cycle (Barczak et al., 2007)**

## 7.10.3 Support Design Consideration

1. In the design of an open entry support, support resistance and support materials are the two major factors. Support resistance, which more or less determines the type of open entry supports required, must match roof geology, mining, and stress conditions. The support materials must have sufficient strength and be disposable (i.e., easily cuttable by the shearer, and the cut-out fragments are small so that they will not got stuck in the AFC).

2. Intuitively, the second method, supplemental roof with or without rib bolt reinforcement, seems to be the most desirable if all requirements can be met. But the most frequently cited criticism for this type of support is that it is too expensive. All factors considered, if cut-through entries must be used in longwall panels, the fail-proof measure is to drive the roof bolts in at an angle approximately 30 degrees from the roofline toward the face and supporting the entries with the third method, standing supports with or without supplemental roof/rib bolts (Barczak et al., 2007; Heasley et al., 2003; Tadolini et al., 2002; Zhang et al., 2006).

3. If the first and third methods (complete backfill and standing supports with or without supplemental roof/rib bolts) are employed, consideration should be given to the cuttability and disposal of the backfilled and standing support materials. Harder materials, either by nature or due to compression by the abutment pressure, will take longer to cut, which may eventually offset the time gained from not wiremeshing. When cutting under high pressure, these materials may also break in large pieces and cause handling problems in the armored face conveyor.

4. Wood cribs alone are too soft to use as standing supports. They also present problems for cutting and handling in the slope belt and separation in the preparation plant.

5. Since the normal width of a recovery room is 22 to 24 ft (6.71-7.32 m) wide, wiremeshing prior to the face reaching the stop line may still be required if the roof is very weak. In such cases, the advantage of using a pre-driven recovery room may not be obvious. Therefore, in order to take full advantage of a pre-driven recovery room, the open recovery room must be 32 to 36 ft (9.75-10.98 m) wide. In such cases, the third method, rows of standing supports plus supplemental roof bolt reinforcement, must be used.

6. Everything considered, the safest approach for open entry support is the third method, standing support with supplementary support. The standing support system itself or in combination with soft inserts, must be chosen so that it can absorb the initial onslaught of the front abutment pressure without cracking up. In other words, the chosen standing supports should yield somewhat as the front abutment first arrives and then maintain high supporting capacity to the end (see Section 7.13.3 for various types of standing supports)

## 7.11 HARD-TO-CAVE ROOF

### 7.11.1 Introduction

On occasion, the stable or hard-to-cave strata (Fig. 7.3.6), mainly thick sandstone, limestone, or conglomerate dives down to near the coal seam top and will overhang for a considerable length before it caves. When and if caving occurs, it generates a wind blast that poses a severe hazard to miners working around the face. Therefore, for hard-to-cave roofs, special measures are required both for safety and production purposes.

Various measures have been developed to evaluate the cavability of roof strata (Haramy et al., 1988; Sarkar, 1998; Singh and Dubey, 1994; Wu and Karfakis, 1993). In general, cavability is evaluated based on two types of caving mechanisms; first caving and periodic caving. For first caving, fixed-end beams are used, and for periodic caving, cantilever beams are used for calculating the caving length and stored energy in the roof or coal. It is important to emphasize that hard-to-cave roof strata do not necessary mean a strong rock type, such as massive sandstone and conglomerate. Massive shale is also hard to cave (Sarkar, 1998). The cavability of cantilevering strong roofs is controlled by the roof geometry, overburden load, rock mechanics properties (UCS and thickness), and equivalent moduli. For bridging strong roofs, the cavability is also affected by the concentrated abutment pressure and floor characteristics. The front abutment pressure is the largest contributor to the strain energy stored in the roof and coal seam. The highly concentrated front abutment pressure causes most of the strain energy to be stored in close proximity to the working longwall face.

### 7.11.2 Methods of Controlling Hard-to-Cave Roofs

Methods of alleviating the adverse effects of the hard-to-cave roof can be broadly classified into two categories: strengthening roof support in the longwall face area and treatment of hard-to-cave roof in the gob (Xu, 1986; Haramy et al., 1988) (Figs. 7.11.1 and 7.11.2).

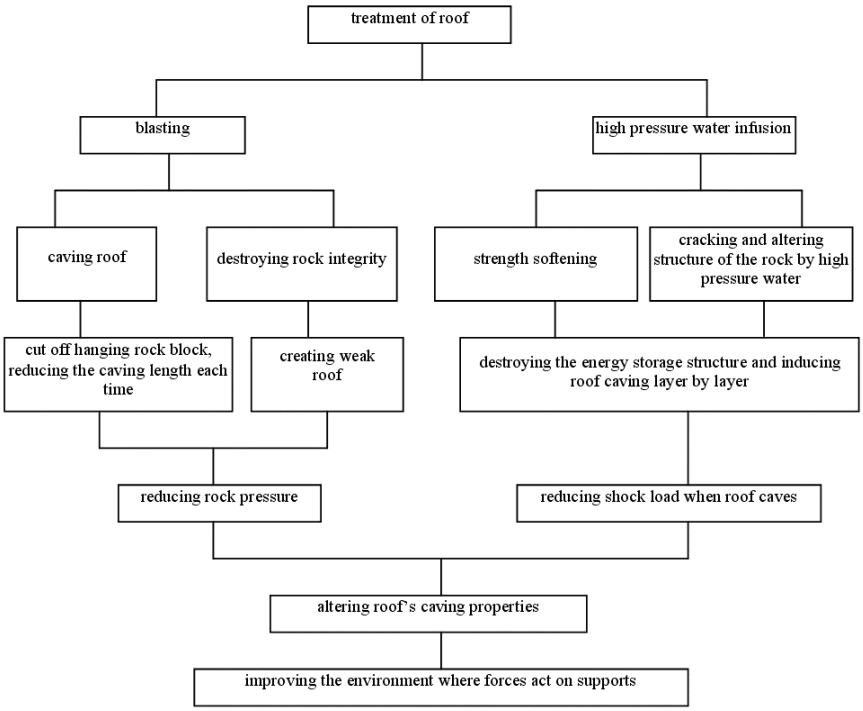


**Fig. 7.11.1 Flow chart for handling hard-roof caving (modified from Xu, 1986)**

Moderating the hard-to-cave roofs is to reduce the intensity of roof action by altering the mechanical properties of the rock strata, thereby reducing the forces acting in the face. Face working conditions can be improved by increasing shield support capacity and its working characteristics to resist shock and horizontal force. Methods of raising the support's ability to cope with the impact of hard-to-cave roofs include selecting a proper shield capacity and the shield's supporting characteristics. A shield should have the capacity to induce caving of the roof at its rear edge. In addition to sufficient capacity, the structural components of shields should be sufficiently strong to resist the instantaneous shock load from the caving roof and the horizontal force acting from the gob to the face and repeated pounding of large falling rock blocks (Fig. 7.11.2).

The major methods employed to moderate hard-to-cave roofs are blasting and hydraulic infusion or fracturing. Blasting involves drilling holes between shields into the roof toward the gob and blast it off with explosives. The number, inclination, and length of holes, plus the amount of explosives per hole and total explosives depend on the roof characteristics (Pal Roy et al., 1997). Infusion with high pressure water can weaken and soften hard rocks such as sandstone. Water infusion can increase caving height, increasing caving angle from the horizontal and reducing the sizes of caved blocks (Niu and Gu, 1982) (Fig. 7.11.1). Hydraulic

fracturing, especially under shallow cover, can split a thick roof into thinner layers, making it easier to cave (Shimada et al., 1998; Su et al., 2002a; Mills et al., 2000). Two examples are discussed below.

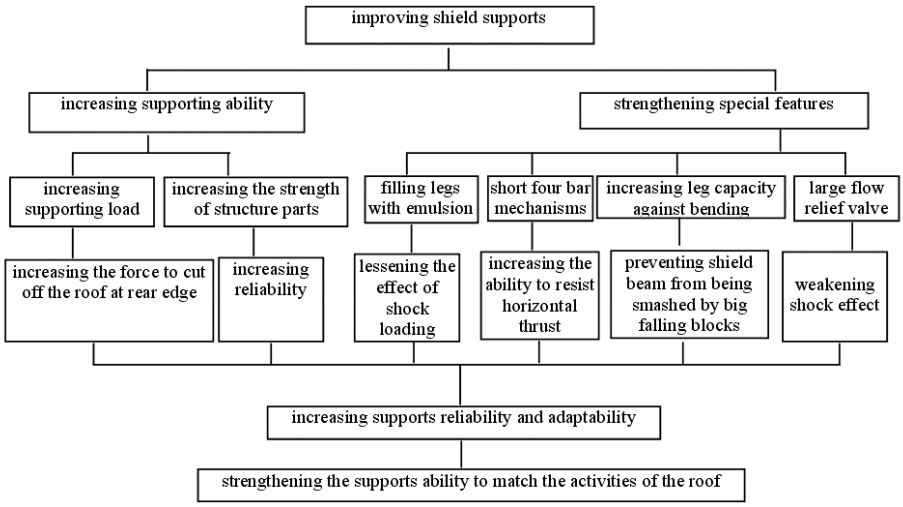


**Fig. 7.11.2 Flow chart for improving support capability (modified from Xu, 1986)**

Su et al., (2002a) described a case in the Pittsburgh seam where a large sandstone channel, 47 - 70 ft (14.3-21.3 m) thick and within 4-5 ft (1.2-1.5 m) of the coal seam top, meandered across three panels, B12, B13, and B14 (Fig. 7.11.3). The uniaxial compressive strength (UCS) and Brazilian tensile strength of sandstone were on average 10,000 psi (68.97 MPa) and 1,000 psi (6.9 MPa), respectively. When the sandstone was first mined under at B12 panel, no preparation was done. The face advance rate was slowed to 9.8 ft/shift (2.99 m/shift) and took seven weeks to mine through, with a total production downtime due to bad top of 30,600 minutes. Surface hydraulic fracturing using nitrogen foam in 5-in. and 6-in. diameter holes was then implemented in B13 and B14 panels. Due to the shallow depth at which the vertical stress would be the minimum of the three principal stresses, a horizontal (pancake) fracture, rather than a vertical fracture (as often observed for the cases of deep oil reservoirs), was created in the sandstone stratum.

Furthermore, since the two horizontal principal stresses were not equal, the horizontal fracture created would be elliptical, not circular, with axes of the ellipse in relative proportion to the principal stress magnitudes. With hydraulic fracturing the average advance rates were 16.6 and 17.1 ft/shift (5.06 and 5.21 m/shift) with total downtime of 3,655 and 3,265 minutes for B13 and B14 panels, respectively. Overall production rates for B13 and B14 were 70 percent better than that for B12.

Mills et al., (2000) performed a successful case of forced caving in Australia. The conglomerate roof was 30-50 m thick with UCS 7,250 $\pm$ 1,450 psi (50 $\pm$ 10 MPa) and tensile strength 580 psi (4 MPa) and would overhang over an area 984 ft (300 m) long by 1,324 ft (100 m) wide. Once caved, the windblast generated would be extremely hazardous to miners at the face. A surface trial of hydraulic fracturing showed that a horizontal fracture could be created parallel to and within 16.4 ft (5 m) of a free surface and that this fracture would grow to a radius of 82 ft (25 m).

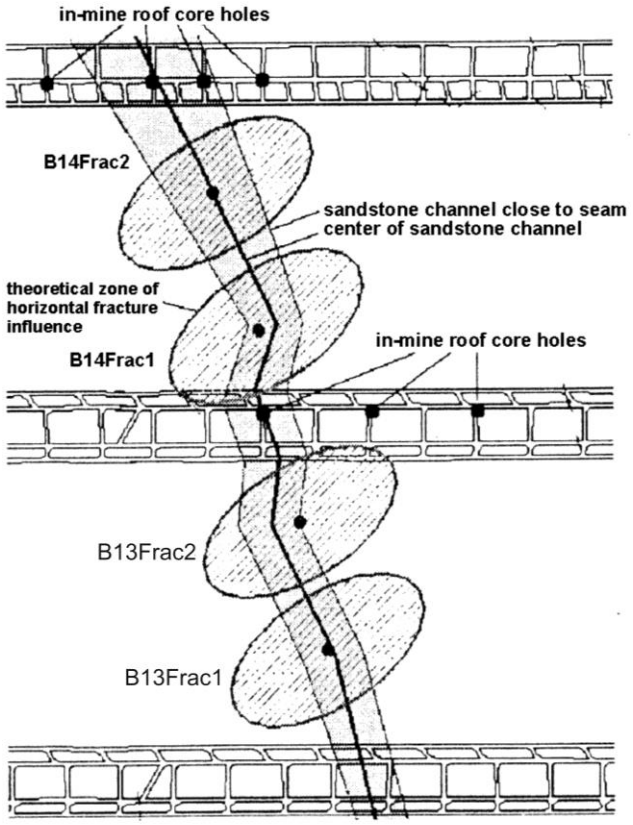


**Fig. 7.11.3 Sandstone channel and frac holes over three longwall panels (Su et al., 2001)**

Underground observation and surface borehole monitoring also confirmed that after caving, the shape of the roof top would resemble a flat arch (Fig. 7.11.4), 39.4 - 49.2 ft (12-15 m) high at the center. In the first underground hydraulic fracturing operation, an inclined hole was drilled upward from the headgate toward the center of the panel to induce caving (Fig. 7.11.4B and C). The results indicated that approximately 70,000 tons of rock (15 m of standing gob) had been induced to cave.

The hard-to-cave roof generally induces severe first and periodic weightings, causing various degrees of roof control problems that range from severe roof falls at the face to support failures and face collapse (Gupta and Ghose, 1992; Hsiung and Peng, 1985b; Singh and Hebblewhite, 2000). In some cases, even caving of the thick, hard-to-cave roof strata in the immediate previous panel caused windblast and sizable seismic events around the tailgate of the active panel (Akinkugbe et al., 2007). Therefore, for safety and production's sake, detailed mapping of the stronger units in the overburden through surface borehole drilling or geophysical methods are strongly recommended. Armed with the knowledge of characteristics of the hard-to-cave units (i.e., strength, thickness, and relative location with respect to the coal seam), their adverse effects, such as weighting, can be estimated using Fig. 7.11.5 which relates weighting severity to panel width and thickness of massive strong units (Frith et al., 2000; Frith and Creech, 1997).

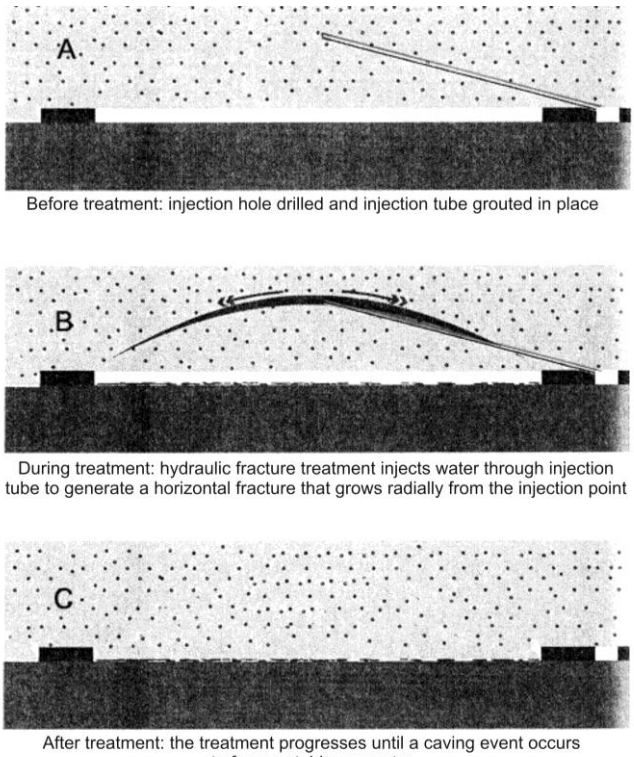


**Fig. 7.11.4 Sequence of induced caving of conglomerates by hydro fracturing (modified from Wischusen, 1999)**

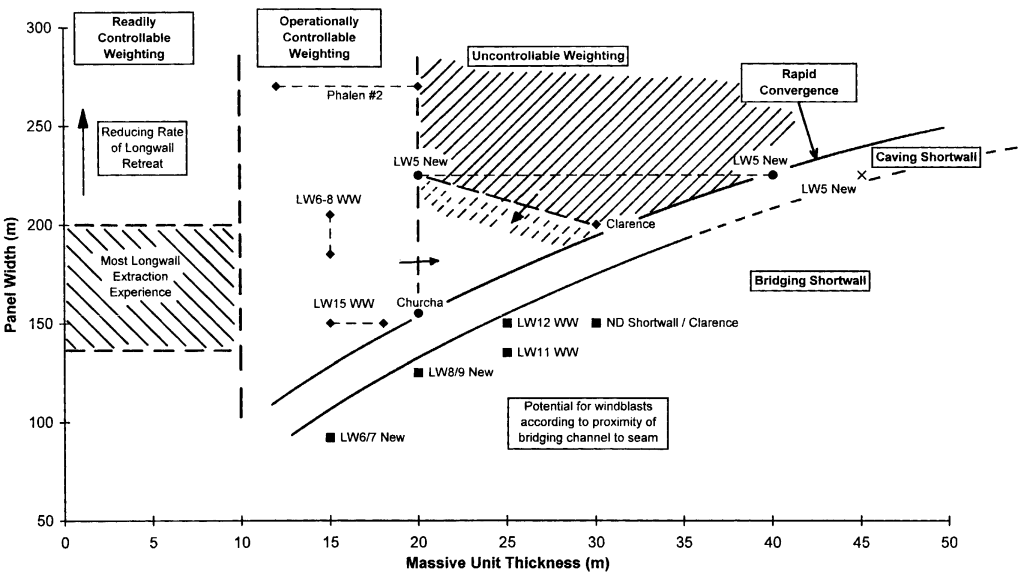


**Fig. 7.11.5 Classification of weighting condition with respect to panel width and thickness of massive unit (Frith et al., 2000)**

## 7.12 BRIDGING AND CYCLIC FAILURE OF STRONG ROOF LAYERS

Experience in longwall mining shows that ground pressure in gateroad systems is low in the 1st and 2nd panels in a virgin reserve. Ground pressure increases in the 3rd panel, especially the tailgate side, and continues to increase as more panels are developed side by side in sequential order. Depending on geological conditions, ground pressure in the 4th or 5th panel may be so high that roof control problems occur in the gateroad systems. Thereafter, the same events repeat again in a cyclic manner (Carmen, 1965: Agapito and Goodrich, 2000).

Numerical modeling using the Pittsburgh seam geological column of 1 to 5 longwall panels (Peng and Su, 1983) showed that caving height increases with the number of panels and that for the 5- panel model, the caving height of the central panel is deeper than those on both sides due to the interaction between panels (Fig. 7.12.1). The 43 ft (13.1 m) immediate roof fails all at once upon mining. Thereafter the failure areas progress upward at a much slower pace until the final stable configuration is reached. The final caving height in the 1-panel model stops immediately below the 25 ft (7.62 m) limestone layer. In the 2-panel model, it stops short of breaking through the 25 ft (7.62 m) limestone layer; and in the 3-panel model and 4-panel models, it stops just short of breaking through the 20 ft (6.1m) sandstone layer. In the 5-panel model the final caving height at the central panel stops at the middle of the 50 ft (15.2 m) thick limestone layer, with the caving height of the two immediate neighboring panels stopping at the middle of the 20 ft (6.1 m) sandstone layer. The convergence on the gateroads increases with the number of panels mined.

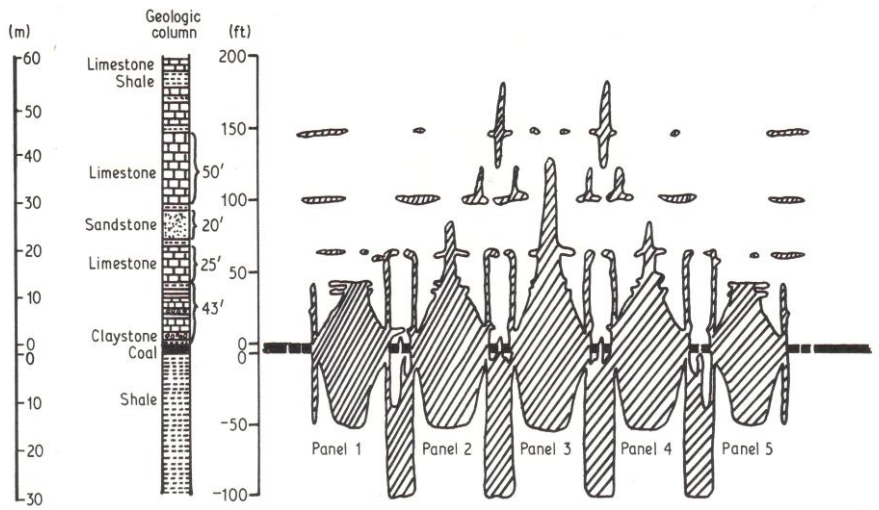


**Fig. 7.12.1 Areas of roof failures in the 5-panel model (Peng and Su, 1983)**

The effectiveness of the bridging and breakthrough of the main roof competent strata depends strongly upon the relative location of these strata with respect to the roof line and their thickness. The closer the strata are to the roof line, the more effective are their bridging and breakthrough. Therefore, the amplitude of cyclic maximum ground pressures on the gateroads depends strongly on the thickness of the main roof competent strata and their relative locations with respect to the roof line. As to the cyclic period, the timing of breaking through the most effective main roof competent strata appears to be the dominant factor. This timing, however, depends not only on the thickness and location of the competent strata, but also the panel

width, mining height, overburden depth, and strength of the competent layers. The most effective way to control the adverse effects of cyclic ground pressure is to put a barrier pillar of sufficient width at regular intervals, for instance, every 4-5 panels depending on mining and geological conditions, to isolate the effect of previous panels.

## 7.13 TAILGATE AND HEADGATE SUPPORTS

### 7.13.1 Introduction

As stated in Section 1.3.2 (p. 18), entry roof support can be divided into two types: primary and secondary or supplementary supports. The primary support, mainly roof bolts, are installed in cycles immediately or soon after the continuous miner's cutting. Secondary supports, on the other hand, are installed sometime or long after the continuous miner's cutting. Secondary supports are usually longer bolts/cable bolts or standing supports that require more time and labor to install. For longwall mining, the secondary supports are additional supports installed to cope with the moving front and side abutment pressures during face retreat. This way of installing supports, i.e., two-stage support installation, allows rapid development of gateroads.

### 7.13.2 Primary Supports for Gateroads

For entries, 17-20 ft (5.2-6.1 m) wide that are developed by conventional continuous miners (place change method), the primary supports are 3/4-in. (19 mm) or 7/8 in. (22 mm) diameter by 6-8 ft (1.8-2.4 m) long in a 4×4 ft (1.2 × 1.2 m) pattern. They can be either fully-grouted resin, combination, or resin-assisted high-tension bolts.

For those entries 15-16 ft (4.6-4.9 m) wide that are developed by the in-place method, two side bolts, 7-9 ft (2.1-2.7 m) apart and 3-4 ft (0.91-1.2 m) between rows, are installed in cycle with or without a strap. A center bolt, if needed, is installed immediately afterward. Bolt types are similar to those for the entries developed by the place-change method. In the entry/crosscut intersections, one to four cable bolts, 0.6 in. (15.2 mm) diameter by 14-16 ft (4.3-4.9 m) long may be added soon after development.

### 7.13.3 Supplementary Supports

#### 1. Headgate

Depending on the severity of the front abutment pressure, supplementary supports in the form of cribs or props/engineered props, such as posts, wood cribs, ACS, and propsetters may be added at the headgate T-junction, especially at the entry side of the headgate and crosscut intersection located immediate outby the face.

#### 2. Tailgate

#### A. Type of tailgate supports

Prior to 1985, when gateroad chain pillar design was in its infancy, there were many tailgate problems. Since then a combination of properly designed chain pillar system plus tailgate secondary support has resolved the problems, even though the tailgate has been designated by law since 1985 as an emergency escapeway that must be kept open all times.

Traditionally, tailgate support employs one or two rows of wood cribs, either side by side or staggered. But as panel lengths grow longer, timber for tailgate supplementary support has

distinctive disadvantages, mainly for reasons of safety and cost (Peng, 2006). Subsequently, various alternative tailgate supports have been developed. There are seven types of secondary supports: (1) conventional wood cribs, (2) engineered wood cribs, (3) conventional and engineered wood posts, (4) non-yielding concrete, (5) deformable concrete, (6) yielding steel, and (7) cribless supports (Barczak et al., 2004; Frith, 2000; Mucho et al., 1999; Tadolini and Trackemas, 1995; Tadolini et al., 2000).

Conventional wood cribbing (Fig. 7.13.1) is made of 2, 3 or more crib blocks per layer, making it a 4-, 9- or more point crib. Each successive layer is placed perpendicular to the previous layer to form an open box arrangement. The most common one is the 4-point crib. A wood crib is the softest type and may not have consistent quality. The wood will not take much load before it deforms substantially. Loads increase with deformation but at a decreasing rate. Wood strength is much higher when stress is applied parallel rather than perpendicular to the grain; conversely, displacement under load is much greater when stress is applied perpendicular rather than parallel to the grain (Schissler, 1993). Parallel to the grain, it is very stiff but fails suddenly. Perpendicular, it is soft but yields indefinitely. In selecting a wood crib, strength, stiffness, and stability are major factors; wood cribs should be constructed from wood of the same species or similar compressive strength; with a minimum overhanging distance ½ the width of the crib block and with height-to-width ratio between 2.5 and 5 (Barczak and Gearhart, 1993). The stiffness of wood cribs can be increased by increasing the number of crib blocks per layer or by increasing the width of the crib block.

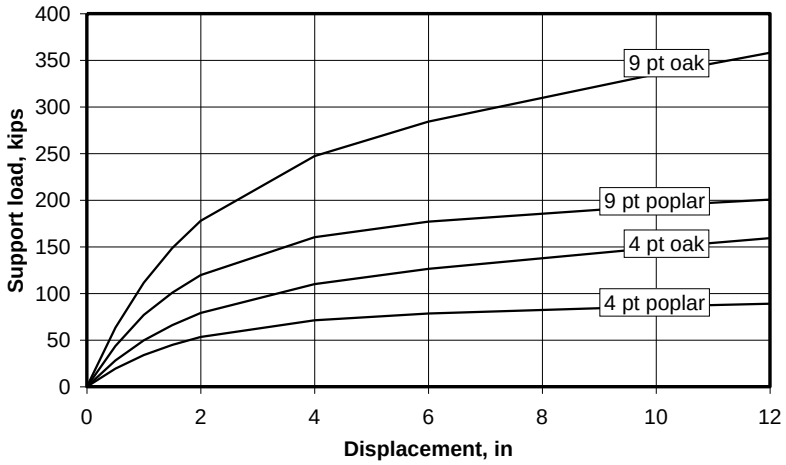


**Fig. 7.13.1 Load-displacement curves for conventional wood cribs (Mucho et al., 1999)**

The engineered wood cribs (Fig. 7.13.2), such as Hercules and Link-N-Lock cribs make use of timber loaded parallel and perpendicular to the grain. Maximum effect is made of the orthotropic properties of timber resulting in cribs having superior strength, high initial stiffness and controlled post yield deformation (Faure, 1993). Blocks and timbers can be combined in many different ways, each of which has a specific combination of block on block, timber on timber, and block on timber contact area, resulting in a unique performance. The quality of engineered cribs is uniform, and the cribbing takes loads faster than the conventional type. The crib reaches the peak load at around 2 in. (52 mm) deformation. Thereafter, load increase is minor or becomes steady. Link-N-Lock cribs constructed from thinner blocks have failure loads much less than thicker ones (Galvin and Offner, 2000).

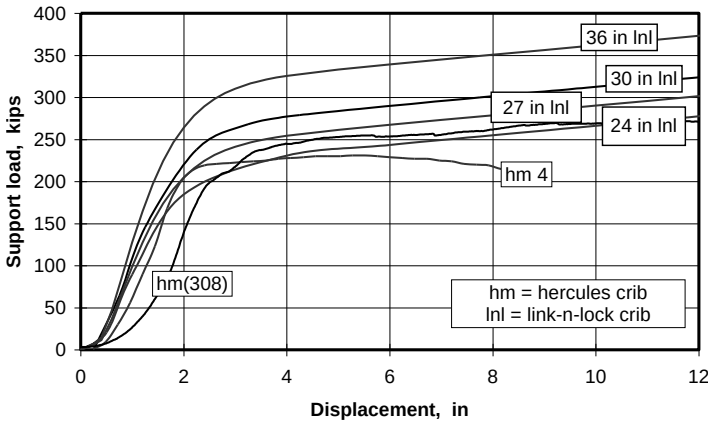


**Fig. 7.13.2 Load-displacement curves for engineered wood cribs (Mucho et al., 1999)**

Conventional timber props (Fig. 7.13.3) take loads quickly but fail quickly soon after. The engineered timber props (Propsetters) (Fig. 7.13.4) are designed to improve the yield capability of a conventional timber prop by engineering the bottom section of the post to deform in a controlled manner and limit the load development in the main body of the post so that it does not buckle (Barczak and Gearhart, 1995). The standard 8.5 in. (215.9 mm) diameter Propsetter, installed and prestressed, is capable of supporting over 50 tons of load at 2 in. (50.8 mm) of deflection. The standard base has a total of 400 $in^2$ (0.258 $m^2$) contact with the floor and 462 $in^2$ (0.298 $m^2$) with the roof (McCartney et al., 1995). It will take a load quickly but maintain that peak load as it deforms for a considerable length of time.

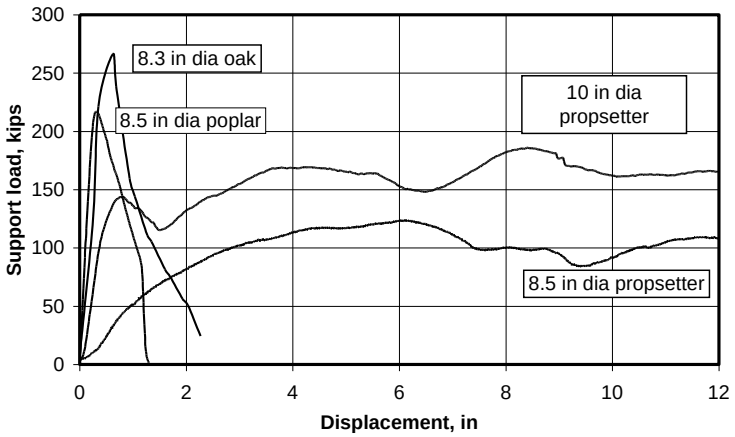


**Fig. 7.13.3 Load-displacement curves for conventional and engineered timber props (Mucho et al., 1999)**

Non-yielding concrete supports (Fig. 7.13.5) will also take a load fairly quickly until it reaches the peak load, which is the highest among all six types of supports. But these supports fail quickly after the peak load is reached.

ACS yielding steel props (Fig. 7.13.6) can be adjusted by using different head plates so that the peak load is reached at different rates and after that drops gradually to a residual load.

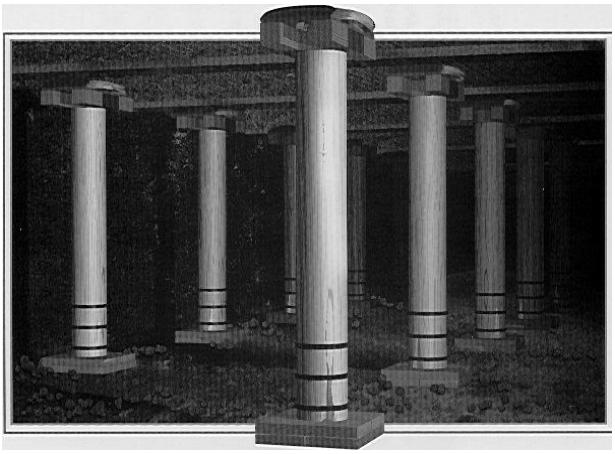

**Fig. 7.13.4 Propsetter™ (Barczak and Tadolini, 2006)**

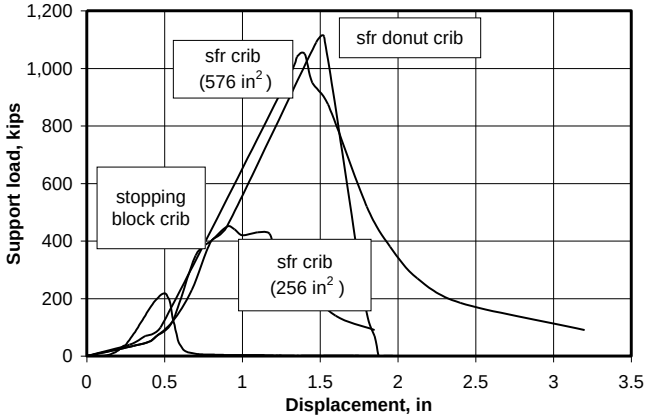


**Fig. 7.13.5 Load-displacement curves for non-yielding concrete supports (Mucho et al., 1999)**

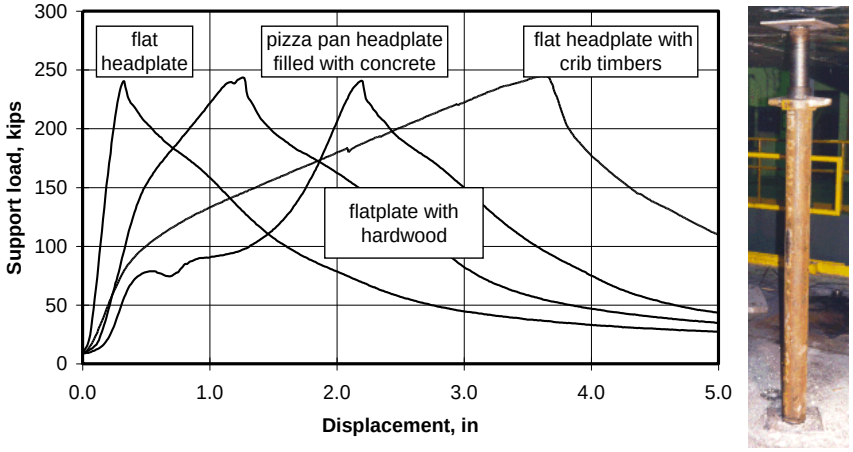


**Fig. 7.13.6 Load-displacement curves for ACS (yielding steel) props (Mucho et al., 1999)**

Among the deformable concrete supports (Figs. 7.13.7 and 7.13.8), Cans, made of steel containers filled with concrete, are the most stable. They perform well in both higher mining heights and large deformation environments that include 2-3 ft (0.61-0.91 m) of floor heave, which produces large lateral displacements of the base relative to the roof contact (Barczak and Tadolini, 2005). In this respect, no other support can match the stability and high yield performance of the Can support. The Cans take the load quickly and reach peak load fairly quickly. After that they maintain peak load for a considerable time. The only disadvantage of the Can is that it has to be topped off with conventional wood crib blocks to establish roof contact (Fig. 7.13.8B). These wood blocks reduce the initial stiffness of the Cans by up to 50 percent. For this reason, a prestressing unit has been introduced recently (Fig. 7.13.8A).

The support loading profiles of pumpable cribs is characterized by a high initial stiffness with peak loading occurring at less than 1 in. (25.4 mm) of roof-to-floor convergence, followed by significant load shedding with a post failure capacity comparable to that of wood cribbing (Figs. 7.13.7 and 7.13.9) (Barczak et al., 2003). The strength of the cribs decreases with increasing water-to-solid ratio and length of curing time.

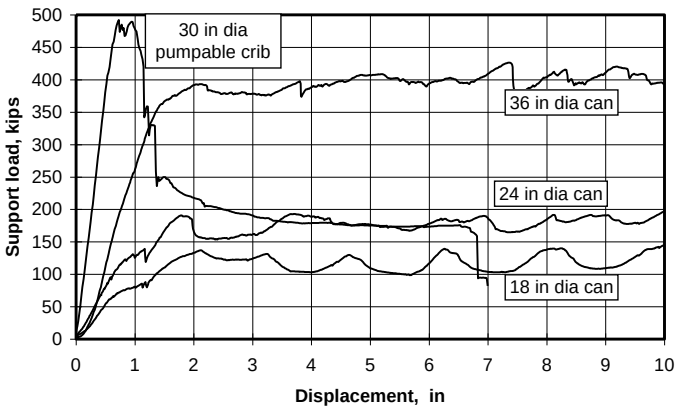


**Fig. 7.13.7 Load-displacement curves for deformable concrete support (Mucho et al., 1999)**

**A** **B** **C**

**Fig. 7.13.8 Can supports**

**Fig. 7.13.9 Pumpable cribs**

Cable bolts have also been used successfully for tailgate supplementary support in soft and stable roofs (Frith, 2000; Koehler et al., 1996; Tadolini et al., 2000; Tadolini and Trackemas, 1995). This type of support, contrary to standing supports, facilitates air ventilation in the tailgate. Fig. 7.13.10 shows an example of a successful cable support system for tailgate support for weak roof. The cable should be pre-tensioned as high as possible and the roof covered with wiremesh.

### B. Selection of tailgate support

Strength, stiffness, and stability are the criteria that must be met for an acceptable crib design. Strength is the crib capacity to support a load. Stiffness is the force developed by a crib to resist a unit of displacement. Stability is a measure of the capability of a structure to maintain equilibrium without sudden or severe loss of load capacity (Barczak and Gearhart, 1993). The key is to match those properties with those of the underground structure. The support capacity required can be determined by the failure height and maximum allowable displacement of the immediate roof and, from a roof control point of view, a standing support should provide an adequate initial resistance to the immediate roof shortly after installation and can still maintain a large percentage of its peak capacity after yield (JS Chen et al., 2003).

Based on the characteristics of load-displacement curves (Figs. 7.13.1-7.13.7), two types of approaches can be used for tailgate secondary support design: stiff and soft. The **stiff type** refers to those that take a load quickly and fail soon after reaching the peak load (see Figs. 7.13.3, 7.13.5, and 7.13.4.6). This type of support, having lost its load-bearing capacity after failure, must be designed such that the supporting load density is sufficiently high so that it would not fail when the longwall face, and thus, the front abutment pressure is approaching. Conversely, the **soft type** refers to those that take the load slowly, say after 10-12 in. (25-30 mm) of displacement before they reach the peak load and, after failure, still maintain a large proportion of the bearing capacity for considerable displacement (see Figs.7.13.1, 7.13.2, and 7.13.7). Since the post-failure bearing capacity of this type of support is still high, roof convergence of the tailgate continues until the roof, floor, and support reach equilibrium. For the soft type of support, the post-failure supporting density must be sufficient so that the roof-to-floor convergence will not be excessive leading to roof collapse.

Barczak (2000 and 2001a), using the concept of ground reaction curve, developed a tailgate support design method, STOP (Support Technology Optimization Program). The

three-dimensional finite element method has also been used for standing supports design for open entries or pre-driven recovery rooms (Tadolini et al., 2002; Zhang et al., 2007a). The advantage of the finite element method is that a prior knowledge of the ground reaction curve is not needed

Underground tests of several types of supplementary tailgate supports (Table 7.13.1) in the Pittsburgh seam showed that from the standpoint of escapeway safety, all of the test configurations provided adequate support on the tailgate corner and outby the face (Molinda et al., 1997). The only difference was that different degrees of rib sloughage, roof sag, and floor heave, occurred in the outby area, and that in the inby area all standing supports provided different degrees of air passageway, but in the cribless section, the tailgate airway was not maintained for the full pillar length.

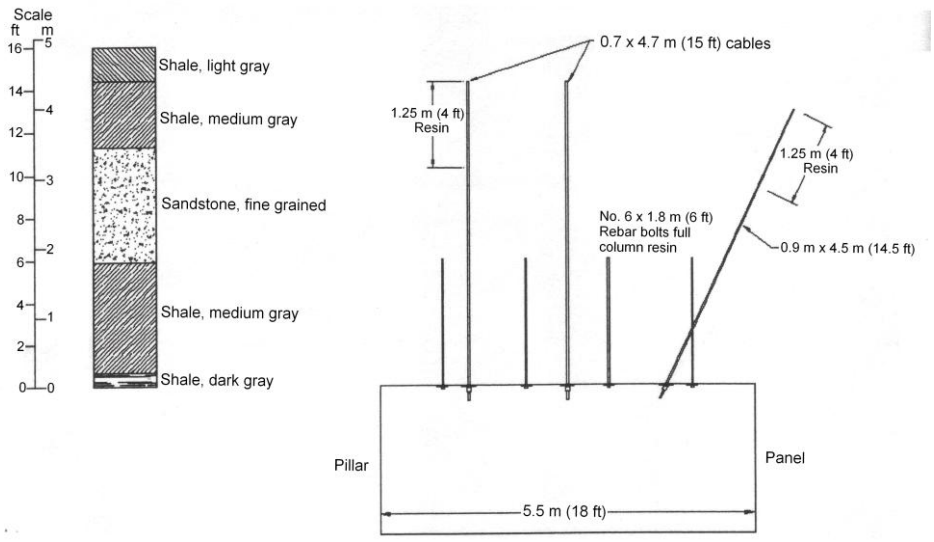


**Fig. 7.13.10 Cribless tailgate support using cable bolts (Tadolini et al., 2000)**

**Table 7.13.1 Test configuration of tailgate supplementary supports (entry was 16 ft or 4.9 m wide)**

| Type | Support components |
|---|---|
| Wood cribs with cable truss and no cable bolt | A single row of wood cribs at 6 ft (1.8 m) centers; cable trusses on 8 ft (2.4 m) centers |
| Link-N-Lock cribs with cable truss and cable bolt | A single row of Link-N-Lock cribs on 6 ft (1.8 m) centers with a 12 ft (3.7 m) long cable bolt in the roof on 6 ft (1.8 m) centers located 4 ft (1.2 m) from the rib. Cable trusses were on 8 ft (2.4 m) centers |
| Wood crib with cable truss and cable bolt | A single row of wood cribs on 6 ft (1.8 m) centers, with the cable truss on 6 ft (1.8 m) spacing and with a 12 ft (4.7 m) cable bolt on 6 ft (1.8 m) added on the tailgate side rib |
| Propsetter posts with cable truss and cable bolt | A single row of 10 in. (254 mm) diameter Propsetter posts on 6 ft (1.8 m) centers and 4 ft (1.2 m) from the tailgate side rib. Cable trusses were on 8 ft (2.4 m) centers and the 12 ft (4.7 m) long cable bolts were on 6 ft (1.8 m) centers |
| Cribless with cable truss and cable bolt | The cable trusses were on 8 ft (2.4 m) centers and a single row of 12 ft (4.7 m) long cable bolts on 6 ft (1.8 m) centers |